Characterizing innate immune cell activation by fungal pathogens

Dissertation

Zur Erlangung der Akademischen Grades

„doctor rerum naturalium" (Dr. rer. nat.)

vorgelegt dem Rat der Fakultät für Biowissenschaften

der Friedrich-Schiller-Universität Jena

von Diplombiologin Alessandra Marolda

geboren am 18.05.1988

Jena, September 2020

Date of the defense: 17.09.2021

Committee members:

Prof. Dr. Oliver Kurzai. Medical Microbiology and Mycology, University Würzburg, Germany

Prof. Dr. Thilo Figge. Leibniz Institute for Natural Product Research and Infection Biology – Hans Knöll Institute (HKI), Jena, Germany

Prof. Dr. Lehrnbecher Thomas. Division for Pediatric and Oncology, Johann Wolfgang Goethe University, Frankfurt, Germany

Prof. Dr. Ilse Jacobsen. Leibniz Institute for Natural Product Research and Infection Biology – Hans Knöll Institute (HKI), Jena, Germany

Prof. Dr. Claudia Waskow. Leibniz Institute on Aging - Fritz Lipmann Institute (FLI), Jena, Germany

Prof. Dr. Peter Zipfel. Leibniz Institute for Natural Product Research and Infection Biology – Hans Knöll Institute (HKI), Jena, Germany

The work included in this thesis was carried out in the Septomics Research Center of the Friedrich Schiller University Jena and Leibniz Institute for Natural Product Research and Infection Biology, Hans Knöll Institute, Jena, in the research group "Fungal Septomics" under the supervision of Prof. Dr. Oliver Kurzai.

Table of content

Figure index

1 Abstract

Candida albicans (*C. albicans*) and *Candida glabrata* (*C. glabrata*) are the two most prevalent *Candida* species causing bloodstream infections. Patterns of innate immune activation triggered by the two fungi differ considerably. To analyze human natural killer (NK) cell activation by both species, we performed *ex vivo* whole-blood infection assays and confrontation assays with primary human NK cells. Isolated NK cells get stronger activated by *C. albicans* than *C. glabrata*. In contrast, activation of blood NK cells was more pronounced during *C. glabrata* infection. NK cell activation in blood is mediated by humoral mediators released by other immune cells and does not depend on direct activation by fungal cells. Cross-talk between *Candida*-confronted monocyte-derived dendritic cells (moDC) and NK cells resulted in the same NK activation phenotype like NK cells in human blood. Blocking experiments and cytokine substitution identified interleukin 12 as a critical mediator in regulation of primary NK cells by moDC-derived cytokines that was also partially responsible for stimulation of blood NK cells.

On the other hand, we focused on the identification of changes in polymorphonuclear cells (PMN) behavior induced by *C. albicans* and *C. glabrata* since these immune cells are of outstanding importance in the response against invasive *Candida* infections. Sorting and extraction of PMN were performed after a one-hour confrontation in human whole blood in presence of fungal cells. Then, infected isolated PMN were used for separate analysis in live cell imaging experiments to visualize their dynamic features in comparison to mock-infected PMN. PMN in the acquired microscopic images were analyzed using the latest version of a migration and interaction tracking algorithm and further classified using different morphokinetics features. Compared to mock-treated PMN, PMN isolated from whole-blood infected with either *C. albicans* or *C. glabrata* presented a higher percentage of PMN with a spreading morphology. Furthermore, *C. glabrata* presented a significantly higher number of cells with a spreading morphology compared to *C. albicans*.

Combination of live cell imaging with automated analysis allowed a classification and distinction of PMN isolated from mock-infected blood and *Candida*-infected blood based on their morphology.

2 Zusammenfassung

Candida albicans und *Candida glabrata* sind die beiden am häufigsten vorkommenden *Candida*-Arten, die Infektionen der Blutbahn verursachen. Die durch die beiden Pilze ausgelösten Muster der angeborenen Immunaktivierung unterscheiden sich erheblich. Um die Aktivierung der humanen natürlichen Killerzellen (NK-Zellen) durch beide Spezies zu analysieren, führten wir ex vivo-Vollblut-Infektionstests und Konfrontationstests mit primären menschlichen NK-Zellen durch. *C. albicans* aktivierte isolierte humane NK-Zellen stärker als *C. glabrata*. Im Gegensatz dazu war die Aktivierung von Blut-NK-Zellen, die durch eine hochregulierte Oberflächenexposition des frühen Aktivierungsantigens CD69 und des Todesrezeptorliganden TRAIL sowie der IFN-γ-Sekretion gekennzeichnet ist, während der Infektion von *C. glabrata* stärker ausgeprägt. Die Aktivierung von NK-Zellen im Blut wird wahrscheinlich durch humorale Mediatoren vermittelt, die von anderen Immunzellen freigesetzt werden und hängt nicht von der direkten Aktivierung durch Pilzzellen ab. Cross-talk zwischen *Candida*-konfrontierten Monozyten-abstammenden dendritischen Zellen (moDC) und NK-Zellen führte zum gleichen NK-Aktivierungsphänotyp wie NK-Zellen im humanen Blut. Blockierexperimente und Zytokinsubstitution identifizierten IL-12 als einen kritischen Mediator bei der Regulation primärer NK-Zellen durch moDC-basierte Zytokine, der auch teilweise für die Stimulation von NK-Zellen im Blut verantwortlich war, insbesondere im Hinblick auf höhere IFN-γ-Spiegel, die bei einer Infektion mit *C. glabrata* freigesetzt werden.

Darüber hinaus konzentrierten wir uns auf die Identifizierung von Veränderungen im PMN-Verhalten, die durch *C. albicans* und *C. glabrata* induziert werden, da diese Immunzellen von herausragender Bedeutung für die Reaktion auf invasive Candida-Infektionen sind. Die Trennung und Extraktion von PMN wurde nach einer einstündigen Konfrontation in menschlichem Vollblut in Gegenwart von Pilzzellen durchgeführt. Dann wurden infizierte isolierte PMN zur separaten Analyse in bildgebenden Live-Cell-Experimenten verwendet, um ihre dynamischen Eigenschaften im Vergleich zu Mock-infizierten PMN sichtbar zu machen. Die manuelle Analyse der erhaltenen Aufnahmen zeigte zwei unterschiedliche dynamische Morphologien: PMN in einer abgeflachten und PMN in einer nicht abgeflachten Morphologie. Aus dieser ersten Beobachtung wurden in Zusammenarbeit mit der Gruppe von Prof. Thilo Figge die PMN in den aufgenommenen mikroskopischen Bildern mit der neuesten Version eines Migrations- und Interaktionsverfolgungsalgorithmus (AMIT-v3) analysiert und anhand verschiedener morphokinetischer Merkmale weiter klassifiziert. Im Vergleich zu Mock-behandelten PMN zeigten PMN, die aus Vollblut isoliert wurden, die entweder mit *C. albicans* oder *C. glabrata* infiziert waren, einen signifikant höheren Prozentsatz von PMN mit einer abgeflachten Morphologie.

Darüber hinaus wies *C. glabrata* im Vergleich zu *C. albicans* eine signifikant höhere Anzahl von Zellen mit einer abgeflachten Morphologie auf.

Die Kombination der Bildgebung lebender Zellen mit automatisierter Analyse ermöglichte eine Klassifizierung und Unterscheidung von PMN, die aus Mock-infiziertem Blut und *Candida*-infiziertem Blut isoliert wurden, auf Grundlage ihrer Morphologie.

3   Introduction

3.1 Bloodstream infection

Bloodstream infections (BSI) are characterized by the presence of bacterial or fungal microorganisms in the bloodstream which induce an alteration in clinical, laboratory and hemodynamic parameters and accompanied by an inflammatory response [1]. BSIs can lead to sepsis, an infectious syndrome triggered by organ dysfunction from a dysregulated immune system in response to an infection [2]. In patients with impaired immunity, BSI can be caused by virtually any pathogen, from Gram-positive to Gram-negative bacteria and fungi. BSI afflicts between 1.2% and 6.7% of hospitalized patients requiring intensive care unit (ICU) [3-5], especially in cases of hospitalization longer than 48 to 72 hours [6-8], and is correlated with high mortality rates. A recent study conducted in Germany correlated the mortality rate with the type of pathogens in 937 ICUs considering more than 4 million of patients affected by primary BSI (PBSI) [9]. Among the 13 considered pathogens, Enterococci, *Escherichia coli (E. coli)*, *Stenotrophomonas maltophilia, Pseudomonas aeruginosa, C. albicans* and non-*albicans Candida* species (spp.) were responsible for higher mortality in ICU patients compared to *Staphylococcus aureus*, which was used as reference [9].

3.2 *Candida* bloodstream infection and invasive candidiasis

Candida bloodstream infection, also called candidemia, is the most common form of invasive candidiasis. Indeed, *Candida* BSIs are one of the most frequent fungal infections belonging to hospitalized patients [10] and the fourth cause of nosocomial invasive infections in ICUs patients in North America [11]. Analysis of the Extended Prevalence of Infection in Intensive Care (EPIC II) study showed a prevalence of *Candida* BSIs of 6.9 per 100 patients with an associated morality rate of 43% versus 27% caused by bacterial BSIs [12]. In particular, *C. albicans* and *C. glabrata* account for the majority of candidiasis cases worldwide. *C. albicans* represents the predominant species with 50% of cases, while *C. glabrata* causes 15-25% of invasive *Candida* infections in the US and in the North of Europe [13]. Together both species are responsible for approximately 65%-75% of all systemic candidiasis, followed by *C. parapsilosis* and *C. tropicalis* [13, 14].

3.3 *Candida albicans* and *Candida glabrata*: similarities and differences

C. albicans and *C. glabrata* are ubiquitous commensals of healthy humans. Both fungal species can be found as constituents of the normal microbiota in different human niches (oral cavity, gastrointestinal and vaginal tracts) [15, 16]. Under certain conditions, *C. albicans* and *C. glabrata* can become pathogenic. Predisposing factors responsible for the asymptomatic to pathogenic shift

are long treatment with antibiotics, diabetes, cancer, age, immunosuppression and others described above [13]. Although sharing some characteristics, these two fungal species are very different from a phylogenetically, genetically and phenotypically point of view. Some of these differences also reflect *C. albicans* and *C. glabrata* virulence. The diploid genome of *C. albicans* contains genes involved in its ability to infect the host, such as adhesins which are important in adhesion to the host, secreted aspartyl proteases and phospholipases involved in host barriers degradation and invasion, and proteins for iron transfer [17-20]. On the other hand, *C. glabrata* haploid genome encodes cell wall proteins and aspartic proteases which are, respectively, involved in interaction with the host and immune evasion [21, 22]. Another key virulence factor missing in *C. glabrata* is the ability of *C. albicans* to switch from yeast to hyphal form. This morphological flexibility has a strong impact on the infection [23]. Both yeast and hyphal morphology presents a specific role: yeast cells of *C. albicans* are involved in dissemination during infection, while the filamentous form is required for attachment, invasion and tissue damage [24].

3.4 *C. albicans* and *C. glabrata* adhesion

C. albicans and *C. glabrata* can attach to mammalian host cells (epithelial, endothelial and immune cells), other microbes (bacteria and other *Candida* species), and abiotic surfaces (medical devices) [24, 25]. Adhesion to host cells is considered closely related to *C. albicans* and *C. glabrata* pathogenesis and biofilm formation.

The main players involved in this process are adhesins. Agglutinin-like sequence (Als) proteins (Als1-7 and Als9) and hypha-associated glycosylphosphatidylinositol-linked (GPI-linked) protein (Hwp1) are the most important adhesins in *C. albicans* adhesion [25, 26]. It was shown that deletion of Als3 induces a strong reduction in *C. albicans* adhesion to the epithelial cells [25, 27], in iron acquisition from ferritin [28], in biofilm formation [29], in induction of endocytosis by host cells [27, 30], demonstrating the importance of this protein. On the other hand, epithelial adhesin (Epa) family is involved in attachment process of *C. glabrata* [31]. Among all adhesions expressed by *C. glabrata*, Epa1 is most important virulence factor mediating *in vitro* adhesion to epithelial cells [32] . Furthermore, Epa6 and Epa7 have been identified as important for kidney and bladder colonization as well as in biofilm formation [33, 34].

3.5 *C. albicans* and *C. glabrata* invasion

3.5.1 *C. albicans* invasion

Adhesion is followed by invasion in the pathogenesis process of *Candida*. Depending also on the host cells, *C. albicans* presents two different mechanisms to invade the attached substrate: induced

endocytosis and active penetration by *C. albicans* hyphae [27, 35]. Induced endocytosis is an active process which involved both host cells and *C. albicans*. In fact, Als3 can interact with mammalian cadherins (such as N-cadherin and L-cadherins) and leads to establishment of adherence junctions, resulting in host cytoskeletal rearrangements and fungal internalization [30]. Active penetration can occur by *C. albicans* hyphae elongation associated with lytic enzyme secretion. Interestingly, hyphal cells can growth directionally after contact with solid surface (thigmotropism) [36] and through to a combination of physical pressure and lytic enzyme secretion can invade the cell layer [27]. In addition, temperature, pH, serum and CO_2 are involved in *C. albicans* yeast to hyphal transition [37, 38]. Lytic enzymes, as hydrolytic enzymes (as Secreted Aspartyl Proteinases (SAP)) and phospholipases, are released by *C. albicans* to facilitate the entry of *C. albicans* into or between host cells digesting surface cell components [39]. Another important peptide released by *C. albicans* is the cytolytic toxin Candidalysin encoded by extent of cell elongation 1 gene (*ECE1*) which is expressed by *C. albicans* hyphae during infection [40]. It was shown that *ECE1*-deficient strain presents less ability to damage and induce immune activation in zebrafish model and it is not virulent in immunocompromised murine model during oropharyngeal candidiasis [41].

3.5.2 *C. glabrata* invasion

Invasion ability and the consequent tissue/cell damaging caused by *C. glabrata* is lower compared to *C. albicans*, but *C. glabrata* is still able to reach the bloodstream and cause infection.

This fungal species can grow only as yeast during its infection. This means that *C. glabrata* pathogenicity is not correlated with its morphology. Surgery, catheter, parental nutrition, and burn injury allow the invasion and colonization of *C. glabrata* of different tissues in the host [13]. Another possible way for *C. glabrata* to invade the host is to be co-infected with other fungal species, like *C. albicans* [42-44], or even with other pathogens, like *Clostridium difficile* [45]. In oropharyngeal candidiasis it was shown that *C. glabrata* binds *C. albicans* hyphae, which increases *C. glabrata* colonization and spreading in the bloodstream [46]. Furthermore, *C. glabrata* was found in the cytoplasm of oral epithelial cells [47] and vaginal epithelial cells [16], suggesting that *C. glabrata* internalization could be also triggered by endocytosis into host cells. Secretion of hydrolytic enzymes is important during induce tissue damage induced by *C. albicans*, but these enzymes are not released or the secretion is very low by *C. glabrata* [48-51]. *C. glabrata* infiltration is facilitated by the release of phospholipases which can be only two types and are the same produced also by *C. albicans* [52]. High secretion of phospholipases is correlated with persistent candidemia and they are mainly important in the early stage of infection during host penetration and damage [19].

3.6 Interaction with human immune cells / immune system

Upon invasion into the tissue and entry into the bloodstream, fungal cells interface with the host innate immune system. The detection of pathogenic fungi occurs mainly through the recognition of cell wall constituents such as β-glucans, mannans and cell wall proteins [53, 54], also called pathogen associated molecular pattern (PAMPs), which are recognized by specific subset of pattern recognition receptors (PRRs) expressed on the surface of innate immune cells.

These immune receptors include C-type lectin receptors (CLRs), NOD (nucleotide-binding-oligomerization-domain)-like receptors (NLRs) and Toll-like receptors (TLRs) [55]. Every immune cell presents an individual set of PRRs, which are involved in varying degrees in the recognition of a pathogen. It is therefore suspected that, depending on the cell type, different receptors are involved in the detection of *Candida* [55, 56].

3.7 Interaction of *C. albicans* and *C. glabrata* with immune cells

Due to the differences that characterized *C. albicans* and *C. glabrata*, there are also evidences that the interplay between these two fungal species and the host immune system is quite different [57]. Consequently, distinct targeting of immune cell populations results in a strong response driven by PMN cells during *C. albicans* infection [58]. In fact, PMN rapidly phagocytose *C. albicans* upon confrontation and are the only immune cells able to inhibit intracellular filamentation of *C. albicans* [59]. In contrast, *C. glabrata* induces a low-grade inflammatory response, recruiting and activating monocytes rather than PMN in human blood and during murine infection [58].

Circulating monocytes, macrophages and dendritic cells also play a role in immune response against several pathogenic fungi especially in linking innate and adaptive responses [60]. These mononuclear phagocytes present different functions like: phagocytosis, antigen presentation, immune activation/modulation, and intracellularly pathogen killing using oxidative and non-oxidative mechanisms. Phagocytosis occurs by identifying antibodies (IgG) or complement components (C3b) which bind to Fc-gamma (Fcγ) and complement receptors (CR3), respectively, or to PPRs. It is known that the direct recognition and uptake of *C. albicans* occurs via Dectin-1 in the contest of tissue, while receptors involved *C. glabrata* recognition are still unknown [61]. However, monocytes represent a minor player in the early stage of immune response against *Candida* infections and they present lower capacity to kill *C. albicans* compared to blood neutrophils [62, 63], but it was shown that monocyte deficient mice are quickly affected by *Candida* dissemination into organs.

On the other hand, macrophages play an important role after tissues invasion. In addition to recognize and eliminate fungal cells, they are also able to produce inflammatory cytokines and chemokines which recruit others immune cells to the infection site. Although the monomorphic fungus *C. glabrata* has no hyphae, it has developed mechanisms to survive and even replicate within macrophages. The proliferation of the fungus eventually leads to the lysis of the macrophages and to the exit into the extracellular space [64].

3.8 *Polymorphonuclear cells* (**PMN**)

PMN cells, also called neutrophils, are the most common type of white cells in the bloodstream, representing 40-75% of leucocytes in human with their main role as pathogen-fighting immune cells. They are generated in the bone marrow in response to several stimuli (*e.g.* cytokines as granulocyte colony-stimulating factor G-CSF) [65] and their production can increase, for example, during bacterial infection. PMN present a relatively short life span. They can survive only 8-12 hours in the circulation and up to 1-2 days in tissues [66-68]. Blood PMN levels increase naturally in response to infections, injuries and other type of stress and their main role is to prevent infections by blocking, disabling, digesting particles and microorganisms.

Circulating PMN are quiescent but upon inflammatory stimuli they can migrate through the endothelium and reach infected and inflamed tissue in a process called extravasation. This process can be initiated by the production of chemotactic signals like the secretion of IL-8 or the complement derived anaphylatoxin C5a [69]. Once in the inflamed tissue, PMN become fully activated and explicate their cytotoxicity using different effectors mechanisms like phagocytosis, degranulation, generation of reactive oxygen species, and production of neutrophil extracellular traps (NETs) which are all designed to increase their pathogen-destruction ability [70].

Phagocytosis represents the internalization of a targeted organism or particle in an active receptor-mediated process [71]. For example, uptake of opsonized microbes depends on the binding by opsonic receptors, such as FcγRs [72, 73]. This process is accompanied by cytoskeletal rearrangements: phagocyte plasma membrane extends around its target, initiating a process which creates a membrane-bound vacuole called phagosome. Uptake is followed by fusion of the phagocytic vacuole with preformed granules in a process called phagosomal maturation. These granules contain hydrolytic enzymes and nicotinamide adenine dinucleotide phosphate oxidase (NAPDH) subunits that initiate killing mechanisms [71].

PMN degranulation is the release of proteinases and antimicrobial peptides which are stored in granules. Three main groups of granules are present inside PMN: (i) azurophilic (primary) granules which contain myeloperoxidase (MPO), defensins, β-glucuronidase, lysozyme and proteases (as

neutrophil elastase and cathepsin G (CG)); (ii) secondary granules which are characterized by the presence of lactoferrin, neutrophil gelatinase-associated lipocalin (NGAL) and matrix metalloproteinases (as MMP9) as well as (iii) tertiary granules [65, 74]. Furthermore, the secondary and tertiary granules contain also gelatinase and components of the NADPH oxidase. During the phagocytosis process, granules fuse with the phagosome and the plasma membrane, the latter resulting in the release of granule contents in the extracellular space. Furthermore, generation of reactive species coincident with the phagocytosis process require the translocation of the cytosolic NADPH oxidase components to the membrane [75].

Generation of oxygen derivates (like hypochlorous acid HOCl) is another direct (though decarboxylation, deamination, or peroxidation of proteins and lipids) and/or indirect (through modulation of phagocyte proteinase activity) killing mechanism used by neutrophils [76]. During PMN oxidative burst, NADPH oxidase is able to produce highly reactive compounds, such as the superoxide.

Finally, PMN are able to release NETs which are composed of decondensed chromatin (DNA and histones) and proteins contained in PMN granules like neutrophils elastase (NE), MPO, lactoferrin (LTF), gelatinase, CG, leukocyte proteinase 3 (PR3), calprotectin, cathelicidins, defensins [77]. Once NETs are released, they can trap and kill pathogens in the extracellular space. NET formation requires also reactive oxygen species. Following activation and reactive oxygen species (ROS) production, neutrophil elastase is transferred from the azurophilic granules to the nucleus where it can cleave histones and induce chromatin decondensation. In addition, MPO binds to chromatin and promotes further decondensation which leads to cell rupture and NET release [78].

PMN are not only involved in pathogen killing but also in immune response modulation by the release of cytokines and chemokines. Chemokines produced by PMN are IL-8/chemokine (C-X-C motif) ligand 8 (CXCL8) and growth-regulated alpha protein (GRO-α)/CXCL1 which exert their function on PMN themselves as well as macrophage inflammatory proteins 1α (MIP-1α)/chemokine (C-C motif) ligand 3 (CCL3) and MIP-1β/CCL4 that are involved in recruitment of monocytes, dentritic cells (DC), and T-lymphocytes, thereby affecting among other things immune cells that belong to the adaptive immune system [79-81]. Different studies show the beneficial role of neutrophils on DC recruitment to sites of infection through their release of lactoferrin, α-defensins and chemokines [82, 83]. Interestingly, in a murine model neutrophils have been also shown to act as antigen presenting cells to direct differentiation of T helper 1 (Th1) and Th17 lymphocytes [84].

3.8.1 PMN in fungal infection

PMN act as first line of defence in the control of early stages of many infections and show high capacity in killing invading pathogens.

Observations in patients affected by neutropenia, immunodeficiencies, and chronic granulomatous disease (CGD) helped to understand the central role of PMN in *Aspergillus fumigatus*, *C. albicans*, *C. glabrata* and *Cryptococcus neoformans* infections [85].

An example is represented by patients with leukocyte adhesion deficiency I (LAD-I) which are predisposed to invasive bacterial and fungal infection and lack the complement receptor CR3 due to a mutation of the CD18 subunit [86]. Consequently, studies using isolated neutrophils from LAD-I patients revealed an impaired uptake capacity of these cells for *C. albicans* and *A. fumigatus* conidia [87, 88].

Lack or functional defects in NADPH oxidase in CGD patients are also critical for host defence due the reduced or absent production of oxygen radicals (*e.g.* superoxide) by patient neutrophils. For this reason, CGD patients are more predisposed to invasive aspergillosis often caused by non-*fumigatus* species like *Aspergillus nidulans* or *Aspergillus viridinutans* and other mould infections [89].

The most common PMN defect is the MPO deficiency which involves the enzyme for generation of hypochlorous acid from reactive oxygen intermediates in azurophilic granules. However, MPO-deficient PMN showed *Candida* and *Aspergillus* killing defects *in vitro*, but the majority of patients are asymptomatic and not predisposed to fungal infections [90, 91].

Like most other immune cells, PMNs also express soluble and membrane Pattern Recognition Receptors (PRR) able to recognize and bind fungal PAMP. PAMPs-PRRs binding, but more in general the contact of PMN to the fungus, triggers the activation of signal transduction pathways that results in the stimulation of different cytotoxic responses like phagocytosis, oxidative burst mediates by the NADPH oxidase complex, release of antimicrobial peptides from neutrophilic granules and NET formation that all together contributes to the killing of fungi.

PPRs include the CLRs, TLRs, integrins like CR3, and FcγRs. Integrin CR3, for example, is the major human PMN receptor in recognition of non-opsonized or C3b opsonized fungal pathogens. Instead, soluble PRRs are present in PMN granules, like long variant pentraxin 3 (PXT3) which is mainly involved in *Aspergillus* spp. immune response.

While, PMN use two pathways in *C. albicans* killing based on recognition of opsonised or non-opsonised fungal cells [88]. It was shown that when *C. albicans* is unopsonized, the fungal killing is dependent of CR3, tyrosine-protein kinase (Syk), phosphoinositide 3-kinases (PI3K), and caspase recruitment domain-containing protein 9 (CARD9) pathways and independent of NADPH oxidase

activity. While opsonized *C. albicans*, FcγRs, serine/threonine-protein kinase (Sik), and ROS formation are involved in the killing [88].

Among PRR, CLR and their role have been heavily studied in *Candida* recognition [88, 92-94]. Belonging in this receptor class, there is Dectin-1 which is expressed on PMN surface (paper: Dectin 1 promotes fungicidal activity of human neutrophils) and recognises *C. albicans* β-(1,3)-glucan, after which it mediates protective cytokine production via Syk-CARD9 signalling [95]. It was shown that Dectin-1 also promotes fungicidal activity of human PMN and indeed its inhibition prevented binding and phagocytosis of β-glucan-rich zymosan by PMN [93].

Further, several studies suggest that CR3 is a major receptor for *C. allbicans* yeast and hyphae on human PMN [88, 96, 97]. Indeed, it was shown that CR3, which is expressed on circulating PMN and moves from intracellular compartments to the cell membrane upon activation, mediates phagocytosis of unpsonized of *C. albicans* cells by PMN [98].

All together, there are a lot evidences suggested that PMN play a central role in the immune response against invasive *Candida* infections and this is particularly true during *C. albicans* infection [59, 62, 99]. Indeed, it is known that PMN are of central importance in coordinating the response against *C. albicans* in human blood and there are the only immune cells able to inhibit intracellular filamentation of *C. albicans* [59]. Furthermore, PMN trigger several forms of stress response in *C. albicans* that can contribute to killing of the fungus [100-102].

On the other hand, the role of PMN during *C. glabrata* infection is not well characterised. Although PMN seems to play a role in this infection, other immune cells, such as monocytes, have been shown to be more relevant in human blood [58]. Indeed, PMN are less effective in taking up *C. glabrata* [58]. Another interesting aspect about the interaction of PMN with *C. glabrata in vitro* is the release of phagocytosed and intracellularly killed fungal cells, a process called dumping. Thus, dumping differs from vomocytosis, which is characterized by the release of viable intracellular fungal cell without damage of the host cell [103, 104]. Moreover, dumping occurs more frequently than vomocytosis.

CR3, Dectin 1 and 2, TLRs (but not TLR3) and FCγ receptors are the PRR on PMN which can recognise *C. glabrata* [55]. Recently an important role for dectin 2 which recognises fungal mannanns has been described [94]. Murine PMN lacking dectin 2 were defected in phagocytosis and ROS secretion upon confrontation with *C. glabrata* and were thus diminished in their capacity to kill the fungus.

3.9 Natural killer (NK) cells

NK cells belong to the group 1 of innate lymphoid cells (ILC1) and are characterized by the presence of the neural cell adhesion molecule CD56 and the absence of T-cell receptor CD3 on their surface [105-107]. Depending on the cell surface density of CD56 and the Fcγ receptor III (CD16), two main NK subpopulations are identified which differ in their localization and function: the cytotoxic CD56^{dim}CD16^{bright} and the immune regulatory CD56^{bright}CD16^{dim} subsets [108]. NK cells are regulated by various receptors which positively or negatively control their activation status. This regulation takes place through intracellular activation or inhibition domains (ITAM or ITIM) [109].

NK cells have different effectors mechanisms to eliminate target cells: (i) exocytosis of cytotoxic granules containing perforin and granzymes, (ii) death receptor-induced target cell apoptosis through expression of tumor necrosis factor (TNF) receptor ligands and (iii) antibody-dependent cellular cytotoxicity mediated by Fcγ-receptor III (FcγRIII, CD16) [110].

Exocytosis of cytotoxic granules occurs with a formation of immunological synapse between NK cell and the target cell which provides actin cytoskeleton rearrangement like the microtubule organizing center (MTOC) and secretory lysosome polarization. These changes are followed by the attachment of lysosome with NK cell membrane and then fusion of these secretory lysosomes with the target cell membrane which lead to the secretion of cytotoxic molecules as perforin and granzyme (the molecular mechanism of natural killer cells function and its importance in cancer immunotherapy [111]. It was shown that perforin can perforate the plasma membrane of tumor cells, resulting in an influx of water, loss of intracellular molecules and cell lysis [112, 113]. In addition, disruption of the target cell membrane by granulysin causes ion fluxes leading to an increase of cytosolic calcium and a decrease of potassium levels which induce caspase activation and consequently apoptosis in the target cells [114-118].

During NK cell degranulation process, some proteins appear on NK cell surface due the fusion of lysosomes with the plasma membrane. This is the example of the lysosomal-associated membrane protein-1 (LAMP-1 or CD107a) and -2 (LAMP-2 or CD107b). Interestingly, CD107a regulation and expression are used as cytolytic activity markers of NK cells [119].

The importance of this granule-specific protein was demonstrating through CD107a silencing which shows inhibition of NK cell cytotoxicity. Further, the disruption of CD107a leads to slowing down of granules movement and interfering of perforin recruitment to lytic granules [120].

Another process by which NK cell mediates killing of target cells involves death receptor-induced target cell apoptosis. Belonging to the death receptor family, there are: TNF receptor (TNFR), Fas ligand (also known as CD95 or APO-1), DR3 (also known as APO-3, LARD, TRAMP and WSL1), TRAIL and nerve growth factor receptor (NGFR) [121, 122]. All these death receptors contain an

intracellular globular protein domain called death domain (DD) of ~80 residues which transmits the death signal to intracellular signaling pathways [123]. Once the binding occurred between the death receptor and its ligand on the target cells, activated death receptor recruit an adaptor protein called Fas Associated Death Domain (FADD) [124] which is composed by two protein interaction domains: a death domain and a death effector domain (DED). After its recruitment, FADD binds to the receptors through interaction between DDs and to pro-caspase-8 through DED interactions to form a complex at the receptor called the death inducing signalling complex (DISC). Recruitment of caspase-8 through FADD leads to its auto-cleavage and activation [125]. Active caspase-8 in turn to activates effector caspases such as caspase-3 causing the cell undergo apoptosis by digesting upwards of hundred or so proteins [126].

In more details, TRAIL exposed on the NK cell surface belongs to the TNF superfamily and is an important mediator of apoptosis. Five receptors for TRAIL have been found: TRAIL-R1 and TRAIL-R5 are involved in apoptotic signal transduction [127], while the other three (TRAIL-R3, TRAIL-R4 and a soluble receptor TRAIL-R5) may be involved in TRAIL-mediated cell death regulation [128]. The expression of TRAIL is induced on mouse and human NK cells after stimulation with IL-2, IFNs, or IL-15. High expression of TRAIL could be correlated with its actively role in innate immune response [128]. In addition to the previously described mechanism of induction of apoptosis, activation of TRAIL can bring to another form of programmed cell death called necroptosis which brings to cellular death in a caspase-independent manner [129-131].

A lot of evidences suggest that the binding of TRAIL to TRAIL-R1 and TRAIL-R2 can activate different factors as nuclear factor kappa-light-chain-enhancer of activated B cells (NFkB), PI3K/Protein kinase B (Akt), mitogen-activated protein kinase (MAPKs), extracellular signal-regulated kinases 1 (ERK1)/ERK2, c-Jun N-terminal kinase (JNK) and p38, which generate different signals involved in NK cell cytotoxicity and cytokine release [132, 133]. Further, it was shown TRAIL role in tumor growth and elimination of infected cells and also in the regulation of immune system balance.

Finally, NK cells express FcγRIII/CD16 that can bind to the Fc portion of human immunoglobulins which themselves are bound to target cells (tumor cells, infected cells). FcγRIII-immunoglobulin binding results in lysis of the target cells by NK cells without priming. This antibody-dependent cell-mediated cytotoxicity (ADCC) is particularly involved in tumor cell recognition and it is used in cancer treatment, especially in cancer characterized by the over-expression of unique antigens (*e.g.* neuroblastoma, breast cancer) [134].

In addition to their cytotoxic activity, NK cells can produce a wide range of cytokines production of cytokines such as IFN-γ, TNF-α, GM-CSF, IL-10, IL-5, and IL-13 and chemokines such as MIP-1α,

MIP-1β, IL-8, and RANTES [135]. Among them, IFN-γ is one of the most potent effector cytokines secreted by NK cells and present relevant roles in antiviral, antibacterial, and tumor activity. IFN-γ is known to enhance the activity of antigen-presenting cells [136], driving among other things the secretion of Th1-inducing cytokines and killing capacity of macrophages against obligate intracellular pathogens [137]. Interestingly, NK cells also require signals by other immune cells like monocytes, macrophages and DC to exhibit their cytotoxicity and produce cytokines. Several studies demonstrated the functional link between NK cells and DC and showed the reciprocal activation of these cells by soluble factors or direct NK cell / DC interaction [138].

An important role of NK cells is their ability to recognize and kill abnormal cells via missing-self signaling, a down-regulation of constitutively expressed major histocompatibility complex (MHC) class I molecules on transformed cells [139]. Their antitumor function includes activity against acute lymphoblastic leukemia [140], acute myeloid leukemia [141], and neuroblastoma [142, 143]. NK cell importance has also been proven in the elimination of tumor cells of mucin-like carcinoma-associated antigen (MCA)-induced sarcoma [111, 144]. Further evidences suggested NK cell role in MCA-induced sarcoma, indeed, in mice lacking of adaptive immunity and NK cells present higher incidence of this tumor compare to mice lacking only of adaptive immunity [145]. In NK cell elimination process of MCA-induced sarcoma are involved IFN-γ and perforin [146, 147], the latter has also been shown to be involved in the control of B cell lymphomas and mammary carcinoma [148]. Another example is the mouse model of liver carcinoma where the restoration of endogenous p53 in tumor cells stimulate NK cell mediated elimination of senescent tumor cells [149].

Due to all these different roles and their ability to eliminate target cells, NK cells have been tested for use in immunotherapy offering several advantages. Indeed, several therapies have recently been proposed based on the use of NK cells: i) adptive NK cell therapy, ii) cytokine therapy, iii) chimeric antigen receptor (CAR) NK cell therapy and iv) antibody (mAb)-based therapy [111]. In the adaptive NK cell therapy, source of NK cells can be autologous or allogenic from peripheral blood, bone marrow, human embryonic stem cells, and cord blood. After NK cell isolation from patients or healthy donor using CD56 beads, NK cells are activated and expanded *ex vivo* using a cocktail of cytokines (such as IL-2) and after that transfused again in the patient. This approach was used with haploidentical NK cell from Kir-mismatched donor in acute myeloid leukemia (AML) patients inducing a complete remission of this disease [150, 151]. Also cord blood expanded NK cell show *in vivo* antitumor activity against several myeloma using artificial antigen presenting cells [152, 153]. Cytokine therapy is based on the use of different cytokines (IL-2, IL-15, IL-12, IL-18 and IL-21) capable of increasing the functions of the NK cells. For example, infusion of IL-15 in the metastatic malignant patients showed: expansion and proliferation of NK cells together with others

antitumor cells (as CD8^{+}T cells), IL-15 tolerance and the reduction of lung lesions in two patients [154].

Another therapy based on the use of NK cell is the CAR treatment. This approach use engineered NK cells which express specific CAR against tumor antigen and subsequent transfer of these cells; CAR NK cell therapy demonstrated in different preclinical models efficient killing of tumor cell *in vivo* and *in vitro* by engineered NK cells [155-159] which also show enhanced cytotoxic activity and cytokine secretion against osteosarcoma [159].

Finally, mAb-based therapy takes advantages of several activating, costimulatory, and inhibitory receptors on NK cells surface, as for example the expression of CD16 which is involved in the antibody-dependent cell-mediated cytotoxicity (ADCC). Human Ab IgG IPH2101, which is able to block the inhibitory receptor KIR2DL-1,-2 and -3 on NK cells surface, has the effect to induce a complete remission in AML patients but fails in the patient with myeloma [160, 161].

In addition, NK cells play an important role in the host response against various pathogens, including viruses, such as cytomegalovirus (CMV), Epstein–Barr virus [162] or hepatitis B and C virus [163], and bacteria, such as *Salmonella typhi, Escherichia coli* [164], or *Listeria monocytogenes* [165].

3.10   NK cells in fungal infections

Even if the exact role of NK cells in the host response against fungi is not fully understood and clinical data concerning NK cell involvement are lacking, different *in vitro* and *in vivo* studies showed the importance of NK cells in fungal infection [166]. First of all, NK cells exhibit direct antifungal activity against *C. albicans, Aspergillus fumigatus, Cryptococcus neoformans* and other fungal species [167-170]. Dependent on the immune status of the host, NK cells play an essential role on the outcome of systemic *C. albicans* infection and invasive aspergillosis in murine infection models [171, 172]. In line with this, an immune cell reconstitution study with patients subjected to hematopoietic stem cell transplantation (HSCT) that were affected by invasive aspergillosis showed impaired NK cell recovery with NK cell counts remaining below 200 / µL compared to healthy individuals [173]. Unfortunately, it has not been shown whether the infection was due to the lower number of NK cells or dependent on other factors. Similar results were found in a second study with solid organ transplant patients [174]. Patients who developed invasive fungal disease had lower NK cell counts than patients without infection, further demonstrating NK cell involvement in Aspergillus infections. In addition, patients suffering from chronic mucocutaneous candidiasis (CMCC) are characterized by reduced NK cell counts and NK cell cytotoxicity. However, these

patients present a generally impaired cell-mediated immunity and it is hard to define the exact role of NK cells in the pathogenesis of this disease [175-177].

It was shown that NK cells are able to damage *A. fumigatus* and *R. oryzae* hyphae but not their conidia [167, 178, 179] but this NK cell inability could be explained considering that conidia could be protected by capsules as pigments (melanin) which may prevent NK cell recognition [180-183]. The same situation might occur with *C. albicans*. Indeed, the NK cells express their cytotoxicity against germ tubes while they are able to phagocyte against the yeast form of *C. albicans* [184].

NK cells interact with fungi via receptors called natural cytotoxicity receptors (NCR) 1-3 (NKp46, NKp44, and NKp30) that belong to the group of activating receptors expressed on NK cell surface [107]. Recognition of *C. albicans* was shown to be mediated by the natural cytotoxicity receptor NKp30 [170], while NKp46 and its mouse ortholog NCR1 are involved in binding and damage of *C. glabrata* [185]. Interaction studies of NK cells and *A. fumigatus* recently discovered the neural cell adhesion molecule CD56 as pathogen recognition receptor that directly binds to *A. fumigatus* and accumulates at the interaction site [186].

The importance of lytic granule secretion was shown in several studies especially in the induction in the direct damage of fungal cells. Indeed, direct contact between *C. albicans* and primary NK cells results in release of perforin and granzyme B from cytotoxic granules and cytokine secretion, thereby directing fungal damage and enhancing PMN functionality in co-cultivation experiments, respectively [184]. Using an inhibitor of granule secretion (monensin), it was demonstrated that *C. neoformans* growth inhibition was partially abolished by human NK cells showing the importance of granule release also against *C. neoformans* infections [187].

In addition, cross-talk between NK cells and other immune cells during fungal infection was further demonstrated by other studies [188, 189]. The secretion of cytokines by NK cells is involved in the host response against fungi. In this context, secretion of IFN- γ secretion which presents multiple effects on various immune cells.

4 Aims of the work

Candida albicans and *Candida glabrata* are the two most prevalent pathogens in the genus *Candida* and account for the majority of candidiasis cases worldwide. However, there is evidence that the interplay of *C. albicans* and *C. glabrata* with the human immune system differs considerably. In order to get further insights into immune cell interactions in response to *Candida* infection, we are interested in stimuli that lead to different levels of NK cell activation during whole-blood infection with both fungal species.

The specific aims of this work were:

- Identification of changes in PMN behavior induced by C. albicans and C. glabrata
- Visualization of infected PMN dynamic features by live cell imaging
- Automated image analysis of morphological features of infected PMN
- Evaluation of infected PMN morphological changes

- Definition of NK cell effectors mechanisms involved in the response against *C. albicans* and *C. glabrata*
- Comparison between activated primary NK cells and blood NK cells stimulation induced by different fungal species
- Identification of potential factors involved in NK cells activation in the whole-blood infection model and in the DC-NK cell crosstalk

5 Materials and Methods

5.1 Ethics statement

This study was conducted in accordance with the Declaration of Helsinki and all protocols were approved by the Ethics Committee of the University Hospital Jena (permit number: 273-12/09).

5.2 Fungal strains and culture

C. albicans wild-type strain SC5314 [190], *C. glabrata* wild-type strain ATCC2001 [191], GFP-expressing *C. albicans* [62], and GFP-expressing *C. glabrata* [64] were routinely used in all experiments. *C. albicans cph1Δ/efg1Δ* mutant (cph1::hisG/cph1::hisG, efg1::hisG/efg1::hisG-URA3-hisG) was provided by Prof. B. Hube (HKI Jena, Jena, Germany).

C. albicans and *C. glabrata* were seeded in YPD medium (2% D-glucose, 1% peptone, 0.5% yeast extract, in water) and grown overnight at 30°C and 37°C, respectively, in a shaking incubator. Both fungal species were reseeded 1:50 in fresh YPD medium, grown until they reach the mid-log phase followed by harvesting in Hanks balanced salt solution (HBSS, gibco).

When required, *C. albicans* and *C. glabrata* were grown overnight in M199 medium (9.8 g/l M199, 35.7 g/l HEPES, 2.2 g/l $NaHCO_3$), pH4 at 37°C in a shaking incubator, reseeded in M199 medium, pH8 and cultured for 1 h at 37°C, which induced filamentous growth in *C. albicans.* Killing of *C. albicans* germ tubes and *C. glabrata* was performed by incubation for 1 h in 0.1% thimerosal (Sigma-Aldrich) in HBSS at 37°C.

5.3 Bacteria strains and culture

Neisseria meningitidis (WUE2120, from University of Würzburg), *Staphylococcus aureus* (ATCC25923) and *Streptococcus pneumonia* (SP257; from Prof. B. Löffler group from University of Würzburg) were used for one representative experiment in a whole-blood model assay. *N. meningitidis* and *S. pneumonia* were seeded on blood agar plates (Columbia agar with sheep blood plus, Oxoid) and grown overnight at 37°C. *S. aureus* was seeded in Lysogeny broth (LB) medium (0.01% Tryptone, 0.005% Yeast Extract, 5 g/L NaCl) and grown overnight to the stationary phase at 37°C in a shaking incubator. Bacteria were reseeded in fresh specific medium (*N.m*.: PPM medium (Bacto™ 15 g/l proteose peptone, 5 g/l NaCl, 0.5 g/l Starch from potatoes (Fluka), 1g/l K_2HPO_4, 4 g/l KH_2PO_4); *S.a.*: LB medium; *S.p.:* Todd Hewitt Broth (THY medium, 500.00 g/l Beef Heart Infusion, 20 g/l Peptic Digest of Animal Tissue, 2 g/l Dextrose, 2 g/l Sodium Chloride, 0.4 g/l Sodium Phosphate, 2.5 g/l Sodium Carbonate), grown until they reach the mid-log phase followed by harvesting in HBSS.

5.4   Human whole-blood infection model

Human peripheral blood was collected from healthy donors with written informed consent. The whole-blood infection assay was performed as described previously [62]. Briefly, either alive or thimerosal-killed *C. albicans* or *C. glabrata* cells were added to Hirudin-anti-coagulated blood (1×10^6 fungal cells/ml blood) and incubated at 37°C on a rolling mixer for indicated time points. In some experiments, aliquots of whole-blood were either pre-incubated with a blocking antibody against C5a (InflaRx), a blocking antibody against IL-12 (clone 24910, R&D Systems) or the isotype control (mouse IgG1, clone MOPC-21, Biolegend) for 5 min at 37°C. Flow cytometry and plasma collection were performed immediately after incubation. Plasma was collected after centrifugation of blood for 10 min at 13,200 rpm and 4°C and stored at -80°C until further analysis.

5.5   Isolation of human PMN

Human PMN were isolated one hour post infection from peripheral blood of healthy donors. Non target cells were removed by immunomagnetic depletion with MACSxpress beads (MACSxpress Whole blood Neutrophl isolation kit, Miltenyi), while erythrocytes were aggregated and sedimented. Remaining erythrocytes were lysed for 5 min with ACK Lysing Buffer (Life Technologies) and purity of PMN was checked by flow cytometry to be >95%. Obtained PMN were resuspended in RPMI (Biochrom AG) + 5% heat-inactivated human serum (human AB serum, Sigma-Aldrich; heat-inactivated at 56°C for 1 h) and used for live cell imaging and further flow cytometry analyses.

5.6   Isolation and expansion of human NK cells

First, human peripheral blood mononuclear cells (PBMCs) were isolated from buffy coat of healthy donors by standard Ficoll gradient centrifugation (Biochrom AG). Untouched NK cells were isolated from PBMCs by negative selection using the NK cell isolation kit according to manufacturer's instructions (Miltenyi Biotec). NK cell purity was checked by flow cytometry and defined as >95% CD56$^+$/CD3$^-$/CD14$^-$ cells. Primary human NK cells were either used directly after isolation or further expanded by cytokine treatment. To generate cytokine-primed NK cells, freshly isolated NK cells were seeded at a concentration of 2×10^6/ml in Stem Cell Growth Medium (SCGM, Cell Genix) containing 10% human serum (human AB serum, hS, Sigma-Aldrich) and 100 U/ml recombinant IL-2. After three days of incubation (37°C and 5% CO_2), half of the medium was exchanged with SCGM+10% hS supplemented with 100U/ml IL-2, 50ng/ml IL-15, 1000U/ml IFN-α and 2000U/ml IFN-β and incubated for another three days. Recombinant cytokines were

obtained from ImmunoTools. After six days of expansion, NK cells were harvested and resuspended in fresh SCGM+10% hS.

5.7 Generation of monocyte-derived dendritic cells

Monocytes were isolated from PBMCs of healthy donors by positive selection using CD14 microbeads according to the manufacturer's instructions (Miltenyi Biotec). Freshly isolated monocytes were used to generate moDCs by incubation in RPMI containing 10% heat-inactivated fetal bovine serum (hiFBS, Biochrom AG) in the presence of 800 U/ml GM-CSF (Leukine® Sargramostim) and 1000 U/ml IL-4 (Miltenyi Biotec) for 7 days. Differentiation of monocytes into moDC was checked by flow cytometry, with results of > 85% CD1a$^+$/CD14$^-$ cells being used for further experiments. MoDC were collected, resuspended in RPMI + 10% hiFBS and used for confrontation in the transwell assay.

5.8 NK cell confrontation assay

Confrontation of cytokine-primed NK cells with fungi was performed in SCGM + 10% hS at a multiplicity of infection (MOI) of 0.5 for 2 h and 4 h at 37°C and 5% CO_2. To investigate the direct effect of IL-12 on the regulation of NK cell surface marker expression, $1x10^6$/ml freshly isolated NK cells were incubated with 2 μg/ml recombinant IL-12 (ImmunoTools) for 40 h at 37°C and 5% CO_2.

5.9 Transwell assay

Transwell plates (Corning) were used to investigate the cross-talk between moDC and NK cells. $1x10^6$ moDC were seeded into the upper compartment and either mock-infected or confronted with $5x10^5$ thimerosal-killed *C. albicans* germ tubes and thimerosal-killed *C. glabrata*, respectively (moDC : *Candida* ratio of 2:1, MOI = 0.5) in 500 μl of RPMI + 10% hiFBS. The upper compartment was separated by a microporous membrane (pore size: 0.4 μm) from the lower compartment that contained $1x10^6$ freshly isolated NK cells in 1.5 ml of RPMI + 10% hiFBS (Figure 1) The microporous membrane allowed the exchange of soluble factors, while it prevented direct contact of immune cells in the two compartments. When indicated, 10 ng/ml mouse IgG1 or the αIL-12 blocking antibody were present in the upper compartment throughout the course of the experiment.
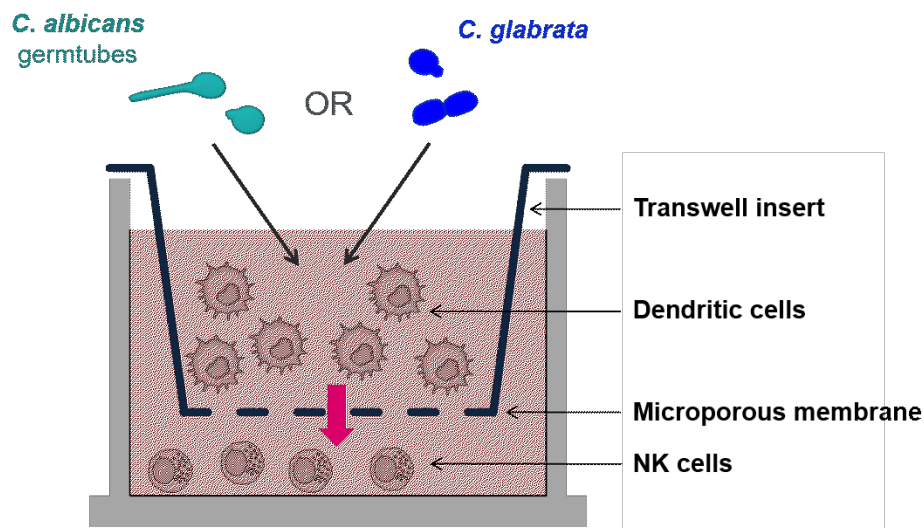
Figure 1. Transswell system layout.

5.10 Flow cytometry

Analyses of isolated immune cells (NK cells and moDC) and NK cells in whole-blood regarding their expression of cell surface activation markers were performed using differential FACS staining and subsequent measurement with the BD FACSCanto II. NK cells were specifically identified by a $CD3^-$ and $CD56^+$ staining using mouse anti-human CD3 (clone REA613) and CD56 (clone REA196) antibodies, both obtained from Miltenyi Biotec. Changes in surface marker expression were investigated using mouse anti-human CD69 (clone REA824, Miltenyi Biotec), CD16 (clone 3G8, Biolegend), CD107a (clone H4A3, Biolegend), TRAIL (CD253, clone RIK-2, Biolegend), FasL (CD178, clone NOK-1, Biolegend), CD38 (clone REA671,Miltenyi Biotec), HLA-DR (clone REA332, Miltenyi Biotec) and NKp30 (CD337, clone REA823, Miltenyi Biotec). MoDC were stained with the following antibodies: mouse anti-human CD1a (clone HI149, Biolegend), CD14 (clone REA599, Miltenyi Biotec), CD86 (clone 2331, BD) and CD83 (clone HB15e, Biolegend).

PMN were specifically identified by CD66b staining using mouse anti-human CD66b (clone G10F5) antibody obtained from BD Biosciences. Changes in surface marker expression were investigated using mouse anti-human CD16 (clone 3G8, Biolegend), CD62L (clone DREG-56, Biolegend), CD11b (clone ICRF44, Biolegend), CD18 (clone TS1/18, Biolegend), CD44 (clone BJ18, Biolegend).

Stained blood samples were treated with BD FACS Lysing solution, which lyses erythrocytes while preserving and fixing leukocytes, followed by washing and harvesting cells in BD Cell WASH solution. Similarly, primary NK cells, moDC and isolated PMN were washed with BD Cell WASH solution after staining.

Analysis of flow cytometry data was performed using FlowJo 7.6.4 software.

5.11 Time-lapse microscopy

Live cell imaging was performed for PMN isolated either from mock-infected, *C. albicans* or *C. glabrata* infected human peripheral blood. For each experiment, 4×10^5 PMN were seeded in a μ-dish (ibidi) in a total volume of 2 ml of RPMI containing 5% hiFBS. 2.5 ng/ml of propidium iodide (PI, Sigma-Aldrich) was added into the medium to distinguish viable cells from dead ones. PI stains only the nucleus in dying cells characterized by a lack in their plasma membrane. PMN were incubated in an environmental control chamber at 37°C and 5% CO_2. Images were acquired every 7 seconds with a LSM780 confocal microscope, which was focused on the bottom of the dish. Cells were monitored with a 20x microscope objective (Plan-APOCHROMAT 20x/0.08NA) using a differential interference contrast (DIC) setting with illumination by 488 nm laser. Image resolution is 0.208 μm/px and image size is 2048 by 2048 px.

5.12 Quantification of secreted proteins

Protein quantification within supernatants of isolated cells or in plasma samples obtained from whole-blood experiments was performed using Luminex technology according to the manufacturer's instructions (ProcartaPlex and High Sensitivity ProcartaPlex Immunoassay, ThermoFisher Scientific). Among a set of 34 cytokines, analysis was focused on the following ones: interleukin (IL)-1β, IL-2, IL-6, IL-12, IL-15, IL-18, IL-23, IL-27, TNF-α and IFN-γ.

5.13 Quantification of C5a in human plasma

C5a concentration was measured in plasma samples obtained from whole-blood infection experiments with either *C. albicans* or *C. glabrata* for 1 hour using the BD Cytometric Bead Array – Human Anaphylatoxin kit, following the manufacturer's instruction.

5.14 Statistical analyses

For all experiments, at least three independent repeats using cells from individual donors were used. Data are presented as arithmetic means ± standard error of mean (SEM). All statistical analyses were performed using GraphPad Prism software. *P* values were determined using one-way ANOVA followed up by multiple comparison tests. When required, *P* values were determined using unpaired, two-sided Student *t* test. Significance is shown as *$P < 0.05$, **$P < 0.01$, ***$P < 0.001$.

5.15 Bioinformatic analysis

5.15.1 Segmentation and tracking of PMNs

Migration and interaction tracking algorithm was used for cell detection and tracking (AMIT) [192-194] in its third release version (AMIT-v3) [195]. This algorithm allows automatic segmentation and detection of positions of label-free immune cells from transmitted light microscopy data. In addition, it provides the possibility to eliminate track segments associated with long-lasting clusters that highly likely are results of overlapping cells or consist of multiple cells. This step is necessary for extraction of non-distorted information about the morphology of individual cells. For further analysis a selection of cells with track durations of more than 1 minute (i.e., at least nine frames) was performed.

5.15.2 Measurement of PMN speed

Computation of instantaneous cell speed was performed for pairs of consecutive time steps in *μm/min*. The arithmetic mean was calculated from the instantaneous speed values and these values were collected per each video.

5.15.3 Extraction of gradient-based cell features.

For each frame in the videos from time-lapse microscopy, a sequence of contrast-limited adaptive histogram equalization followed by a Sobel gradient operator was used to compute an image gradient magnitude map. This map is transformed into a scaled intensity image that contains values in the range from 0 (minimal value of the map) to 255 (maximal value of the map). Afterwards, the intensity of the image is adjusted and for each previously segmented PMN, the value range of percentiles in the pixel intensity is used as a descriptor of cell surface roughness in the intensity space. We refer to this feature, which is based on the percentiles of the histogram for the transformed gradient magnitudes, as pHG descriptor.

6 Results

6.1 Combining whole-blood infection model with live cell imaging to identify PMN morphokinetic parameters for infection classification

The aim of this project was to generate a dynamic hemogram from whole-blood infection assays that goes beyond standard blood count examination by integration of information on migration, morphology and interaction of blood cells, with particular attention on PMN.

Automated processing of microscopic images and imaging data was performed in collaboration with the group of Applied System Biology of Prof. Dr. Marc Thilo Figge and his PhD student Ivan Belyaev.

6.1.1 Infected PMN by fungal cells show different morphology compared to mock-infected PMN

In previous studies, direct comparison of human PMN activation by *C. albicans* and *C. glabrata* has been performed. In response to these two different fungal species the response of PMN is quite different. It was shown that PMN are more efficient in *C. glabrata* elimination, but at same time this species induces a low-grade and slow inflammatory response preferring the recruitment and activation of monocytes [58]. On the other hand, PMN stimulation is rapid and pronounced in response to *C. albicans* which results in a rapid phagocytosis of fungal cells with the only recruitment and activation of PMN. This different immune response is also reflected in the human whole blood where *C. glabrata* is higher associated with monocytes and while *C. albicans* with PMN. These previous experiments were performed on PMN isolated from human whole blood and then infected by fungal cells for different time points. After PMN- fungal cells co-incubation, different assays were performed to investigate PMN activation in response to *C. albicans* and *C. glabrata*.

In this current study, peripheral blood was infected for one hour either with *C. albicans* or *C. glabrata* and after that PMN isolation was performed from infected-blood. This new approach has allowed us to investigate a new aspect of PMN behaviour after being in contact with fungal cells in the context of whole-blood with all its constituents and to perform a comparison in the response to *C. albicans* and *C. glabrata* infection.

After PMN isolation from human whole-blood infected either with *C. albicans* or *C. glabrata*, PMN were used to perform live cell imaging and monitored 30 minutes in comparison to PMN isolated from mock-infected blood. Live cell imaging allows investigation of dynamic events of single label-free cells and instead of giving a single picture it turns frames into movies.

Already manual analysis of the movies obtained from the three considered conditions (PMN mock-infected, *C. albicans*-influenced PMN and *C. glabrata*-influenced PMN) showed some differences in PMN phenotype never observed in previous works always performed for primary PMN during direct *Candida* infection [58] (Figure 2).
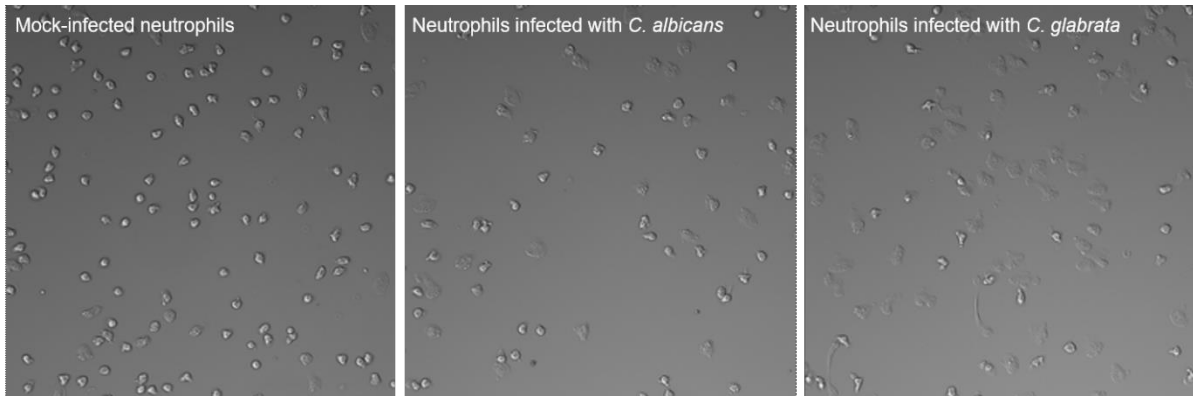
Figure 2. Frames taken from time-lapse microscopy video.
PMN were isolated from blood that was either mock-infected or infected with *C. albicans* and *C. glabrata*. Subsequently, isolated PMN were used to perform live cell imaging using LSM 780 confocal microscope and monitored for 30 min. Pictures show one of nine independent experiments with isolated cells from different donors with virtually identical results.

In more detail, it was possible to distinguish two different dynamically morphologies (Figure 3): PMN in a spreading (S-morphology) and PMN in a non-spreading morphology (N-morphology).
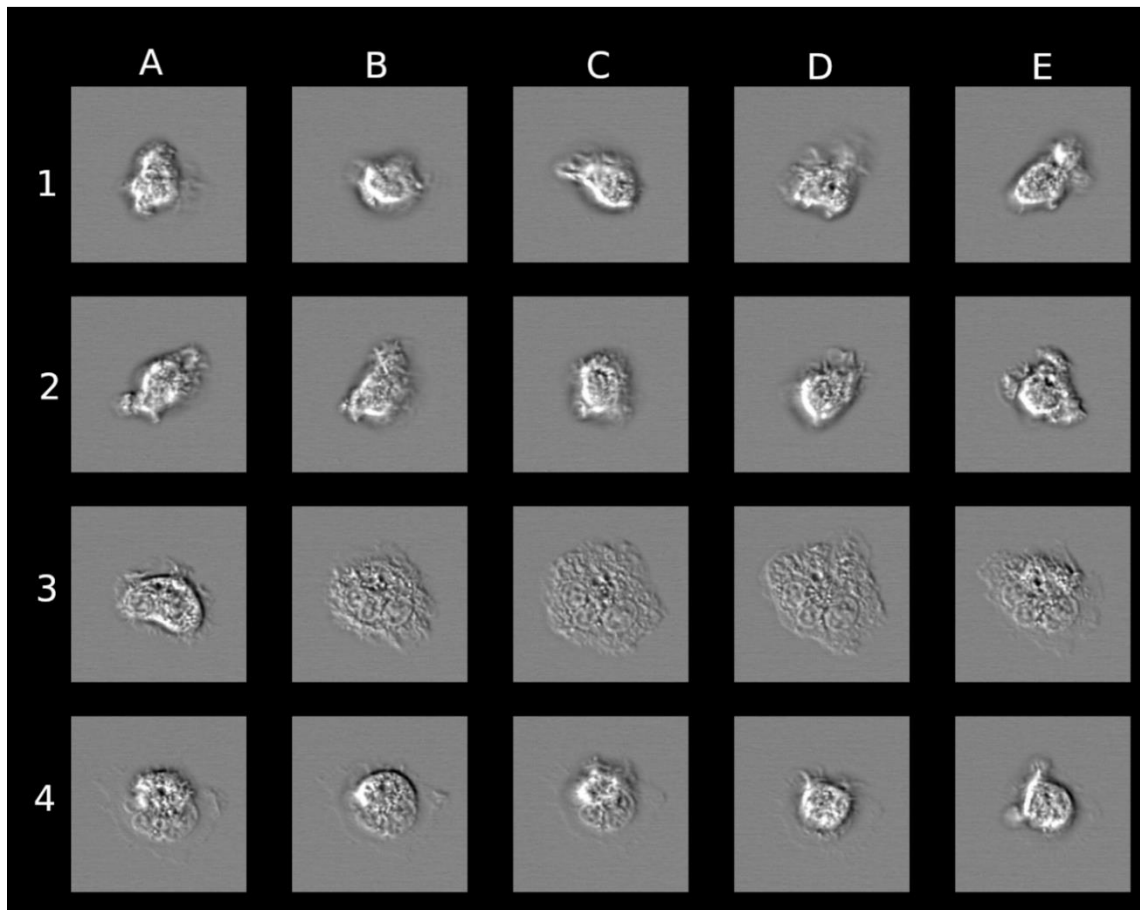
Figure 3. Different morphological phenotypes of single PMN.

A sequence of 20 frames ordered as A1→E1→A2→E2→A3→E3→A4→E4. For instance, A1 shows the spreading (S-morphology) and D4 the non-spreading (N-morphology) phenotype.

To get further insight into this initial observation, PMN in the acquired microscopic images were segmented and tracked over time-frames by the latest version of a migration and interaction tracking algorithm (AMIT-v3) [195]. Furthermore, a method was designed for the automated identification and quantitative evaluation of PMN morphology. Using these approaches, a direct comparison of morphologies of PMN isolated from mock-infected, *C. albicans*- and *C. glabrata*-infected whole blood was made.

Compared to PMN from mock-infected blood which presented mostly PMN in a N-morphology, PMN isolated after whole-blood infection with either *C. albicans* or *C. glabrata* presented a significantly higher percentage of PMN with S-morphology (Figure 3). PMN with S-morphology were only rarely present in mock-infected samples (0.75±0.02%). Furthermore, *C. glabrata* (0.50±0.04%) confrontation resulted in an even higher number of cells with S-morphology compared to *C. albicans* (0.34± 0.02%) (Figure 4).
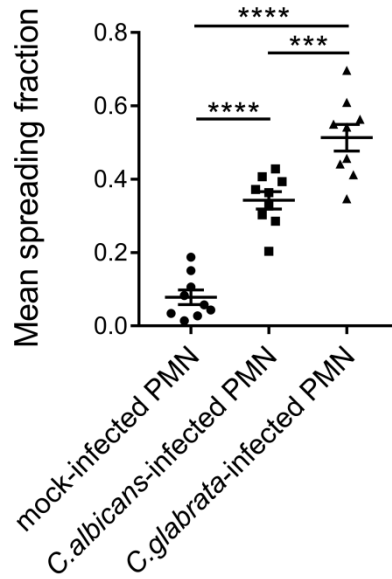
Figure 4. *C. glabrata*-infected PMN present the highest percentage of PMN in a spreading phenotype.
Percent of spreading fraction was calculated using AMIT-v3. Bars show means ± SEM of 9 independent experiments with blood from different donors. *P* values were determined using one-way ANOVA followed up by multiple comparison tests. Significance is shown as ***$P < 0.001$.

Interestingly, difference between PMN with S- and N-morphology was also reflected by differences in PMN size and surface roughness in intensity space (Figure 5). One single *Candida*-infected PMN presented a bigger area (~ 6000 px) (Figure 5C) compared to ~ 3000 px of a single mock-infected PMN (Figure 5A). Another important aspect was the time span a PMN exists in the S-morphology and how often this cell switches between S- and N-morphology over the time-lapse microscopy acquisition. From the PMN behaviour diagrams, it was quite clear that while *Candida*-infected PMN was constantly and stably in the S-morphology (1.0) (Figure 5D), mock-infected PMN was dynamically fluctuated between N-morphology and S-morphology over the time (Figure 5B), showing that N- (0.0) to S-morphology (1.0) switching was a rapid event for mock-infected PMN movement in the surrounding space.
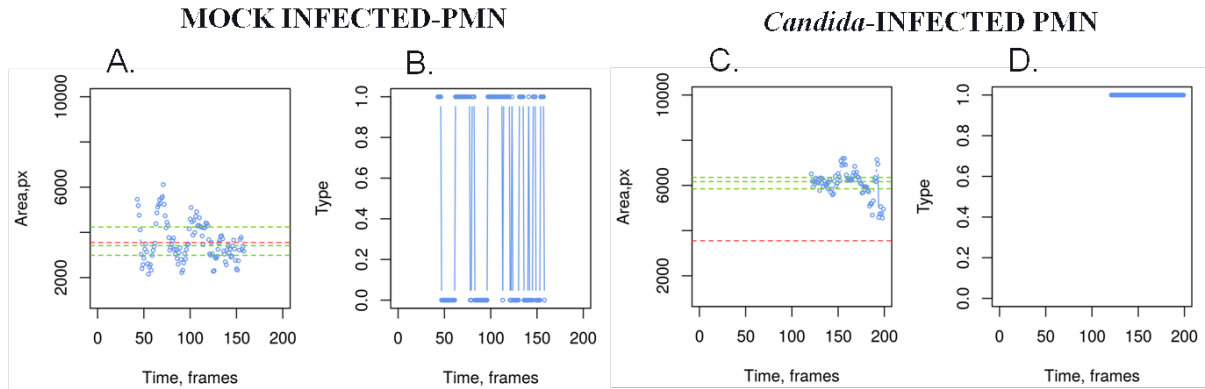
Figure 5. PMN behavior diagrams.

Examples of one mock-infected PMN and one PMN isolated from *Candida*- infected blood are shown that were analyzed for (A, C) area and (B, D) switching from N-morphology (0.0) to S-morphology (1.0).

Taken together, combining live cell imaging and automated analysis allowed a classification and distinction between PMN isolated from mock-infected and *Candida*-infected blood based on PMN morphology.

6.1.2 Analysis of morphokinetics

Compared to mock-infected PMN, PMN isolated from blood infected with *C. albicans* and *C. glabrata* showed a different phenotype. Including tracking and time-evolution of cell descriptors information, it was possible to improve the accuracy of the distinction between *C. albicans* and *C. glabrata* infection.

Combining the N-morphology detector with tracking information allowed the rejection of some PMN from the classifier, which were considered in a S-morphology state. Furthermore, following each PMN for the entire video acquisition permitted the quantification of spreading event duration. Moreover, we used the distribution percentiles of these durations as an additional descriptor. A support vector machine was trained on these descriptors. To keep the training set balanced, a leave-one-out sampling was applied for each analyzed condition. In the end, samples that were left out were used as test set and their classification results were recorded. A visual inspection of samples with high misclassification value revealed their similarity with the data from *C. glabrata* infected samples (Figure 6).

Figure 6. The ratio of correct/erroneous classification based on spreading cell ratio for each video over all iterations for *C. albicans* infected, *C. glabrata* infected blood samples.

The ratio of correct/erroneous morphokinetic-based classification for each video over all iterations for C. albicans infected and C. glabrata infected blood samples.

6.1.3 PMN with spreading morphology are slower compared to PMN with a non-spreading morphology

Cellular migration has an important role among immune cell function and is involved in the mobilization, homing and phagocytosis of PMN [196, 197]. Among other things, reduction of PMN migration was correlated to a severe disease course in sepsis [198, 199] and suggested as potential prognostic biomarker [196].

These observations led to the further analysis of PMN speed as marker to discriminate between *C. albicans* and *C. glabrata* infection. Unfortunately, this approach did not work since comparison between PMN isolated from blood infected by *C. albicans* and PMN isolated from blood infected by *C. glabrata* did not show any significant differences in speed which was also due to the relatively large variation (Figure 7).
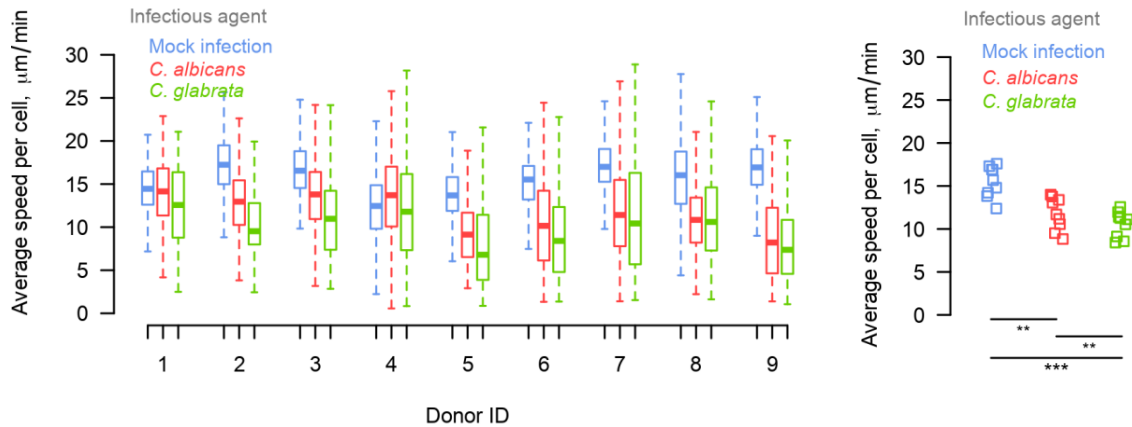
Figure 7. Diagrams of the average speed per cell.

This was quantitatively confirmed by plotting the speed distributions of spreading and non-spreading PMN isolated from blood infected either with *C. albicans* or *C. glabrata* (Figure 8A-B). To estimate and illustrate this difference Δ between cells with S- and N-morphology, we applied the multiple quantile comparison method [200]. As can be seen in Figure 8C, the majority of spreading cells are slower.

we showed the difference between distributions (Fig. 8C) in absolute units (μm/min), where we performed statistical tests and the effect size estimation from a distribution that pools all donor data. AFTER having done the classification into spreading / non-spreading, we could then see the difference in the speed and it is significant and has a high effect size. However, this was not at the per donor level. At the per donor level, a distinction would not work because of donor variability.

For example, the most left red dot (0.1, 1.1) shows that for all *C. albicans* infected samples (we combined data from all samples together) slowest 10% of PMNs with N-morphology are faster than slowest 10% of PMNs with S-morphology for 1.1 μm/min. However, this is the point wise estimation. Therefore, in the test procedure the 95% confidence interval was calculated. Since the confidence intervals (corresponding to the error bars in Fig. 8C) did not include zero value (i.e., do not cross the line Δ=0), the associated difference was considered as being significant. Using this line of reasoning for all other points, we drew the conclusion that the majority of PMNs with S-morphology (at least 90%) were slower than majority of PMNs with N-morphology in both fungal infection.
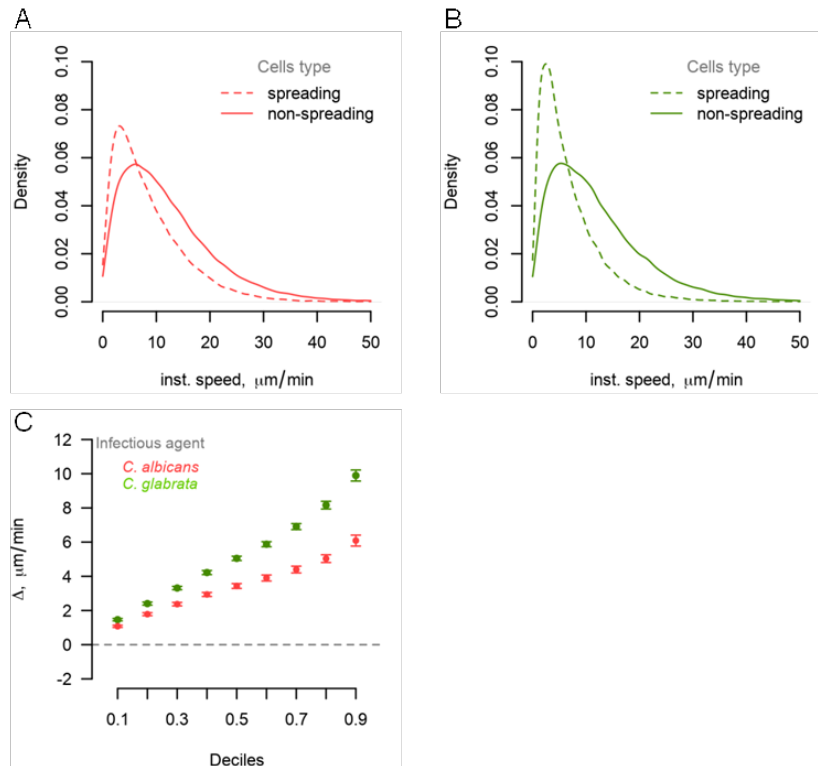
Figure 8. Aggregated distributions for spreading and non-spreading PMN after confrontation with *C. albicans* (A) and *C. glabrata* (B) and corresponding shift functions (C).

6.1.4 *C. albicans* induced a stronger PMN activation compared *C. glabrata* during whole blood infection

Live cell imaging and time-lapse microscopy video were performed using PMN isolated from whole blood infected either by *C. albicans* or *C. glabrata*. To further investigate PMN activation after one hour of fungal infections, the whole-blood infection model was used [62].

Unfortunately using flow cytometry, it was not possible to differentiate between PMN in a N-morphology and S-morphology but PMN activation was investigated.

In agreement with the results obtained after 8 hours post infection (Figure 9) and with published data [58], confrontation with both *C. albicans* and *C. glabrata* led to differential expression of the degranulation marker CD66b and CD16 after one hour of infection. Furthermore, *C. albicans* resulted in a significantly stronger PMN activation then *C. glabrata*. Compared to PMN in mock-infected blood, decrease in CD16 surface levels as well as up-regulation of degranulation marker CD66b on PMN were significantly more pronounced in presence of *C. albicans* compared to *C. glabrata* (Figure 9).
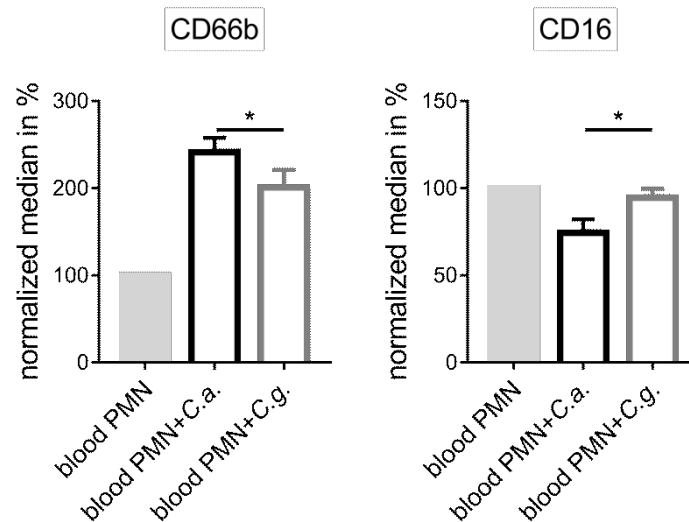
Figure 9. *C. albicans* induces higher activation of blood PMN compared to *C. glabrata*.

Human blood was either mock-infected or confronted with *C. albicans* and *C. glabrata* and analyzed for surface expression of PMN activation markers. Changes of CD66b and CD16 are shown after normalization to basal levels of mock-infected PMN (set to 100%). Compared to mock-infected PMN (light grey filled bars), surface CD66b and CD16 were significantly more increased/decreased during *C. albicans* (black open bars) than *C. glabrata* (grey open bars) infection.

Quantitative analysis was performed for each surface marker using one-way ANOVA followed up by multiple comparison tests. Data shown are means ± SEM and normalized to basal levels on PMN within mock-infected blood (set to 100%, light grey filled bars), *$P < 0.05$.

6.1.5 Blocking of C5a shifts PMN from S- to N-morphology

Different percent of PMN in a spreading phenotype (S-morphology) were found after Candida infections compared to mock-infected PMN where were present mostly PMN in a non spreading state (N-morphology). Further, in response to *C. glabrata* higher percent of spreading PMN were observed compare to *C. albicans*. To identify which could be the factor involved in the different levels of spreading PMN after *C. albicans* and *C. glabrata*, secretion of cytokines particularly involved in PMN activation (TNF-α and IL-1β) and recruitment (IL-8) was checked and found only slightly increased plasma levels (IL-8, TNF-α, IL-1β) upon fungal confrontation compared to mock-infected blood, without any differences between the two *Candida* species after 1 hour post-infection (Figure 10A). Considering that IL-8, TNF-α, IL-1β were usually highly secreted after 8 hours of incubation either with *C. albicans* or *C. glabrata* (data not show).
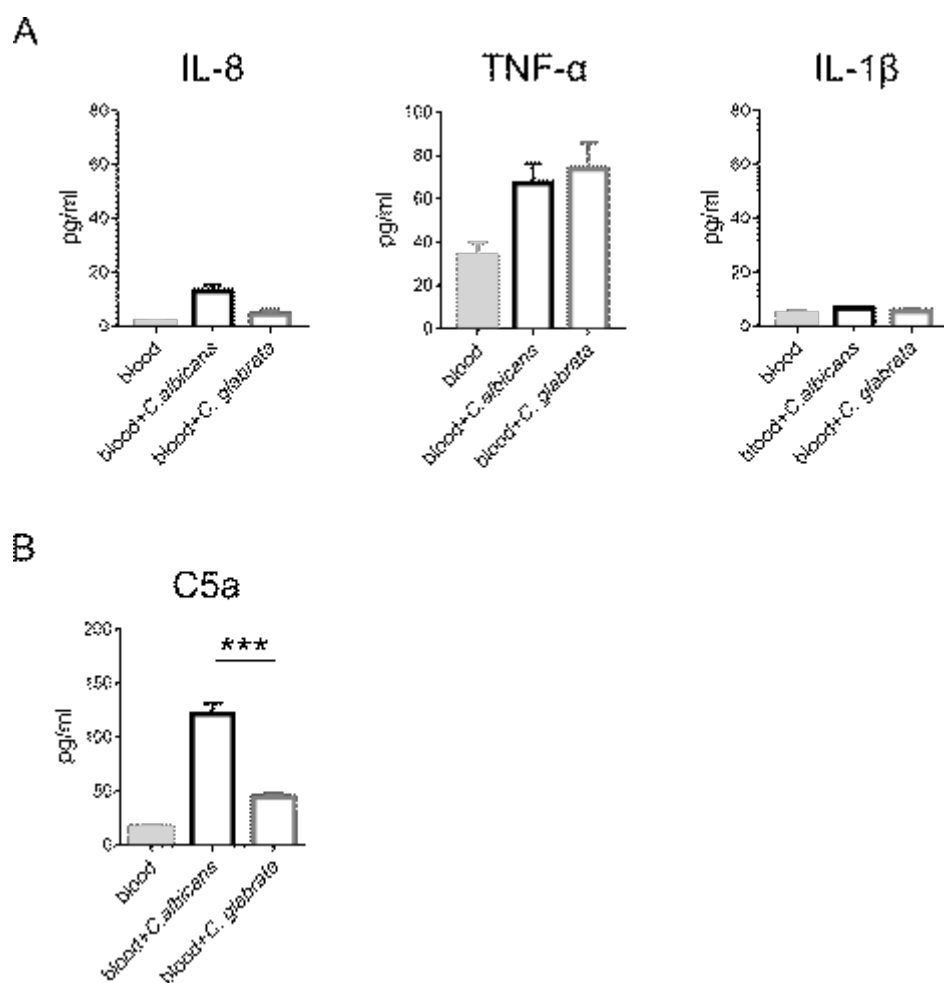
Figure 10. *C. albicans* induces higher C5a secretion than *C. glabrata* infection.

Secretion of (A) IL-8, TNF-α, IL-β, and (B) C5a was measured in plasma samples after 1 hours confrontation of human whole-blood with either HBSS (mock-infected, light grey filled bars), *C. albicans* (black open bars) or *C. glabrata* (grey open bars). Bars show means ± SEM of eight independent experiments with blood from different donors. *P* values were determined using one-way ANOVA followed up by multiple comparison tests, *$P < 0.05$, **$P < 0.01$, ***$P < 0.001$.

Another factor taken into consideration potentially involved in the difference between in the different level of spreading PMN after *C. albicans* and *C. glabrata* infection was the complement product anaphylatoxin C5a. Complement system activation and the subsequently production of anaphylatoxin C5a are important players in the immune response against *Candida* [201]. C5a is a strong chemoattractant and increases effectors functions of PMN [202-204]. A previous study showed the involvement of C5a during *C. albicans*-triggered PMN effector mechanisms, including oxidative burst, phagocytosis, and degranulation especially in the early stage of the *Candida* infection [205]. Furthermore, it has also been shown that C5a is involved in increasing deformability of PMN cell shape which induces morphological changes [206]. Due to these reasons, release of C5a was quantified in plasma collected from infected human blood.

As already published, generation of C5a is rapidly induced by *C. albicans* with high levels already detectable at 10 min after inoculation [205].

It was shown that C5a is a as potential inducer of spreading phenotype and it is particularly important in the immune response against *Candida* [201]. In particular, C5a is a strong chemoattractant and increases effectors functions for PMNs [202-204]. In a previous study we have shown the involvement of C5a production specifically in *C. albicans*-induced PMN effectors mechanisms including oxidative burst, phagocytosis, and degranulation already in the early stage of the *Candida* infection [205]. Furthermore, it has also been shown that C5a is involved in increasing deformability of PMN cell shape and morphological changes [206].

Therefore, we quantified release of C5a from plasma collected from infected human blood 1 hour post-infection. Compared to mock-infected blood (17 ± 2 pg/ml), secretion of C5a was significantly higher during *C. albicans* (122 ± 10 pg/ml, n=8) than *C. glabrata* infection (45 ± 3 pg/ml, n=8) at 1 hour post-infection (Figure 10C).

To confirm the contribution of C5a to *C. albicans*- induced PMN spreading morphology, live cell imaging of PMNs isolated from human blood infected by fungal cells was performed in presence of human anti-C5a Ab (IFX-1) which blocks C5a directly and thereby neutralizes its biologic effects. Then, time-lapse microscopy videos were analyzed using AMITv3 algorithm.

Compared to PMNs isolated from *C. albicans*-infected blood, PMNs isolated from *C. albicans*-infected blood in presence of αC5a showed significantly less in the spreading phenotype and more PMNs with a N-morphology (Figure 11). Blocking of C5a induced an evident decrease of PMNs with a spreading morphology after *C. albicans* infection.
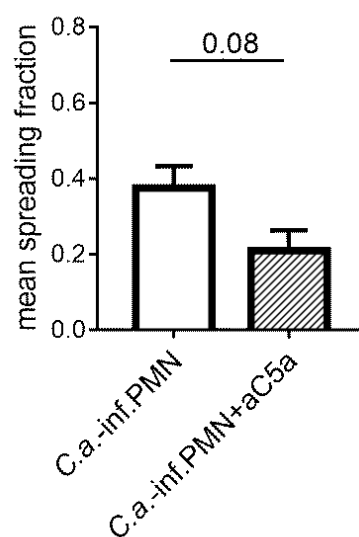
Figure 11. C5a blocking induces PMN switching from S- to N-morphology after *C. albicans* infection.

PMN isolated from blood infected by *C. albicans* (black open bars) was compared with PMN isolated from *C. albicans*-infected blood treated with an anti-C5a (black striped bars) and analyzed using AMITv3 algorithm to quantify and calculate the spreading cell fraction. Bars show means ± SEM of four independent experiments with cells isolated from blood of different donors. *P* values were determined using one-way ANOVA followed up by multiple comparison tests.

These results suggested that C5a was an important factor involved in inducing the spreading phenotype in response to *C. albicans* infection and not after *C. glabrata* infection coherent with its high and low, respectively, secretion in a whole-blood after *C. albicans* and *C. glabrata* confrontation.

Taken together, high levels of C5a during *C. albicans* infection in whole blood correspond to lower percent of PMN in a spreading state, whereas for *C. glabrata* infection lower levels of C5a correspond to a higher percentage of PMN in spreading morphology suggesting that C5a was not involved in response to *C. glabrata* infection.

Other potentials components involved in the spreading phenotype appearance could be P-selectin, involved in PMN adhesion and signaling pathways [207], and Platelet-derived growth factor (PDGF), involved in PMN chemotactic processes [208]. These two secreted factors were differentially secreted during one hour of incubation with *C. albicans* and *C. glabrata*. *C. albicans* induced a significant higher release of P-selection (182 ± 16 pg/ml, *P*< 0.05) and PDGF (340± 60pg/ml, , *P*< 0.05) compared to *C. glabrata* (blood +*C.g.*: 135 ± 7pg/ml; PDGF: blood +*C.g.*: 150±10 pg/ml, *P*< 0.01) (Figure 12).
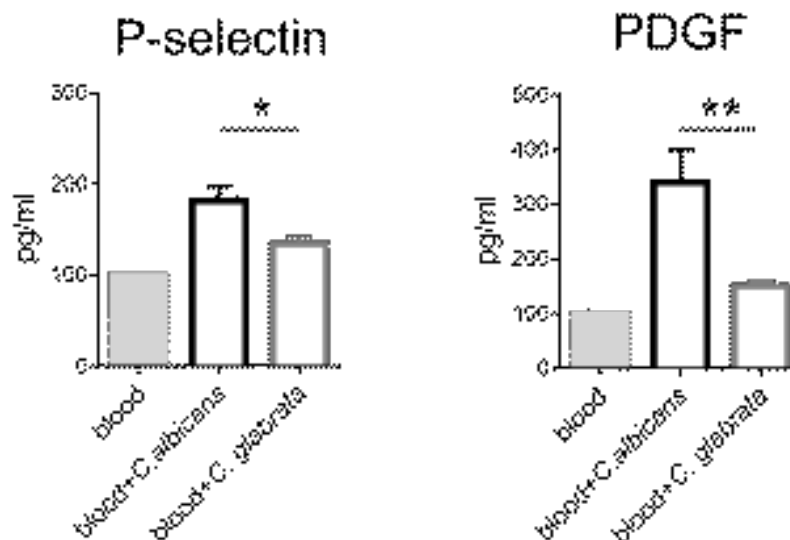
Figure 12. *C. albicans* induces higher P-selectin and PDGF secretion than *C. glabrata* infection.

Secretion of P-selectin and PDGF was measured in plasma samples after 1 hours confrontation of human whole-blood with either HBSS (mock-infected, light grey filled bars), *C. albicans* (black open bars) or *C. glabrata* (grey

open bars). Bars show means ± SEM of eight independent experiments with blood from different donors. *P* values were determined using one-way ANOVA followed up by multiple comparison tests, *P< 0.05, **P< 0.01.

6.1.6 PMN-S-morphology is also present after bacterial infection

Switching from N- to S-morphology was visible in PMN isolated from human blood infected either with *C. albicans* or *C. glabrata*, with a significantly increase after *C. glabrata* infection, compared to mock-infected PMN which were mostly presented in a N-morphology. These evidences allowed a classification of infected- or mock-infected PMN using automated image analysis through the AMIT-v3 algorithm development.

To further investigate S-morphology appearance also after bacterial infection, one representative experiment was performed infecting whole blood either with *Neisseria meningitidis*, *Streptococcus pneumonia* or *Staphylococcus aureus*. Compared to mock-infected PMN (~6%), PMN isolated from human blood infected by different bacterial species showed an higher percent of PMN in a S-morphology: ~47%, ~40% and ~30% after *N. meningitidis*, S. *aureus* and *S. pneumonia, respectively* (Figure 13).
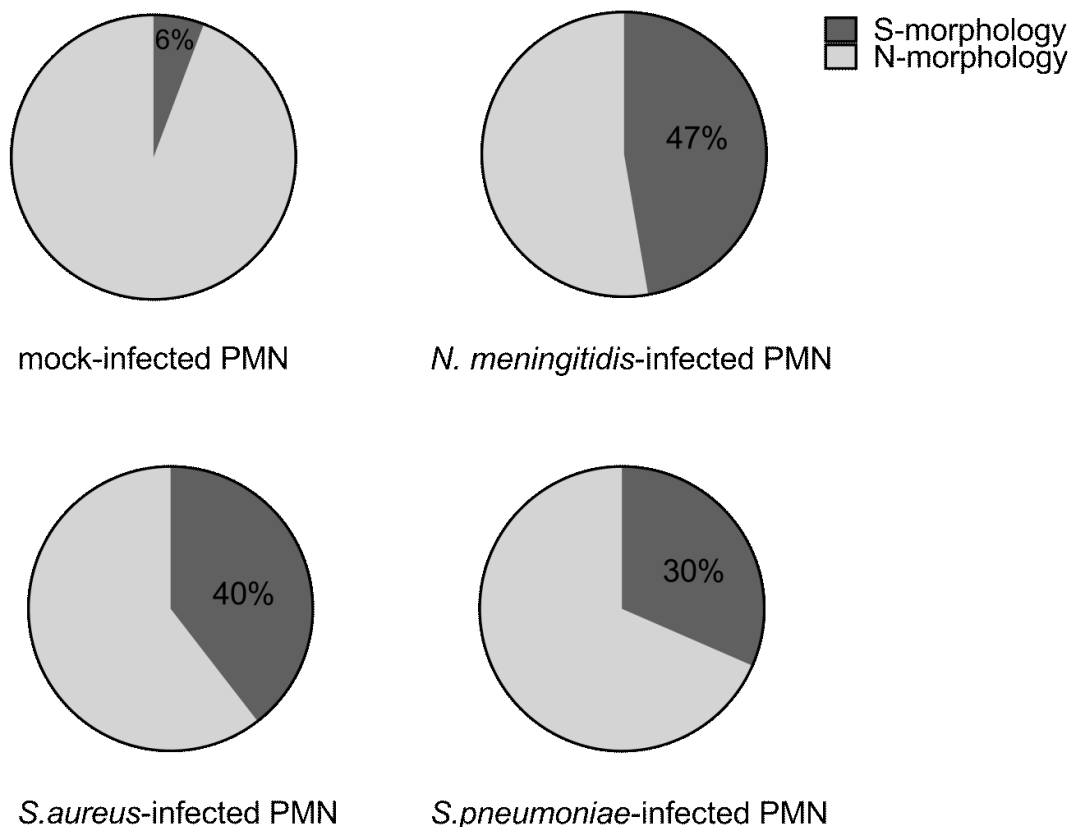
Figure 13. PMN isolated from blood infected by *N. menigitidis*, *S. aureus* and *S. pneumonia*.
The percentage of PMN in S-morphology (dark grey) is represented in a pie chart and compared to PMN in a N-morphology (light grey).

Altogether, switching from N- to S-morphology was a characteristic present not only after fungal infection but also after bacterial infection; although further experiments have to be performed.

6.2 NK cell stimulation in response to *C. albicans* and *C. glabrata* infection

6.2.1 *C. albicans* induces higher activation of primary NK cells compared to *C. glabrata*

NK cells can use different mechanisms to eliminate their potential target: (i) by the release of cytotoxic molecules from their granules (perforin, granzyme), (ii) death receptor-mediated apoptosis mediated by expression of FasL and TRAIL or (iii) antibody-dependent cellular cytotoxicity via Fcγ-receptor III (FcγRIII, CD16) [107]. To analyze the mechanisms being activated by NK cells upon *C. albicans* or *C. glabrata* infection, we used flow cytometry to investigate changes in surface exposure of the respective NK cell markers during direct confrontation of fungi with primary NK cells and during *ex vivo* whole-blood infection.

Previous experiments using cytokine-activated primary human NK cells have shown that *C. albicans* predominantly induces a marked down-regulation of CD16 and increase in CD107a surface exposure, which was in line with an active release of cytotoxic granule content [184]. These data could be confirmed and analyzed in more detail in a novel set of experiments including a comparative analysis using *C. glabrata*.

Cytokine-activated primary human NK cells were obtained after isolation and expansion of primary NK cells by cytokine treatment. Confrontation with both *C. albicans* and *C. glabrata* led to differential expression of CD16 and degranulation marker CD107a. In direct comparison we observed a 1.7-fold lower downregulation for CD16 and 1.5-fold higher CD107a expression for *C. albicans* (CD16: 59 ± 6%; CD107a: 242 ± 32%) compared to *C. glabrata* (CD16: 81 ± 3%, $P<0.01$; CD107a: 160 ± 15%, $P<0.05$) after 2 hours of confrontation (Figure 14).
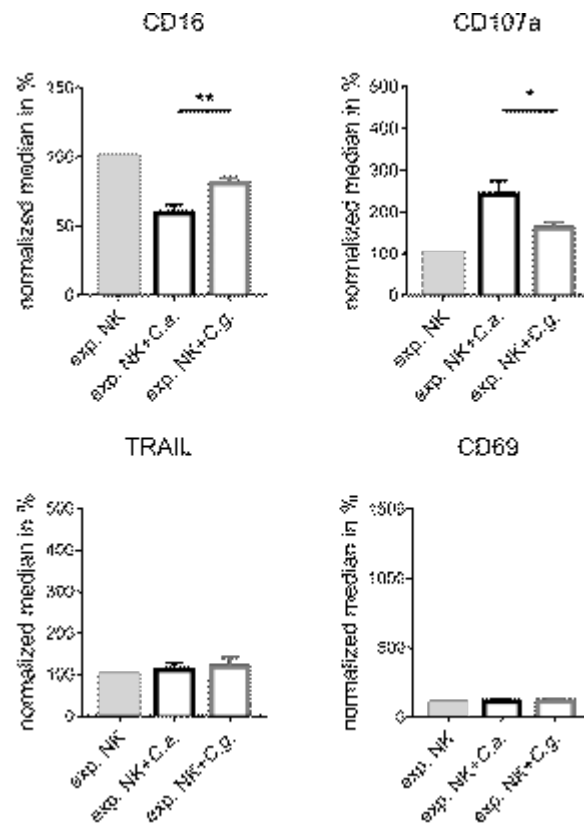
Figure 14. *C. albicans* induces a higher activation of primary expanded NK cells compared to *C. glabrata*.

Changes of CD69, TRAIL, CD16, and CD107a are shown after normalization to basal levels of mock-infected NK cell (set to 100%). Compared to mock-infected expanded NK cells (light grey filled bars), surface CD16 and CD107a were significantly more increased after *C. albicans* (black open bars) than *C. glabrata* (grey open bars) infection for 2 hours on expanded NK cells.

Quantitative analysis was performed for each surface marker using one-way ANOVA followed up by multiple comparison tests. Data shown are means ± SEM and normalized to basal levels of mock-infected NK cells (set to 100%, light grey filled bars), *$P< 0.05$, **$P< 0.01$.

Differences were even more marked after 4 hours post infection: 2.5-fold lower downregulation for CD16 and 2.7-fold higher CD107a expression for *C. albicans* (CD16: 18 ± 4%; CD107a: 847 ± 263%), indicating a weaker NK cell activation potential for *C. glabrata* (CD16: 44 ± 7%, $P<0.001$; CD107a: 317 ± 48%, $P<0.05$) (Figure 14). No regulation of CD69 and death-inducing ligands TRAIL (Figure 14) was detected.

These data suggested that primary expanded NK cells were directly stimulated by fungal cells and this stimulation was stronger during *C. albicans* than *C. glabrata* infection.

6.2.2 *C. glabrata* induces higher activation of blood NK cells compared to *C. albicans*

Experiments with isolated cells do not necessarily reflect *in vivo* conditions due to missing interactions with other components of the host response [205]. Furthermore, primary expanded NK

cells are cytokine-activated and differ from naïve NK cells in peripheral blood. To further analyze NK cell activation in a more complex system of immune cells and humoral factors, a human whole-blood model of infection was used [62]. Interestingly, surface levels of CD16 and CD107a did not change after confrontation of whole-blood with either *C. albicans* or *C. glabrata* (Figure 15B). Both species induced a markedly increased surface exposure of death-inducing ligand TRAIL and early activation antigen CD69 (Figure 15B), while the latter was only slightly regulated on expanded NK cells (Figure 15A). No changes in surface expression of FasL during NK cell activation could be detected for any tested condition (data not shown). Furthermore, in sharp contrast to data obtained for primary NK cells, confrontation with *C. glabrata* induced a significantly stronger activation of blood NK cells (CD69: 1121 ± 128%, *P*<0.01; TRAIL: 389 ± 40%, *P*<0.01) than *C. albicans* (CD69: 583 ± 99%; TRAIL: 253 ± 28%).

Figure 15. Milieu and *Candida* species influence NK cell stimulation.

(A) Primary expanded NK cells (MOI = 0.5, 4 h) or (B) human whole-blood (1×10^6 fungal cells/ml, 8 h) were either mock-infected or confronted with *C. albicans* and *C. glabrata*. Changes in the surface expression levels of NK cell activation markers CD16, CD107a, CD69 and TRAIL are shown in representative histograms after confrontation with *C. albicans* (black line) and *C. glabrata* (grey line). Light grey filled histograms indicate basal expression of NK cells from mock-infected samples. Data from one of at least 9 independent experiments using cells from

different donors with virtually identical results are shown. Graphs show means ± SEM of CD69, TRAIL, CD16, and CD107a expression levels during *C. albicans* (black open bars) and *C. glabrata* (grey open bars) infection after normalization to basal levels of mock-infected NK cell (set to 100%, light grey filled bars). *$P<0.05$, **$P<0.01$, ***$P<0.001$.

6.2.3 Release of IFN-γ depending on the milieu

Altogether, our results identified differences in the stimulation of NK cells dependent on the milieu and *Candida* species between *ex vivo* whole-blood infection with those of expanded primary cells. This is further supported by analysis of IFN-γ release after fungal infection. IFN-γ secretion was measured within supernatants collected following infection of primary expanded NK cells for 4 hours and plasma collected after 8 hours of whole-blood infection with either HBSS (mock-infected), *C. albicans* or *C. glabrata*. The pro-inflammatory cytokine is mainly released by NK cells and stronger induced by *C. albicans* during primary NK cell confrontation (exp.NK+*C.a.*: 489 ± 103 pg/ml; exp.NK+*C.g.*: 224 ± 63 pg/ml, $P<0.05$) compared to the higher levels detected after blood infection with *C. glabrata* (blood+*C.a.*:133 ± 27 pg/ml; blood+*C.g.*: 470 ± 82 pg/ml, $P<0.001$) (Figure 16).
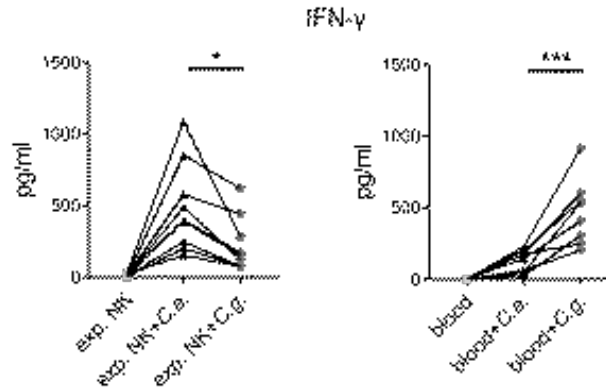
Figure 16. Secretion of IFN-γ by expanded and blood NK cells in response to *C. albicans* and *C. glabrata* infectios. IFN-γ secretion was measured within supernatants of primary expanded NKC from 9 independent experiments (left graph) and plasma of whole-blood infection from 8 independent experiments (right graph) with either HBSS (mock-infected, light grey squares), *C. albicans* (black triangles) or *C. glabrata* (grey circles). Quantitative analysis was performed using paired one-way ANOVA followed up by multiple comparison tests. Lines connect data points from identical donors. Significance is shown as *$P< 0.05$, ***$P< 0.001$.

6.2.4   Different levels of cytokines are induced by *C. albicans* and *C. glabrata* during *ex vivo* whole-blood infection

We already demonstrated that activation of primary human NK cells by *C. albicans* depends on direct contact, whereas the fungus exclusively interacts with PMN and monocytes during *ex vivo* performed whole-blood infection assays, suggesting an indirect induction of NK cell effector mechanisms by soluble blood components released during infection [62, 184]. To further investigate, which stimuli could be involved in the activation of blood NK cells, the release of cytokines/chemokines into plasma generated from whole-blood infection experiments in response to *C. albicans* and *C. glabrata* was quantified. Interestingly, monocytic cytokines, such as IL-1β, IL-6, TNF-α and IL-12 were significantly more released during 4 hours of incubation with *C. glabrata* (Figure 17A), which is in line with our previous published data showing a greater association of *C. glabrata* to monocytes in the whole-blood assay [58]. Whereas differences in the IL-6 and TNF-α secretion profile disappeared after 8 hours, differences in plasma levels of IL-1β (blood+*C.a.*: 436 ± 98 pg/ml; blood+*C.g.*: 1413 ± 268 pg/ml, $P<0.001$) and IL-12 (blood+*C.a.*: 92 ± 35 pg/ml; blood+*C.g.*: 596 ± 161 pg/ml, $P<0.01$) induced by the two *Candida* species were still clearly present (Figure 17B).
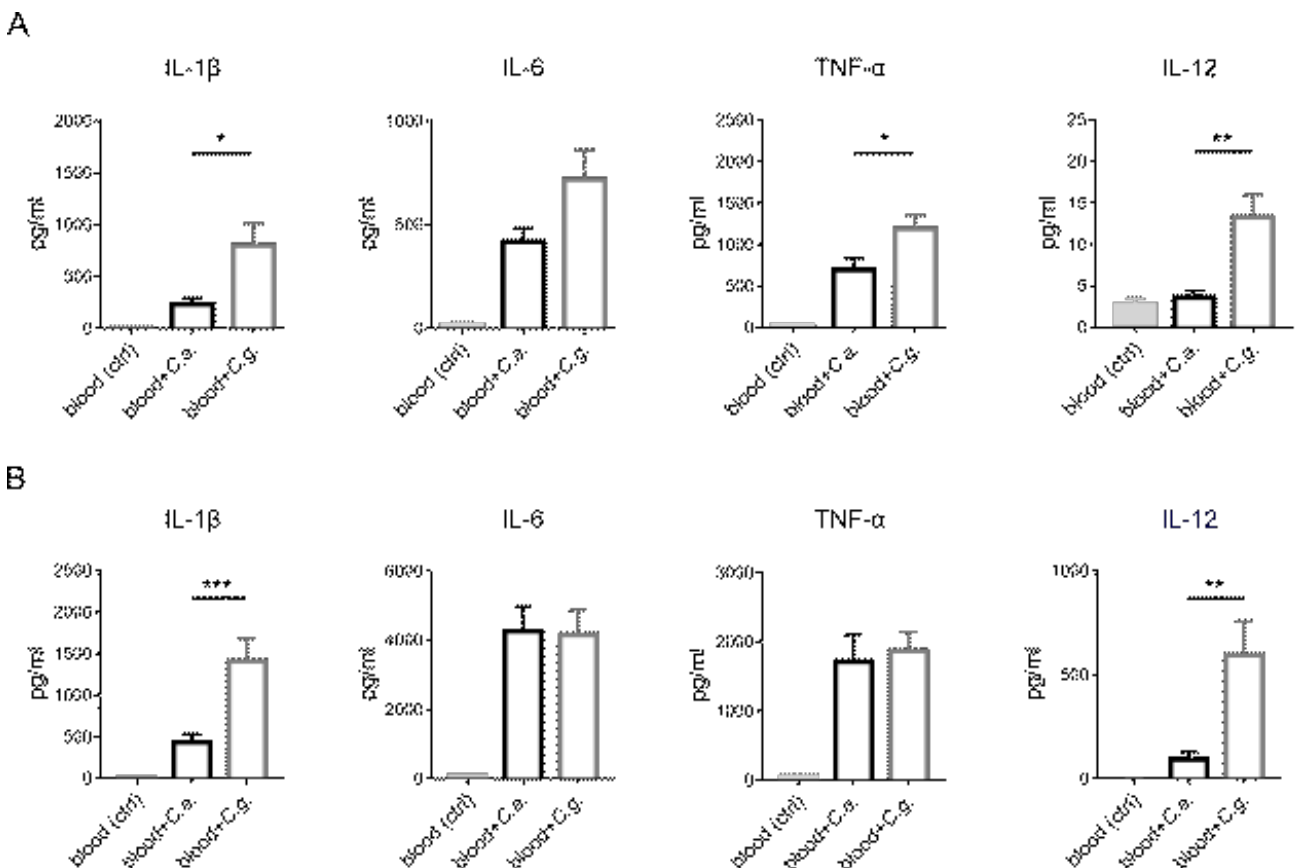
Figure 17. Cytokine secretion during whole-blood infection with *C. albicans* and *C. glabrata*.

Secretion of cytokines was measured in plasma samples after 4 hours (A) and 8 hours (B) confrontation of human whole-blood with either HBSS (mock-infected, light grey filled bars), *C. albicans* (black open bars) or *C. glabrata* (grey open bars) and revealed significantly different levels between both *Candida* species. Bars show means ± SEM of at least four independent experiments with blood from different donors. *P* values were determined using one-way ANOVA followed up by multiple comparison tests, *$P< 0.05$, **$P< 0.01$, ***$P< 0.001$.

Other studies already demonstrated a role for IL-12 in stimulation of IFN-γ production by NK cells, thus making IL-12 an obvious candidate for a putative blood-specific stimulus regulating NK cell function [209]. In addition, we checked the secretion of other cytokines particularly involved in NK cell priming and activation and found no (IL-15, IL-23, IL-27) or only slightly increased plasma levels (IL-2, IL-18) compared to mock-infected blood upon fungal confrontation, without any differences between the two *Candida* species (Figure 18).
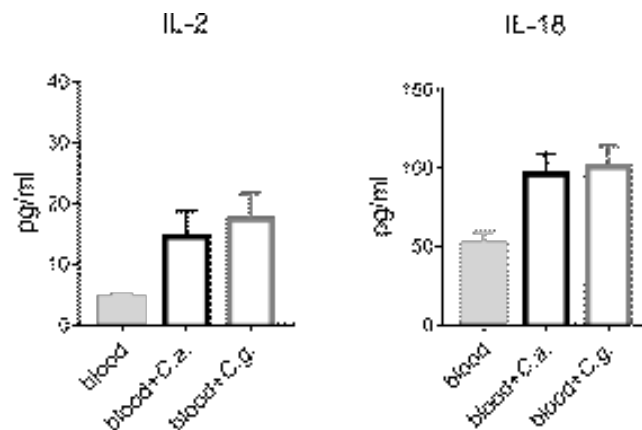
Figure 18. IL-2 and IL-18 secretion in whole blood upon *Candida* infection.
Secretion of IL-2 and IL-18 was measured in plasma samples after 8 hours confrontation of human whole-blood with either HBSS (mock-infected, light grey filled bars), *C. albicans* (black open bars) or *C. glabrata* (grey open bars). Both cytokines were only slightly produced upon fungal confrontation without any differences between the two *Candida* species. Bars show means ± SEM of at least eight independent experiments with blood from different donors.

6.2.5 Blood NK cell stimulation is not dependent on fungal morphology

A key virulence factor of *C. albicans* is its ability to switch between yeast and filamentous forms and thereby adapt to different environmental conditions inside the human host, while *C. glabrata* lacks this property. Interestingly, *C. albicans* morphological plasticity has been linked to its pathogenicity as filamentous forms are associated with tissue invasion and infection. It was already shown that some immune cells, as human PMN, can discriminate between yeasts and filaments of *C. albicans* [59]. Performing whole-blood infection assay using the non-filamentous mutant *C.*

albicans cph1Δ/efg1Δ helped to investigate more deeply *C. albicans* filamentation impact on cytokine secretion and NK cell activation. Secretion of cytokines was quantified from plasma samples collected from whole blood infected either with *C. albicans*, *C. albicans cph1Δ/efeg1Δ* or *C. glabrata* after 8 hours post infection. Infecting whole blood with the non-filamentous *C. albicans cph1Δ/efg1Δ* mutant resulted in the same cytokine release pattern, especially with respect to the lower IL-12 secretion in response to wild type and non-filamentous *C. albicans* compared to *C. glabrata* infection (Figure 19). As observed in previous experiments, no differences in IL-6 and TNF-α plasma concentration could be observed 8 hours post infection. In contrast, IL-1β (blood+*C.a.*: 901 ± 203 pg/ml; blood+*C.a. cph1Δ/efg1Δ*: 468 ± 286 pg/ml; blood+*C.g.*: 1285 ± 188 pg/ml) and IL-12 (blood+*C.a.*: 90 ± 36 pg/ml; blood+*C.a. cph1Δ/efg1Δ*: 56 ± 35 pg/ml; blood+*C.g.*: 225 ± 46 pg/ml) levels induced by *C. albicans cph1Δ/efg1Δ* were in the range of *C. albicans* wild type infection and clearly lower than secreted in response to *C. glabrata* (Figure 19).
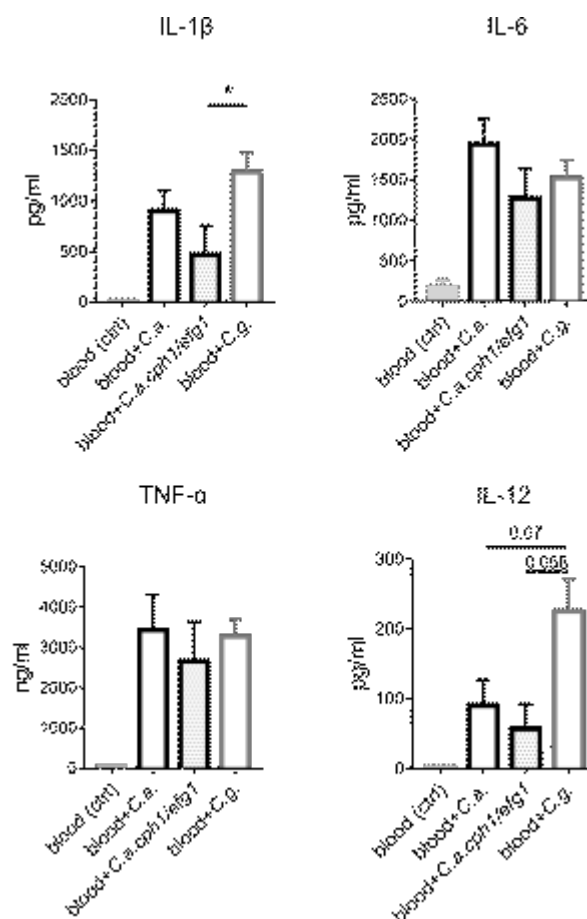
Figure 19. Cytokine secretion during whole-blood infection with the non-filamentous mutant of *C. albicans cph1Δ/efg1Δ* and *C. glabrata*.

Levels of cytokines in plasma samples after 8 hours confrontation of human whole blood with either HBSS (mock-infected, light grey filled bars), *C. albicans* wild type (black open bars), non-filamentous *C. albicans* mutant *cph1Δ/efg1Δ* (black dotted bars) or *C. glabrata* (grey open bars). Bars show means ± SEM of at least four

independent experiments with blood from different donors. *P* values were determined using one-way ANOVA followed up by multiple comparison tests, *P< 0.05.

Additionally, NK cell activation was investigated after whole-blood infection with non-filamentous *C. albicans cph1Δ/efg1Δ*, *C. albicans* wild type and *C. glabrata*, respectively, by analyzing their surface phenotype (Figure 20A) as well as IFN-γ secretion (Figure 20B). No differences in blood NK cell activation between infection with *C. albicans* wild type and *cph1Δ/efg1Δ* mutant could be observed, while differences in NK cell stimulation induced by *C. albicans* and *C. glabrata* were still present. Indeed, CD69 (blood+*C.a.*: 577 ± 137%; blood+*C.a. cph1Δ/efg1Δ*: 451 ± 111%; blood+*C.g.*: 1599 ± 192%) and TRAIL (blood+*C.a.*: 154 ± 28%; blood+*C.a. cph1Δ/efg1Δ*: 160 ± 24%; blood+*C.g.*: 259 ± 19%) were significantly more increased during *C. glabrata* infection compared to *C. albicans* wild type and non-filamentous *C. albicans cph1/efg1* infection on blood NK cells. Despite the high donor-dependent variance, the lower secretion of IFN-γ secretion induced by *C. albicans* was also observed infecting the whole-blood with the non-filamentous form of *C. albicans* and still partially higher during C. *glabrata* infection (blood+*C.a.*: 70 ± 36 pg/ml; blood+*C.a. cph1Δ/efg1Δ*: 51 ± 20 pg/ml; blood+*C.g.*: 177 ± 94 pg/ml). Both *C. albicans* wild type and non-filamentous *cph1Δ/efg1Δ* mutant showed comparable NK cell stimulation, indicating that filamentation is not responsible for a *C. albicans* specific NK cell activation pattern (Figure 20). These results suggested that activation of NK cells in whole blood is not dependent on *Candida* morphology and filamentation is of minor importance for the species-specific differences.
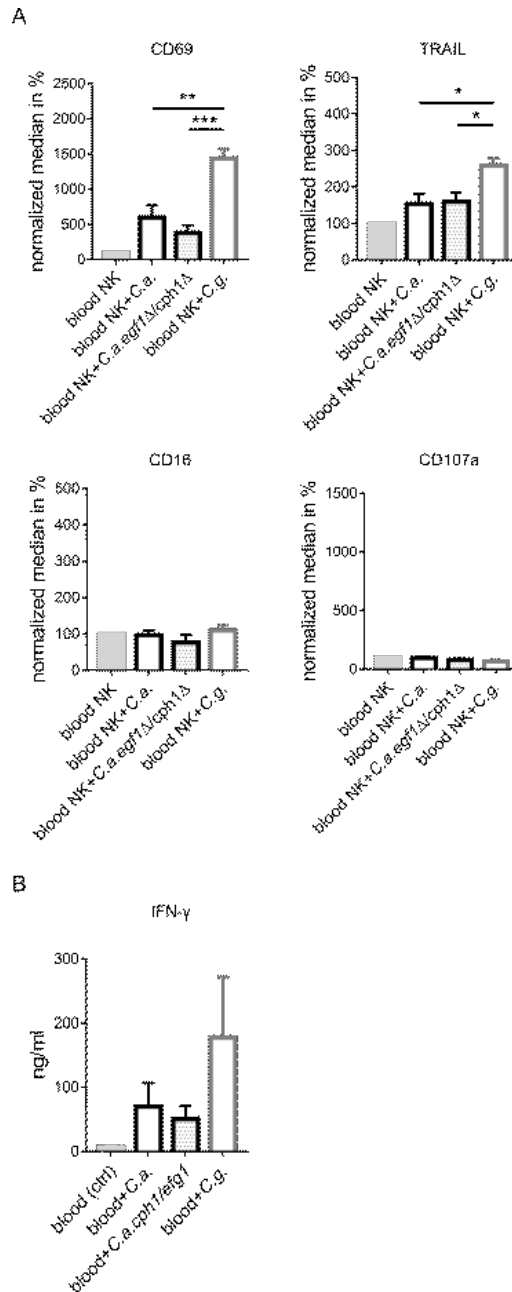
Figure 20. Blood NK cell stimulation is not dependent on fungal morphology.

Non-filamentous *C. albicans cph1Δ/efg1Δ*, *C. albicans* wild type or *C. glabrata* were added to whole blood of healthy donors and NK cell surface phenotype (A) as well as IFN-γ secretion (B) were analyzed following 8 hours of confrontation. Compared to mock-infected blood (light grey filled bars), surface CD69 and TRAIL were significantly more increased during *C. glabrata* infection (grey open bars), while no differences between *C. albicans* wild type (black open bars) and non-filamentous *C. albicans cph1Δ/efg1Δ* (black dotted bars) infection were observed on blood NKC. (B) IFN-γ secretion within plasma samples after 8 hours confrontation of human whole blood with either HBSS (mock-infected, light grey filled bars), *C. albicans* wild type (black open bars), non-filamentous *C. albicans* mutant *cph1Δ/efg1Δ* (black dotted bars) or *C. glabrata* (grey open bars). Bars show means ± SEM of at least four independent experiments with whole blood from different donors. *P* values were determined using one-way ANOVA followed up by multiple comparison tests, **P< 0.05, **P< 0.01, ***P< 0.001*.

6.2.6 Inactivated *Candida* cells induce comparable NK cell response as viable fungi during whole-blood infection

Another *C. albicans* virulence attribute is the secretion of Sap which are able to degrade tissue barriers and facilitate *Candida* invasion [210, 211]. One suggested role for SAPs is modulation of the cytokine milieu due their ability to cleave a broad range of proteins [210]. To analyze a possible correlation between Sap secretion and its potential ability to induce or inhibit pro-inflammatory cytokines secretion, whole-blood infection assay was performed using inactivated fungal cells. *C. albicans* germ tubes and *C. glabrata* were inactivated by thimerosal treatment after which they were not able to release proteases any more. Whereas cytokine secretion was generally lower for inactivated compared with viable fungal cells (Figure 17), cytokine levels of IL-1β and IL-12 showed the same differences using either alive or thimerosal inactivated fungal cells. *C. glabrata* (100 ± 26 pg/ml, $P<0.05$) still induced a significantly higher IL-12 secretion than *C. albicans* (24 ± 7 pg/ml) (Figure 21). Thus, the impact of SAP protease activity during *C. albicans* infection was not responsible for the species-specific difference in IL-12 levels.
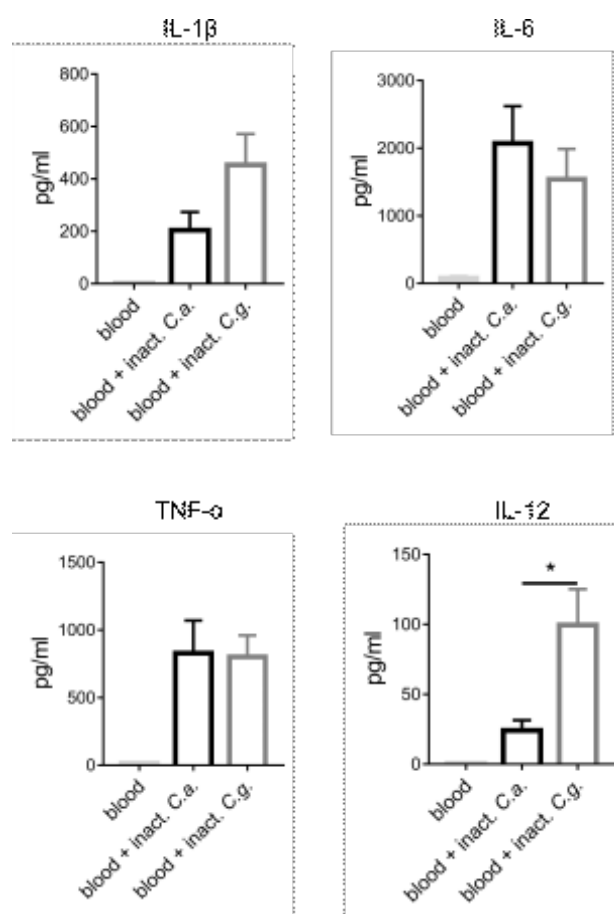
Figure 21. Cytokine secretion during whole-blood infection with inactivated *Candida* cells.
Secretion of cytokines was measured in plasma samples after 8 hours confrontation of human whole-blood with either HBSS (mock-infected, light grey filled bars), thimerosal-inactivated *C. albicans* (black open bars) or

thimerosal-inactivated *C. glabrata* (grey open bars). Bars show means ± SEM of at least four independent experiments with blood from different donors. *P* values were determined using one-way ANOVA followed up by multiple comparison tests, *P< 0.05.

Interestingly, whole-blood infection with inactivated fungal cells revealed the same differences in NK cell activation as induced by alive *C. albicans* and *C. glabrata* (Figure 22). Indeed, *C. glabrata* induced a markedly stronger exposure of NK cell activation markers like CD69 (blood+*C.a.*: 315 ± 43%; blood+*C.g.*: 727 ± 127%, *P*<0.01) and TRAIL (blood+*C.a.*: 167 ± 17%; blood+*C.g.*: 248 ± 11%, *P*<0.01), while only a slight regulation of CD107a and CD16 was presented (Figure 22A). In agreement with data generated for alive fungal cells, IFN-γ secretion was more increased after *C. glabrata* (275 ± 90 pg/ml) than *C. albicans* (69 ± 19 pg/ml) infection using thimerosal-inactivated fungal cells (Figure 22B).

Taken together, alive and thimerosal killed *Candida* species showed comparable NK cell stimulation phenotypes, indicating that Sap secretion or the secretion of other fungal factors are not responsible for *C. albicans* and *C. glabrata* specific NK activation patterns.
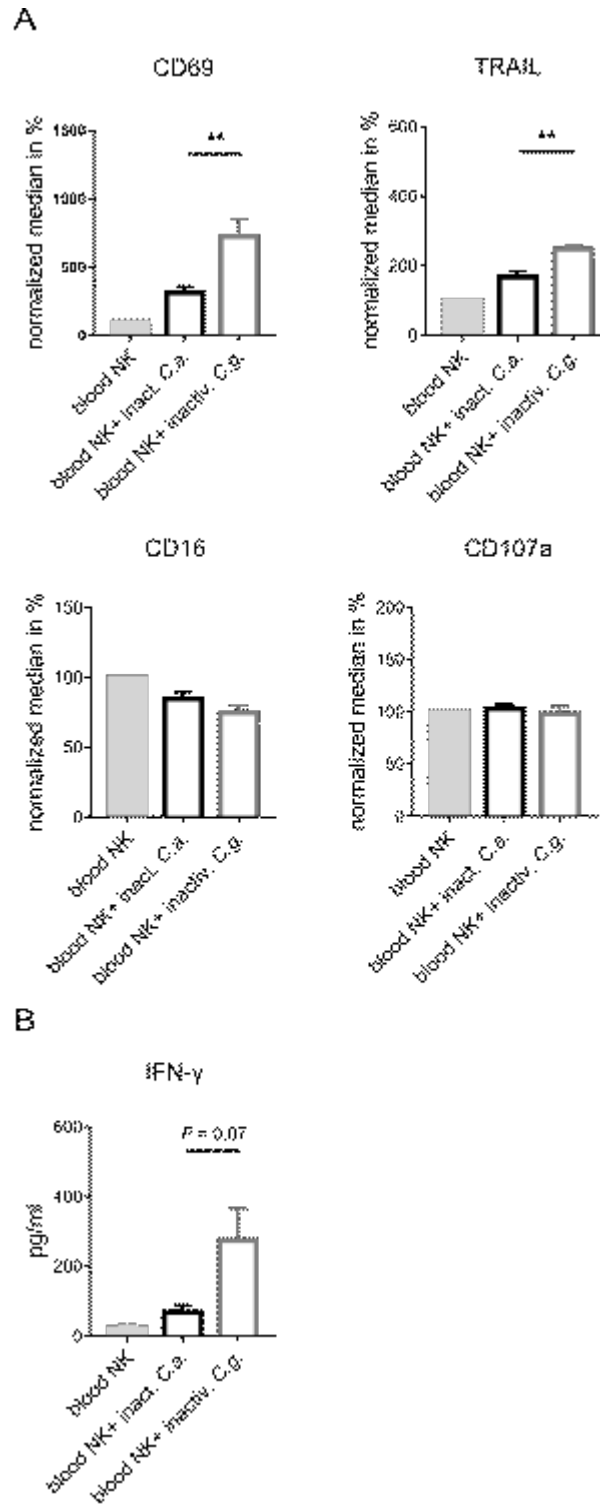
Figure 22. Inactivated *Candida* cells induce the same NK cell response during whole-blood infection as viable fungi.

Thimerosal-killed *C. albicans* germ tubes or *C. glabrata* yeast cells were added to whole blood of healthy donors and NK cell surface phenotype (A) as well as IFN-γ secretion (B) were analyzed following 8 hours of confrontation. Compared to mock-infected blood (light grey filled bars), both the release of IFN-γ and surface CD69 and TRAIL were more increased during *C. glabrata* (grey open bars) than *C. albicans* (black open bars) infection. Bars show

means ± SEM of at least three independent experiments with whole blood from different donors. *P* values were determined using one-way ANOVA followed up by multiple comparison tests, ****P<0.01*.

6.2.7 moDC activation in response to *C. albicans* and *C. glabrata* infection

Among all immune cells involved in the innate immune response in blood, monocytes and DC can release large amounts of cytokines upon activation. Unfortunately, isolated monocytes showed a limited lifespan upon confrontation with inactivated *Candida* cells (Figure 23) and were not suitable for cross-talk experiments with NK cells in a Transwell system. Indeed, confrontation of monocytes with *C. albicans* and *C. glabrata*, respectively, for 16 hours resulted in an almost complete loss of the monocyte population (Figure 23A). In contrast, viability of DC was not affected during 16 hours (Figure 23B) and 40 hours (Figure 23C) of *Candida* co-culture. To further investigate DC viability, evaluation of DC death upon *C. albicans* and *C. glabrata* activation was performed using PI flow cytometry assay. DC population was gated for PI-negative (PI$^-$) and PI-positive (PI$^+$) cells to allow the separation between alive DC and dead DC, respectively. Representative flow cytometry results show comparable small fractions of PI$^+$ cells after 16 h and 40 h of incubation in the mock-infected control sample and for DC infected either with *C. albicans* or *C. glabrata* (Figure 24Figure 23), indicating that the majority of moDC are alive during 40 h of fungal stimulation and able to produce soluble factor(s).

Due to experimental specifications, confrontation of DC needed to be performed with killed *Candida* cells. Previous experiments of whole-blood infection with killed fungal cells as well as a new set of experiments comparing NK cell activation in whole-blood induced by either killed *C. albicans* or *C. glabrata* confirmed the same results obtained for alive pathogens [62] . DC infected either with *C. albicans* or *C. glabrata* located in the upper Transwell compartment were physically separated by a porous membrane from the lower compartment containing primary NK cells, while exchange of soluble factors was permitted. DC were identified by the presence of CD1a and the absence of CD14 on their surface (Figure 25A), while DC activation by *C. albicans* or *C. glabrata* was checked by expression analysis of the two co-stimulatory surface markers: CD86 and CD83. Both markers were upregulated by both fungal species compared to mock-infected DC without any significant differences between *C. albicans* and *C. glabrata* (Figure 25B).
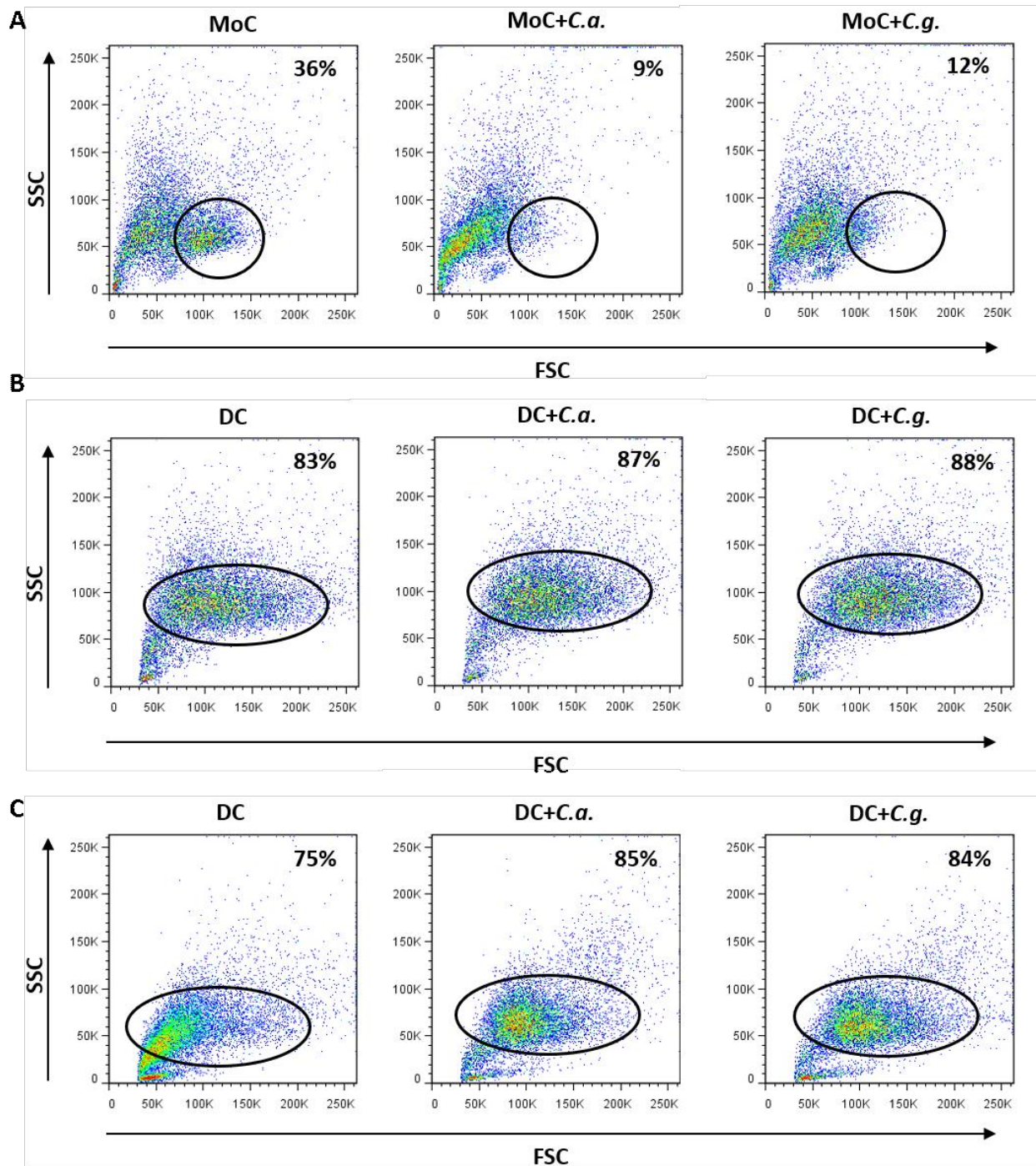
Figure 23. Life-span of monocytes and monocyte-derived dendritic cells during confrontation with *C. albicans* and *C. glabrata.*

(A) Confrontation of monocytes with *C. albicans* and *C. glabrata* for 16 hours and moDC during 16 hours (B) and 40 hours (C) of *Candida* co-culture. Scatter plots show one of at least four independent experiments showing identical results using isolated cells from different donors.
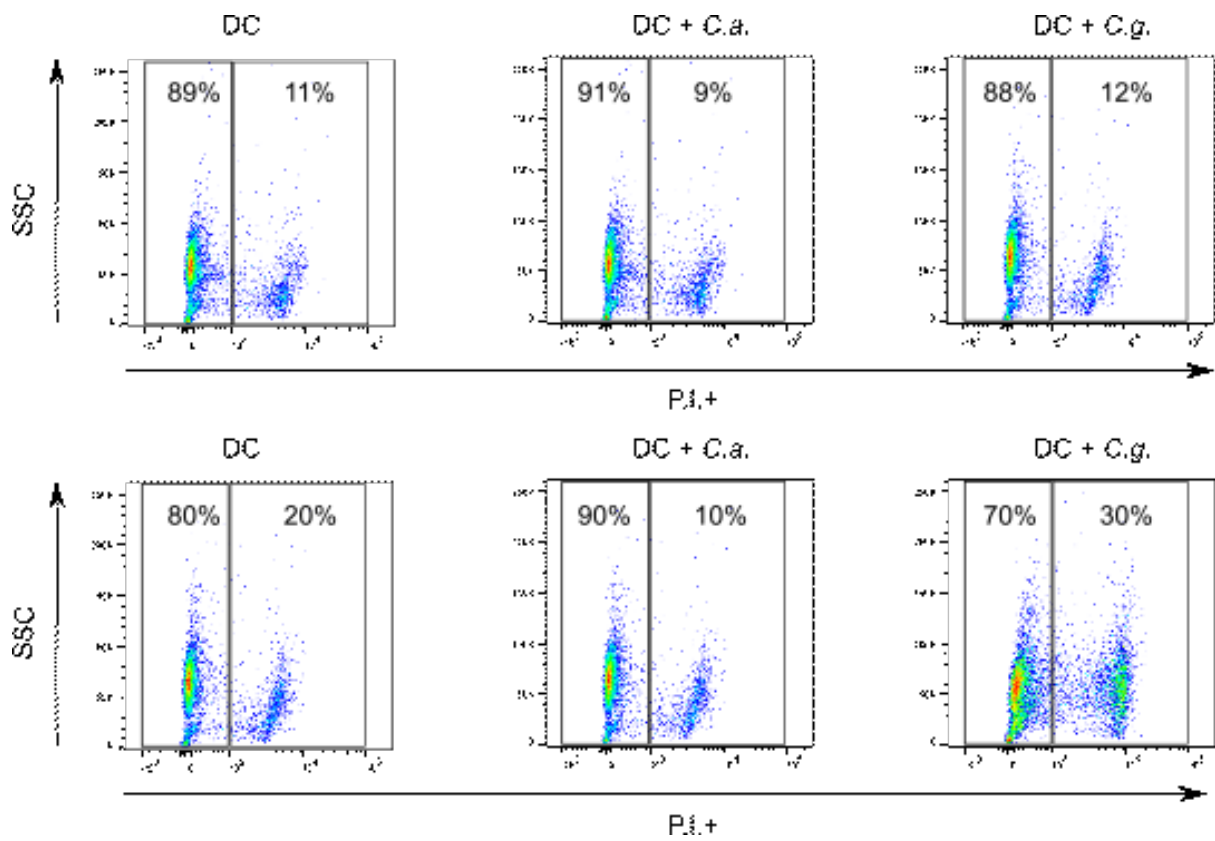
Figure 24. DC death after confrontation with *C. albicans* and *C. glabrata*.

DC population was not affected during 16 hours (A) and 40 hours (B) of *Candida* co-culture compared to the mock-infected control sample. Scatter plots show one of at least four independent experiments with isolated cells from different donors with identical results.
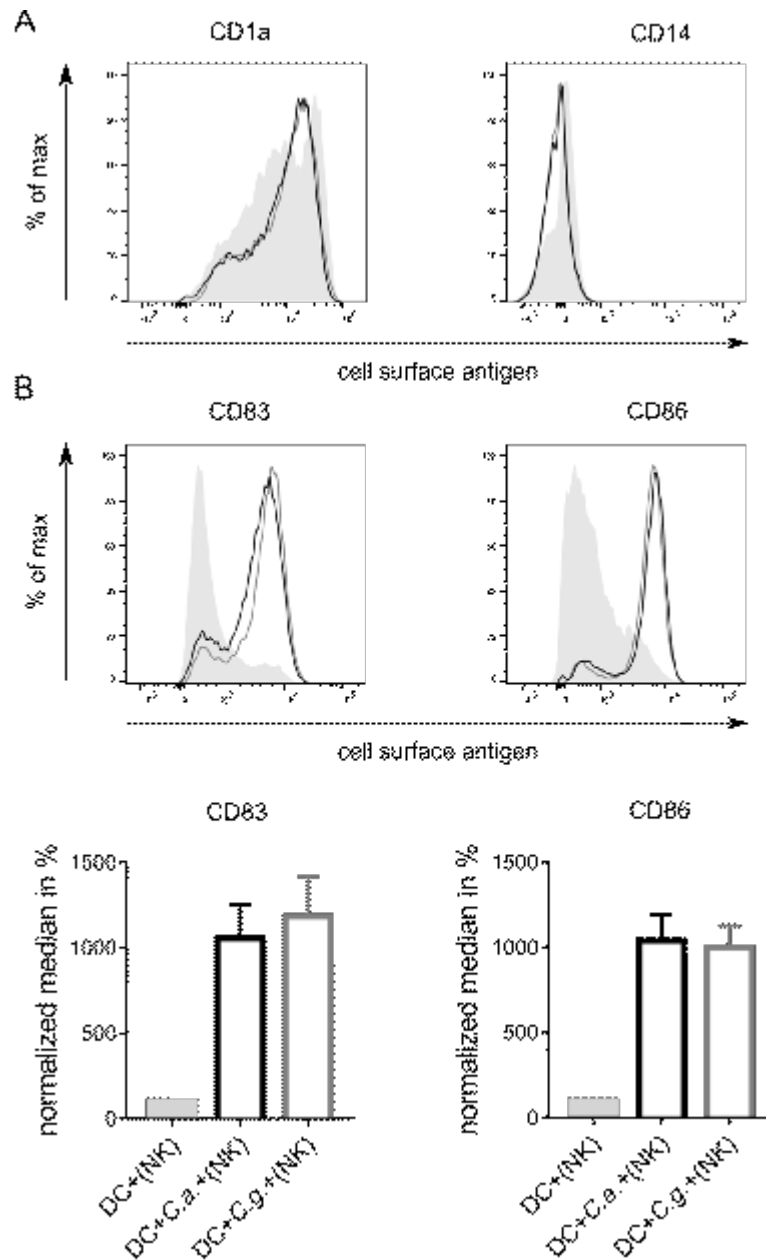
Figure 25. Maturation and activation of DC upon *C. albicans* and *C. glabrata* stimulation.

DC were either mock-infected or confronted with *C. albicans* and *C. glabrata* and analyzed for surface expression of DC identification (CD1a and CD14) and activation markers (CD83 and CD86). Changes in the surface expression levels of DC markers CD1a, CD14, CD83 and CD86 are shown in representative histograms after confrontation with *C. albicans* (black line) and *C. glabrata* (grey line). Changes of C83 and CD86 are shown after normalization to basal levels of mock-infected DC (set to 100%). Compared to mock-infected DC (light grey filled bars), surface CD83 and CD86 were more increased during *C. albicans* (black open bars) and *C. glabrata* (gray open bars) infection on DC. Data shown are means ± SEM.

6.2.8 Dendritic cell-derived soluble factor(s) are released in response to *C. albicans* and *C. glabrata* stimulation

To identify the specific stimulus that mediates NK cell activation, supernatants collected from the upper compartment of the Transwell system were analyzed to gain further insight into cytokines released by stimulated DC during *Candida* confrontation. A set of 34 cytokines/chemokines, including several ones involved in a general immune reaction and others specifically important for NK cell activation, were analyzed by a multiplex immunoassay.

Here, we specifically focused on the monocytic cytokines, such as IL-1β, IL-6, TNF-α and IL-12, which were significantly more released during incubation with C. *glabrata* in the whole-blood assay. Indeed, in agreement with cytokine profiles during whole-blood infection, after 40 hours of confrontation both species induced secretion of IL-6, TNF-α and IL-12 that was higher during *C. glabrata* (IL-6: 10451 ± 1956 pg/ml; TNF-α: 6654 ± 1113 pg/ml; IL-12: 6118 ± 972 pg/ml) than *C. albicans* infection (IL-6: 4411 ± 1057 pg/ml; TNF-α: 4749 ± 973 pg/ml; IL-12: 2517 ± 477 pg/ml) (Figure 26). However, IL-12 amounts released upon DC activation were markedly higher than induced during blood infection (by *C.a.*: 27-fold higher, by *C.g.*: 11-fold higher). The concentration of IL-1β in supernatants of infected DC was at the limit of detection and comparable to the spontaneous release by mock-infected DC, indicating no infection-induced secretion like in whole-blood. Our data also showed the flow of cytokines into the lower compartment, which maintained the same differences in their supernatant levels between confrontation with *C. albicans* and *C. glabrata* (Figure 26B).

Secretion of cytokines particularly involved in NK cell priming and activation were either (i) not detectable (IL-13, IL-15, IL-17A, IL-22, IL-23), (ii) slightly increased, but with equal levels for both fungal species (IL-2, IL-21, IL-27) or (iii) slightly higher released during *C. glabrata* than *C. albicans* stimulation (*e.g.* IL-18, IP-10, RANTES) (Figure 27).
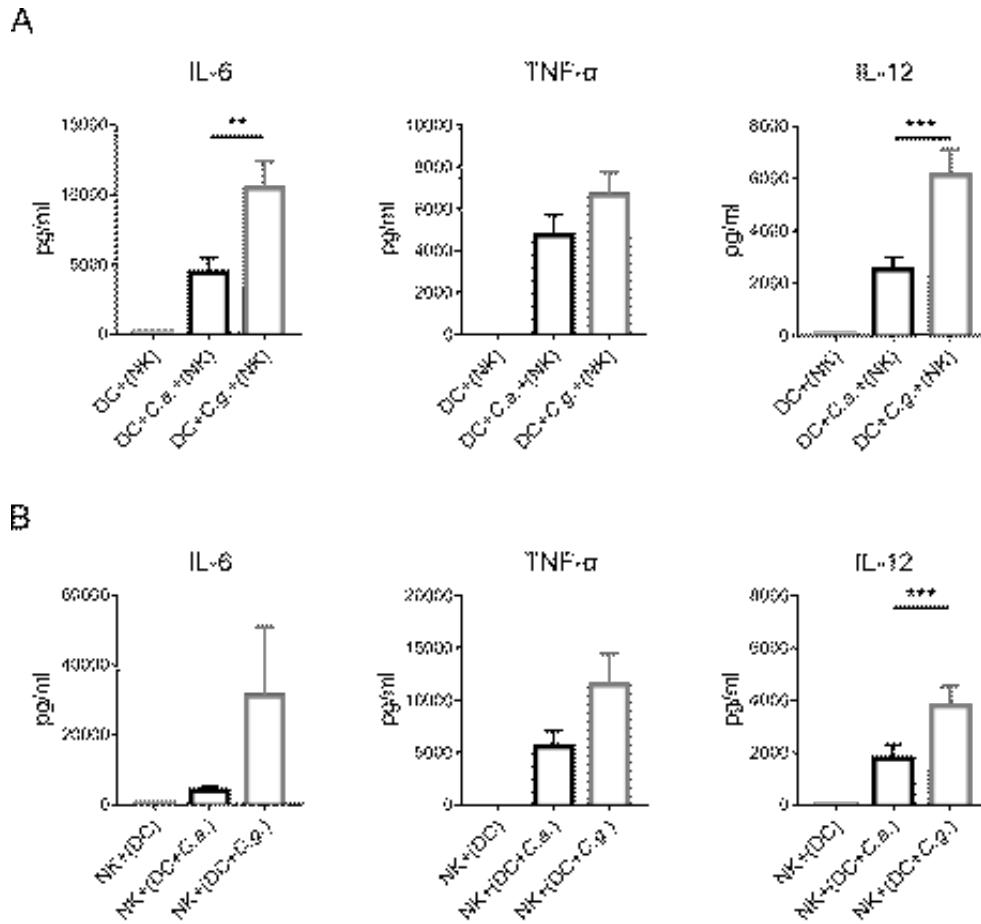
Figure 26. Cytokines released by moDC upon *C. albicans* and *C. glabrata* stimulation.

Supernatants were collected from both the upper compartment (A), where DC were either mock-treated (light grey filled bars) or confronted with *C. albicans* (black open bars) and *C. glabrata* (grey open bars), and the lower compartment of the Transwell system. Bars show means ± SEM of at least four independent experiments with cells isolated from different donors. *P* values were determined using one-way ANOVA followed up by multiple comparison tests, **P< 0.01, ***P< 0.001.
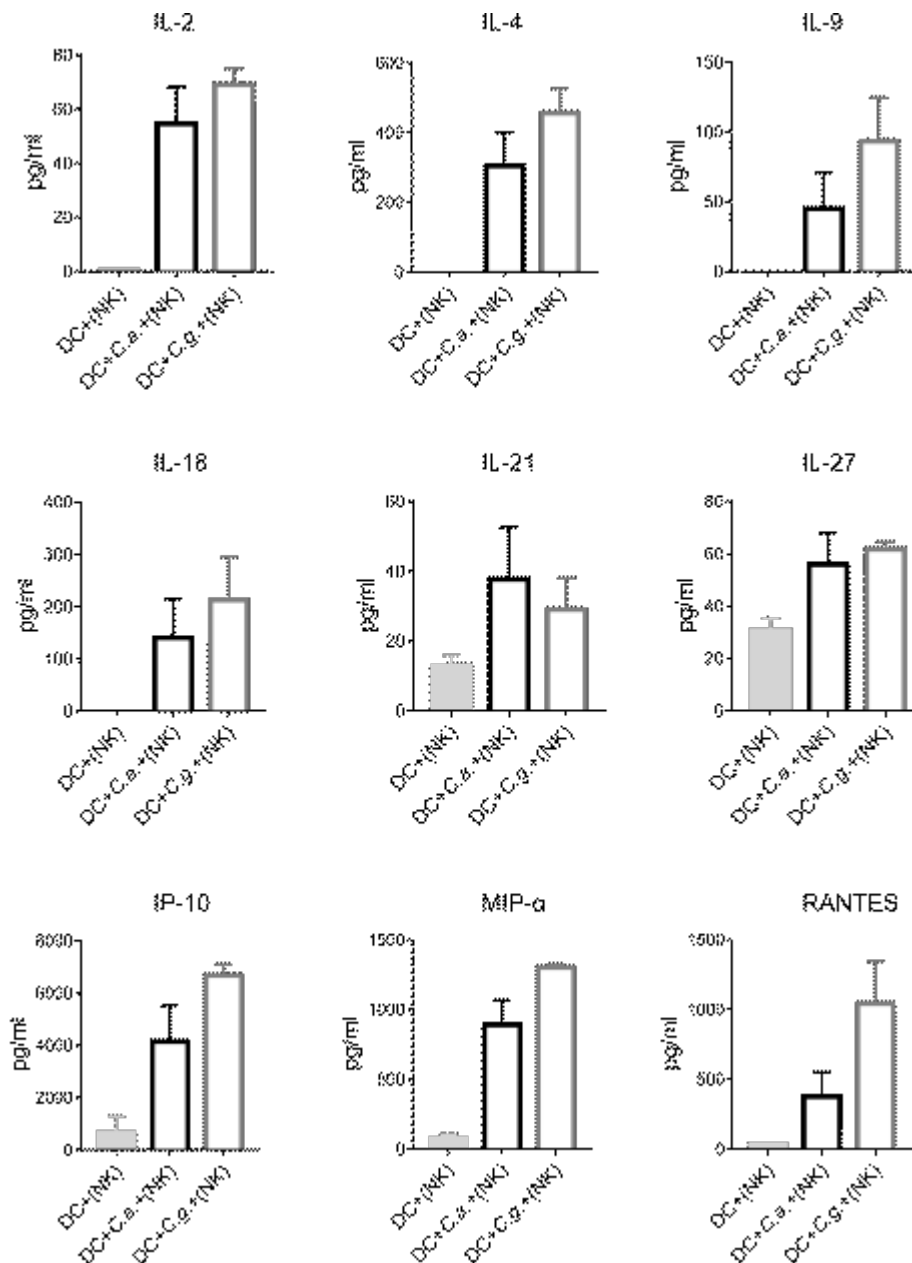
Figure 27. Secretion of cytokines and chemokines particularly involved in NK cell priming by moDC during *C. albicans* and *C. glabrata* infection.

Supernatants were collected from the upper compartment of the Transwell system, where DC were either mock-treated (light grey filled bars) or confronted with *C. albicans* (black open bars) and *C. glabrata* (grey open bars). Bars show means ± SEM of three independent experiments with cells isolated from different donors.

6.2.9 Dendritic cell-derived soluble factor(s) induce differential NK cell activation

We further investigated the induction of NK cell effector mechanisms by cytokines released from stimulated moDC. Interestingly, there was an evident up-regulation of CD69 and TRAIL on primary NK cells as shown for the blood NK cells (Figure 29). In each case, *C. glabrata* confrontation increased surface levels more than *C. albicans* (e.g. CD69: *C.a.* 598 ± 76%, *C.g.* 901

± 107%). In contrast, CD16 and CD107a expression showed only a slight regulation, indicating no role in the NK cell effector mechanisms induced by DC-derived cytokines.
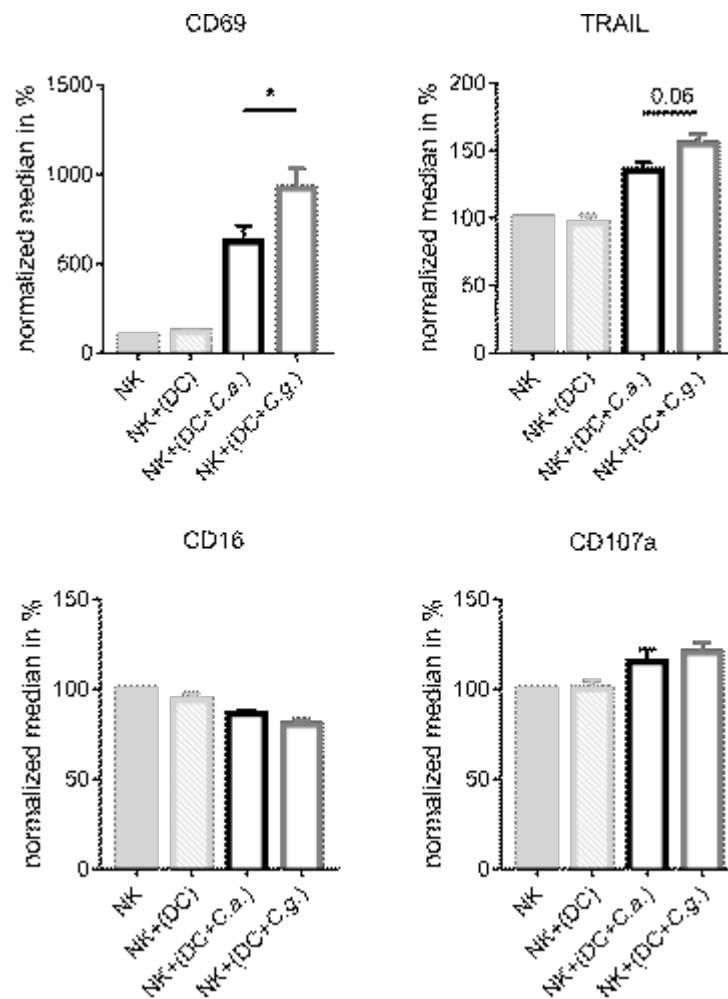
Figure 28. DC-derived soluble factor(s) induce different surface activation marker levels on primary NK cells. NK cells were harvested from the lower compartment of the Transwell system after 40 hours of incubation without DC (light grey filled bars) or co-incubation with DC located in the upper compartment that were either mock-infected (light grey dashed bars) or infected with *C. albicans* (black open bars) and *C. glabrata* (grey open bars). Changes in the surface expression levels of NK cell activation markers CD69, TRAIL, CD16 and CD107a are shown after normalization to basal levels of NK cells in the absence of DC (set to 100%). Bars show means ± SEM of at least three independent experiments with cells isolated from different donors, *$P< 0.05$.

In addition, we analyzed more markers of NK cell activation and found CD38, an adhesion molecule that triggers NK cell cytotoxicity, to be significantly higher induced on NK cell surface in response to *C. glabrata* than *C. albicans* (Figure 29). Other surface markers, such as CD56, HLA-DR and NKp30, were up-regulated in response to cytokines released by DC upon fungal infection, but no differences in the expression between *C. albicans* and *C. glabrata* infection were detected.
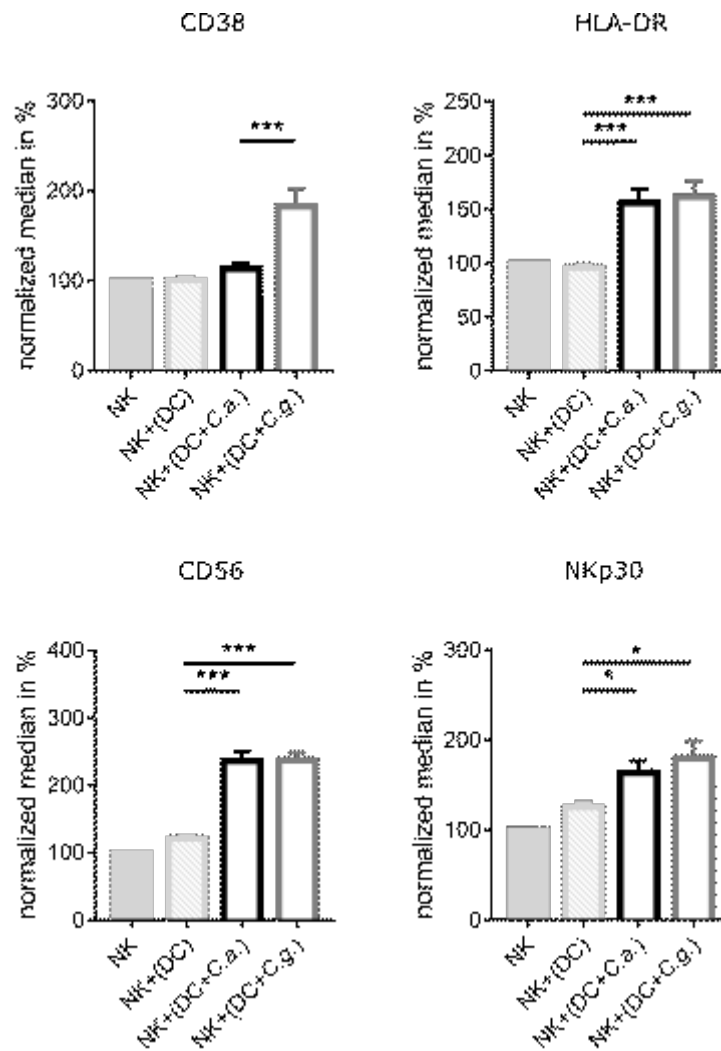
Figure 29. *Candida* species induced DC-derived soluble factor(s) induce different surface activation marker levels on primary NK cells.

Candida species induced DC-derived soluble factor(s) induce different surface activation marker levels on primary NK cells. NK cells were harvested from the lower compartment of the Transwell system after 40 hours of incubation without DC (light grey filled bars) or co-incubation with DC located in the upper compartment that were either mock-infected (light grey dashed bars) or infected with *C. albicans* (black open bars) and *C. glabrata* (grey open bars). Changes in the surface expression levels of NK cell activation markers CD38, HLA-DR, CD56 and NKp30 are shown after normalization to basal levels of NK cells in the absence of DC (set to 100%). Bars show means ± SEM of at least 3 independent experiments with cells isolated from different donors, *$P< 0.05$, ***$P< 0.001$.

Furthermore, supernatants were collected from the lower compartment of the Transwell system that contained primary NK cells and analyzed for IFN-γ secretion in response to DC-derived soluble factors. The lower NK cell stimulation induced by cytokines released from DC in response to *C. albicans* also resulted in lower IFN-γ levels (975 ± 190 pg/ml) present in the NK cell compartment. Despite the high donor-dependent variance, IFN-γ secretion by primary human NK cells was

stronger during NK cell-DC-*C. glabrata* co-incubation in majority of cases (1310 ± 220 pg/ml, *P*<0.05) (Figure 30).
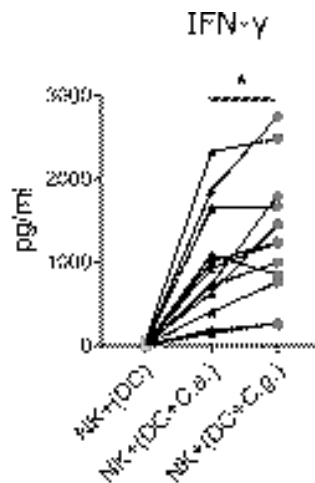
Figure 30. Cytokines released from DC in response to *C. glabrata* induced higher IFN-γ secretion by primary NK cells.

Before-after graph shows the higher IFN-γ release after 40 hours of confrontation with *C. glabrata* (grey circles) compared to *C. albicans* (black triangles) in 12 independent experiments with cells isolated from different donors. *P* values correspond to the means ± SEM of all experiments obtained with the paired two-sided Student *t* test (**P*<0.05).

Taken these results together, we could show that cytokines released by DC upon fungal confrontation were able to drive primary human NK cell activation, which was equal to the differential NK cell activation levels during whole-blood infection between *C. albicans* and *C. glabrata*.

6.2.10 DC-derived IL-12p70 triggers the IFN-γ release by NK cells

DC secrete pro-inflammatory cytokines in response to *C. albicans* and *C. glabrata* infections. IL-12 is a good candidate responsible for the different levels of NK cell activation induced by the two fungal species: on the one hand it is differentially produced by moDC after confrontation and on the other hand it was already shown to induce IFN-γ release by NK cells [138].

To determine the contribution of moDC-derived IL-12 to primary NK cell activation, the induction of NK effector mechanisms was quantified in presence of a neutralizing antibody. Blocking of IL-12 resulted in an inhibited release of IFN-γ by NK cells in response to either *C. albicans* (w/IgG1: 500 ± 97 pg/ml; w/αIL-12: 52 ± 14 pg/ml) or *C. glabrata* (w/IgG1: 728 ± 204 pg/ml; w/αIL-12: 28 ± 3.5 pg/ml) with levels close to background that can be detected during co-incubation of NK cells with mock-treated DC (7.5 ± 3.2 pg/ml) (Figure 31).
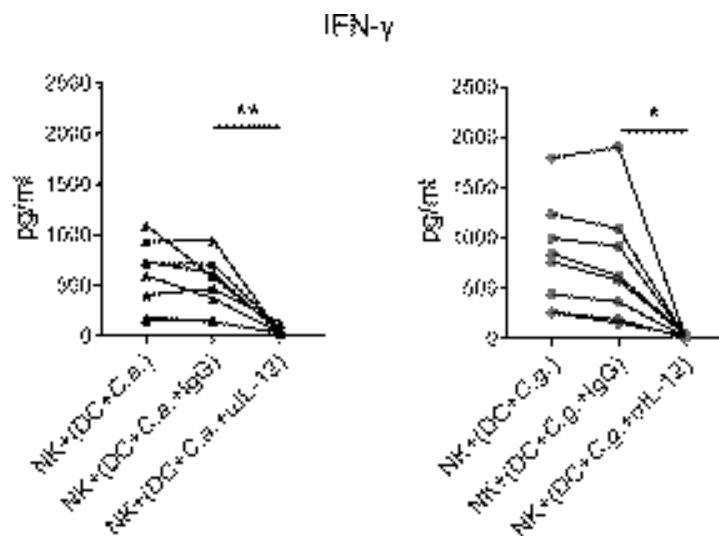
Figure 31. IL-12 contributes to IFN-γ release by primary NK cells.

DC infected with *C. albicans* (black triangles) or *C. glabrata* (grey circles) were either non-treated or incubated in the presence of an isotype control (IgG) or anti-IL-12 blocking antibody (αIL-12). IFN-γ secretion was measured within supernatants obtained from the lower compartment of the Transwell system that contained primary NK cells. Presence of αIL-12 resulted in an inhibited release of IFN-γ by NK cells in response to both *Candida* species. Each data point in the before-after graphs represents an independent experiment and *P* values correspond to the means ± SEM of all experiments, *$P < 0.05$, **$P < 0.01$.

Regulation of surface exposure of CD69, CD56, NKp30 and HLA-DR on primary NK cells after indirect stimulation by *Candida*-activated DC seemed to be regulated by IL-12 (Figure 32). Blocking of IL-12 significantly decreased the strong CD69 up-regulation during *C. albicans* (w/IgG1: 580 ± 83%; w/αIL-12: 256 ± 19%) and *C. glabrata* (w/IgG1: 887 ± 133%; w/αIL-12: 499 ± 85%) infection, whereas CD69 surface levels were not affected by the isotype-matched control Ab. However, the inhibitory effect of the αIL-12 antibody on CD69 regulation was only partially, since we could still detect a 5-fold and 2.6-fold higher CD69 expression in response to *C. glabrata* and *C. albicans*, respectively. Interestingly, increased CD56, NKp30 and HLA-DR surface expression, which showed equal regulation for both fungal infections, were reduced to almost background levels on non-stimulated NK cells (Figure 32). The effect of IL-12 to induce CD56, NKp30, HLA-DR and CD69 on NK cells was confirmed by direct treatment of primary cells with recombinant human IL-12, whereas no changes in the surface expression of TRAIL and CD38 could be detected (Figure 32). In line with this, expression of TRAIL and CD38 showed no significant differences between αIL-12, IgG1-, and non-treated blood in response to both *Candida* species (Figure 32).
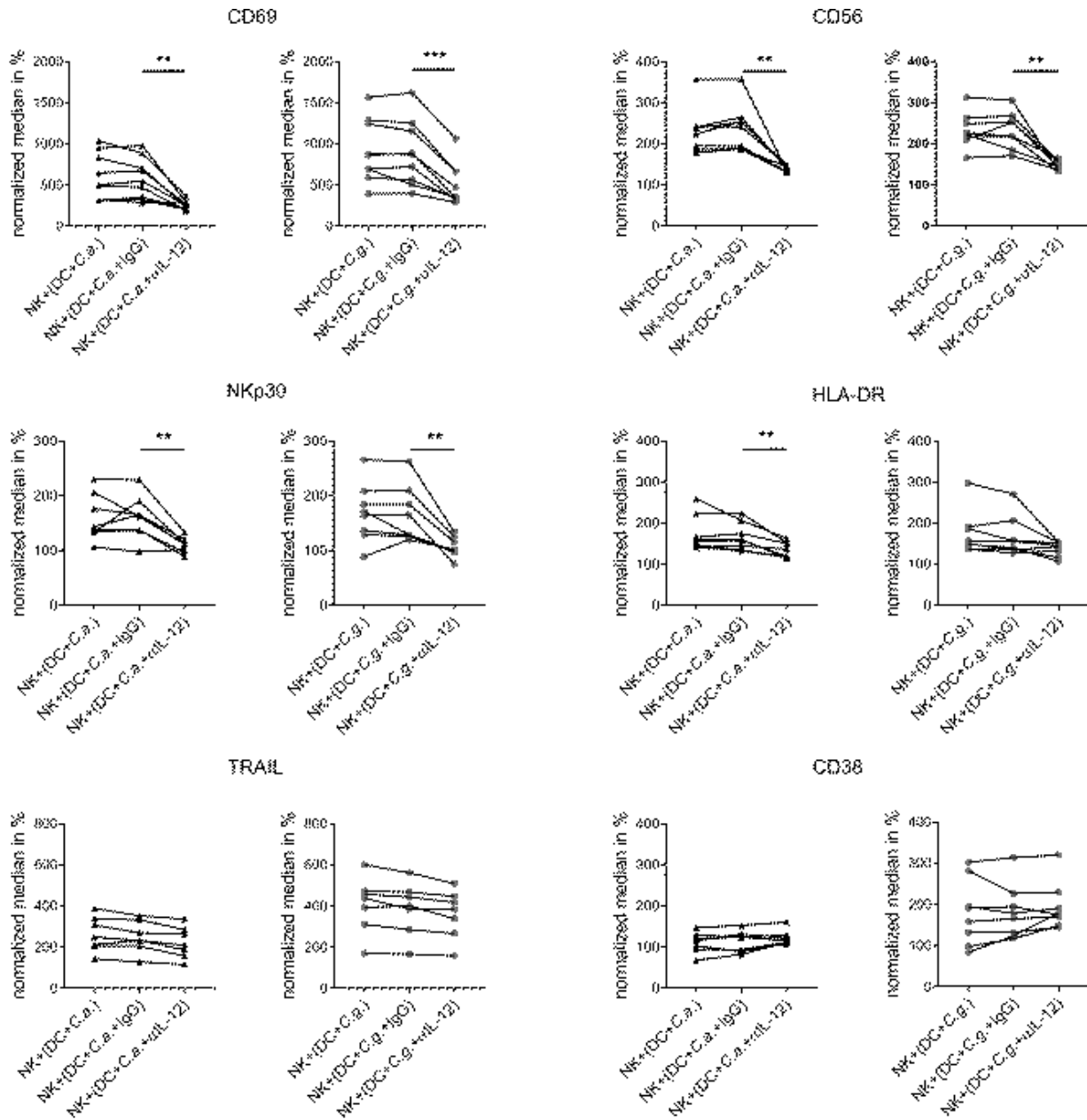
Figure 32. Effects of IL-12 on NK cell surface marker expression.

The surface expression of activation markers on primary NK cells during co-incubation with either *C. albicans*-(back triangles) or *C. glabrata*-infected DC (grey circles) in a Transwell system has been evaluated in presence of IL-12 neutralizing antibody (αIL-12) and compared to non-treated or IgG-treated samples. Changes in the surface expression levels of CD69, TRAIL, CD38, HLA-DR, CD56 and NKp30 are shown after normalization to basal levels of NK cells in the absence of DC (set to 100%, not shown). Quantitative analysis was performed using paired one-way ANOVA followed up by multiple comparison tests. Each data point in the before-after graphs represents an independent experiment of at least 7 experiments. Lines connect data points from identical donors. *P* values correspond to the means ± SEM of all experiments with primary NK cells isolated from different donors, **P< 0.01, ***P< 0.001.

69

Checking CD69 and TRAIL expression on blood NK cells as well as IFN-γ release during whole-blood infection in presence of αIL-12, increased CD69 surface levels and secretion of IFN-γ in presence of *C. glabrata* were partially blocked, whereas TRAIL surface exposure was not affected (Figure 33). In contrast, we observed only marginal effects of the blocking antibody during *C. albicans* infection.
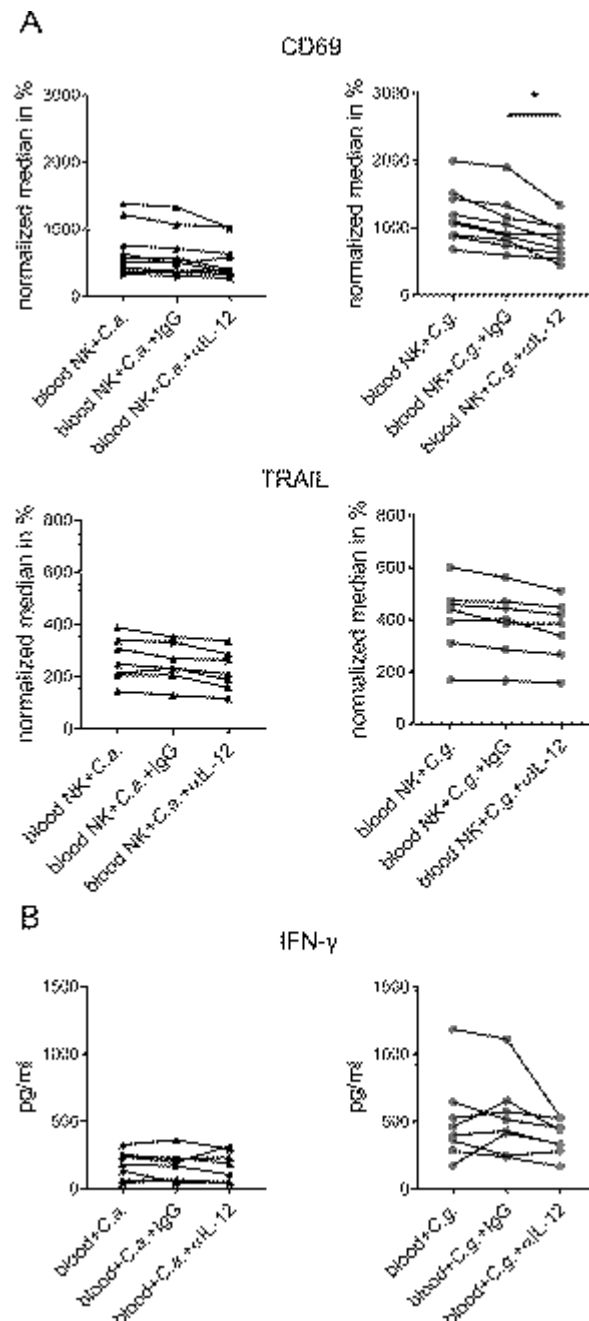
Figure 33. Blocking of IL-12 partially decreases NK cell activation in human whole blood.

Human whole blood was treated with an anti-IL-12 antibody (αIL-12) prior to inoculation of either *C. albicans* (black triangles) or *C. glabrata* (grey circles) for 8 hours to investigate the impact of IL-12 on activation of blood NK cells. Samples were compared with either non-treated or IgG-containing *Candida*-infected blood. After whole-

blood infection, NK cell surface exposure of CD69 and TRAIL (A) and secretion of IFN-γ within plasma samples (B) were analyzed. In comparison with non- and IgG-treated infected samples, presence of αIL-12 partially prevented the increase in CD69 expression and plasma levels of IFN-γ in response to *C. glabrata*. Each data point in the before-after graphs represents an independent experiment. Quantitative analysis was performed using paired one-way ANOVA followed up by multiple comparison tests. *$P< 0.05$.

Taken together, differences in IL-12 secretion by moDC in response to *C. albicans* and *C. glabrata* are responsible for the differential secretion of IFN-γ by NK cells. However, differences in the exposure of surface activation markers CD69, TRAIL and CD38 seemed to be mediated by additional factors that may be also important for regulation within blood.

To further validate the role of IL-12 on NK cell activation, freshly isolated NK cells were treated with recombinant IL-12 for 40 hours and surface markers were analyzed.

Indeed, the effect of IL-12 to induce CD56, NKp30, HLA-DR and CD69 on NK cells were confirmed by direct treatment of primary cells with recombinant human IL-12, whereas no changes in the surface expression of TRAIL and CD38 could be detected (Figure 34).
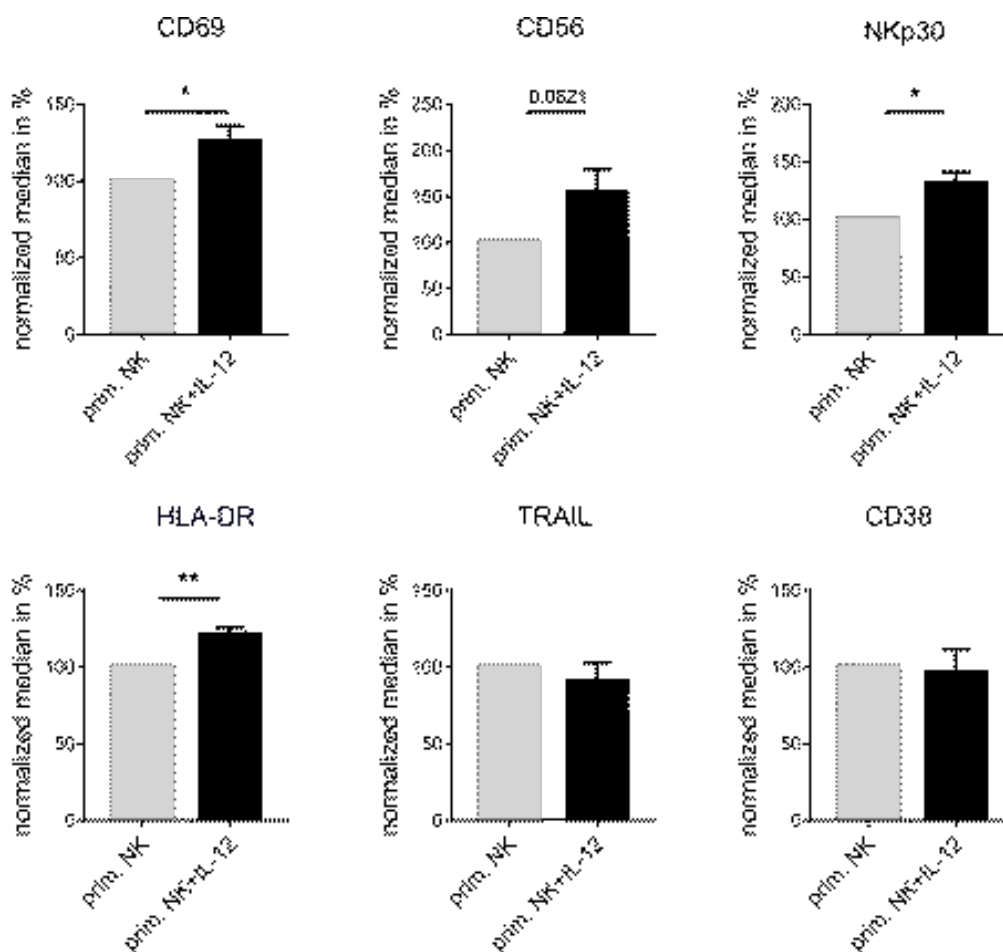
Figure 34. Stimulation of primary human NK cells by recombinant IL-12.

Freshly isolated NK cells were either mock-stimulated (light grey filled bars, set to 100%) or incubated with recombinant IL-12 (black filled bars) for 40 hours and NK cell activation was analyzed by flow cytometry. Compared to mock-stimulated NK cells CD69, CD56, NKp30 and HLA-DR were upregulated on NK cell surface in presence of recombinant IL-12. *P* values were determined using unpaired two-sided Student *t* test. Significance is shown as *$P< 0.05$, **$P< 0.01$. Bars show means ± SEM of four independent experiments with cells isolated from different donors.

In this second part of this study, different NK cell stimulation was showed depending on the milieu and *Candida* species. Whereas activation of blood NK cells was stronger with *C. glabrata*, contact-dependent stimulation of expanded primary NK cells was higher in presence of *C. albicans* and triggered degranulation of secretory granules. The immunophenotype of blood NK cells with upregulation of death receptor ligand TRAIL and CD69 was also observed for NK cells in the presence of DC-derived cytokines released upon fungal contact, proving an indirect NK cell activation by soluble factors during blood infection. Furthermore, differences in IL-12 secretion by DC and in blood induced by the two *Candida* species are responsible for different levels of NK cell activation at least as regards the IFN-γ secretion and the regulation of some NK cell surface markers. However, additional cytokines are required to fully stimulate the NK cells and will be in the focus of future studies.

7   Discussion

Invasive fungal infections are emerging as a significant health risk for humans. In this regard, *C. albicans* and *C. glabrata* are two most prevalent pathogens in the genus *Candida* and account for the majority of candidiasis cases worldwide. Although these two species share some of the same virulence factors, they are phylogenetically quite distinct. Consequently, there are also evidences that the interplay of *C. albicans* and *C. glabrata* with the human immune system differs considerably.

7.1   PMN behavior in response to *C. albicans* and *C. glabrata* infection

The aim of the first part of this study was to generate a dynamic hemogram from whole-blood infection assays that goes beyond standard blood count examination by integration of information on migration and interaction of blood cells, especially PMN, for a fast identification of pathogens causing bloodstream infections and positive treatment outcome. There are already molecular-based diagnostic tools available [212], some of them especially designed for the identification of the most common *Candida* species in whole-blood which show a high and accurate efficiency [213, 214].

The techniques currently most used in the detection of causative pathogens in blood infections are blood cultures (BDs) and PCR-based assays which are not exempt from some limitations [215]. BDs are based on the isolation and identification of microorganisms [216]. This method requires between 6 h and 5 days to organism growth followed then by pathogen identification and antibiotic susceptibility test for a total of approximately 8 days [217]. While, PCR-based analysis allows directly molecular pathogen detection and identification however, contamination problems have been found with this technique [216].

On the other hand, quantification of leukocytes, including also PMN, is an important marker of infections due their involvement in fighting against a wide range of pathogens [218]. Several studies have showed the importance of total white blood cells (WBC), absolute neutrophils count and bad count as markers in the prediction of infection [219, 220]. Also, evaluation of immature granulocytes was also taken into consideration as a parameter of infection and sepsis. It was shown that in infected patients the percentage of immature granulocytes was significantly higher compared to non-infected patients demonstrating that this marker has biologically and clinically relevance but with low sensitivity and specificity [218]. Indeed, leukocyte-related parameters have different limits in predicting infection because their increase it is not only correlate to infection or sepsis, but it can be observed also in other conditions (chronic inflammatory diseases, neoplasia, tissue damage or necrosis, myeloproliferative disorders) [220]. For this reason, additionally to leucocyte count, other factors are considered for infection prediction as, for example, acute phase reactants (C-reactive

protein) [221], circulating inflammatory mediators (C3a, IL-6) [222] and serum levels of procalcitonin [223].

These different diagnostic approaches are based on the idea that human immune cells after encountering with a pathogenic agent undergo changes or carry features – e.g. with regard to cell morphology and/or their surface receptor expression – by which (i) the type of pathogen may be identified indirectly, (ii) information about the therapy efficiency may be provided and (iii) prognosis about therapy outcome may become possible [224]. One possible example in this context is the imaging mass cytometry which is a powerful tool that allows analyzing up to 40 cell surface markers simultaneously [225]. Diagnosis improvement came with the introduction of serologic test such as the galactomannan and 1,3-β-glucan antigens [226, 227].

Furthermore, there are already molecular-based diagnostic tools available [212], some of them especially designed for the identification of the most common *Candida* species in whole-blood which show a high and accurate efficiency [213, 214].

Overall, diagnosis of invasive fungal infections is still challenging due to the low specificity and sensitivity, or the long time required to yield a result to be clinically useful which bring to delay in the patient treatment and therapy [228, 229].

Future diagnostic techniques should aim to have certain requirements, as: early detection, strong negative predictive value, short time result, low cost with inexpensive equipment, minimal number of steps and uncomplicated interpretation [228].

7.1.1 PMN morphology after *C. albicans* and *C. glabrata* infections

The choice to use PMN was dictated by their importance already demonstrated in defense against invasive candidiasis [230] and indeed neutropenia represents a major risk for systemic candidiasis development [231]. It was also showing the different behavior of PMN against infection by different fungal infection, in particular against *C. albicans* and *C. glabrata:* PMN activation differ between this two *Candida spp*. Indeed, activated PMN can rapidly engulf *C. albicans* in a filamentous form and inhibits its elongation resulting in efficient killing of fungal cells and they are the only immune cells able to do this [59]. In contrast, *C. glabrata* induces a low-grade inflammatory response, recruiting and activating monocytes rather than PMN in human blood and during murine infection [58].

One approach to our aim was sorting and extraction of PMN following *ex vivo* whole-blood infection for separate analysis in live cell imaging experiments which provides spatial and temporal information of dynamic events in single cells.

Live cell imaging in combination with automated image analysis is considered to be an important tool in the understanding of host-pathogen interaction field [193, 232]. In a previous study, live cell imaging helped to identify differences in PMN recognition of *C. albicans* and *C. glabrata* showing that PMN are less effective in *C. glabrata* than *C. albicans* uptake and enhance recruitment and phagocytosis of *C. glabrata* by monocytes [58]. Using this powerful technique our lab discovered the ability of PMN to release *C. glabrata* fungal cells after phagocytosis and intracellular killing, a process called "dumping", which may enable the pathogens to be subsequently taken up and processed by professional antigen presenting cells [104].

Different methods have been proposed over the time such as the use of stained cells but this approach could change cell behaviour or induce cell death [233-235]. Previously, an algorithm for migration and interaction tracking (AMIT) was developed to perform quantitative motility analysis of label-free human cells in bright-field microscopy videos [193, 194]. This algorithm has also been improved with new versions up to number 3 which was used in this study [236].

To identify changes in PMN behavior induced by *C. albicans* and *C. glabrata*, fungal cells were added to human whole blood and compared to mock-infected control samples. Following a one hour confrontation, PMN were purified from whole blood and introduced to time-lapse microscopy to visualize their dynamic features. Manual analysis of microscopy videos already identified differences in cell shape and migration behavior between PMN from *C. albicans* and *C. glabrata* compared to PMN from mock-infected whole blood. However, to get quantitative information, imaging data were used for automated image analysis. Features of immune cells that have been studied previously include (i) changes in cell size [237], (ii) modifications of membrane topography [238, 239] and (iii) variations in the migration behavior [196]. In this study combination of all these features was used to identify those that allow the identification of mock-infected PMN from infected PMN and to establish an automated pipeline based on live cell imaging data.

In fact, the cellular behavior was classified by cell segmentation, tracking and the detection of different morphological features (area, perimeter, convex full area, etc.). By combining all different features, it was possible to generate a Kinetic Feature Vector that can be used to discriminate *Candida*-infected from mock-infected PMN and which was able to identify two different dynamic morphologies of PMN: PMN with a S-morphology and PMN with a N-morphology already observed manually. The highest percent of PMN with S-morphology were identified for PMN isolated from human blood infected by *C. glabrata* followed up by PMN from blood infected by *C. albicans*, while PMN isolated from mock-infected blood were mostly presented in a N-morphology and showed the lowest percent of PMN in a S-morphology. PMN with a S-morphology phenotype have been only observed after PMN isolation from infected whole blood. In previous studies, where

PMN were first isolated from freshly drawn blood and subsequently infected during live cell imaging, this characteristic morphology could be never observed [58, 104, 236].

The difference between PMN with N- and S-morphology was also correlated with differences in PMN size and surface roughness. Taking PMN size into account enabled the distinction between mock-infected PMN and infected PMN, while the classification between PMN isolated from blood infected by *C. albicans* and *C. glabrata* was not possible. PMN in a spreading phenotype presented in both fungal infections showed the same characteristics. PMN isolated from blood infected either by *C. albicans* or *C. glabrata* showed a bigger area (~ 6000 px) compared to mock-infected PMN which are spherical with a smaller area of ~ 3000 px.

It was already described that the ability of PMN to rapidly change their shape (from N-morphology to S-morphology) is one of the most important PMN feature [240]. Several evidences suggest that PMN undergo morphological changes, such as from spherical to flattened shape, during migration process and subsequent penetration into infected tissues [241]. In addition, PMN phagocytosis requires morphology changes like formation of pseudopodia [240]. In both cases these changes occur rapidly and imply an expansion of the plasma membrane of almost 200% [242, 243]. Scanning electron microscopy shows that PMN spherical surface present high number of wrinkles and others "microridged" structures which can help PMN to expand their plasma membrane during their switching from N-morphology to S-morphology state observed in our time-lapse microscopy video [244]. Indeed, PMN wrinkles give additional membrane function in this morphological transition and allow PMN to spread on a surface. This transition has been well described as a process in three steps: i) disconnecting surface wrinkles from underlying cortical actin, ii) wrinkle unfolding and iii) acquisition of a new PMN morphology [240].

Considering which stimulus can induce PMN morphological switching, it was shown that exposure of PMN to different chemoattractants, such as N-formylmethionine-leucyl-phenylalanine (fMLP), IL-8 and C5a, induces actin filament polymerization and cytoskeletal rearrangements which are both involved in PMN shape changes and PMN interstitial migration [245, 246]. In particular, C5a induces alterations in cellular morphology and changes in surface adhesion in different cell types, including PMN, using the C5aR1-dependent intracellular signalling pathway which results in osmotic swelling and cellular cell shape [206, 247]. Furthermore, C5a has broad effects on immune system like the secretion of inflammatory cytokines from PBMCs during *C. albicans* infection [248].

It was also shown that complement system cascade is activated during *Candida* whole-blood infection and results in the production of C5a [248]. Consequently, we found C5a to be highly secreted in the plasma of blood infected by *C. albicans* after one hour of co-incubation, while C5a

release was significantly lower during *C. glabrata* infection. To rule out the role of C5a in PMN switching from N- to S-morphology, we performed live cell imaging experiments of PMN isolated from blood treated with an antibody against C5a, which blocks C5a activity, and subsequently infected by *C. albicans*. Performing automated identification and quantitative evaluation of PMN morphology, it was possible to correlate the presence of C5a with PMN morphology changes. In presence of the anti-C5a blocking antibody, the fraction of PMN in a spreading phenotype was reduced compared to PMN isolated from blood infected by *C. albicans* and not treated with the antibody. On the other hand, C5a production in response to *C. glabrata* infection was quite low and for this reason the interpretation of relative results using the blocking C5a-antibody was not clear.

Secretion of other cytokines/chemokines was analysed within plasma of blood infected either by *C. albicans* or *C. glabrata* for 1 hour. The secretion of IL-8, TNF-α and IL-1β was very low compared to levels induced after 4 hours [58] and 8 hours [249] of fungal infection. On the other hand, humoral factors already known to be involved in PMN adhesion and signaling pathways (such as soluble P-selectin) [207] and PMN chemotactic process (such as PDGF) [208] were higher released during *C. albicans* than *C. glabrata* infection.

Since PMN also play an important role against bacterial infection, we further investigated PMN switching after isolation of PMN from human blood infected with three different bacteria (*N. meningitidis*, *S. pneumonia* and S. *aureus*) in one representative experiment. After one hour of bacterial infection and isolation from infected blood, PMN showed an increase of cells with a spreading phenotype compared to the mock-infected PMN. Indeed, as for Candida infection, neutropenia or PMN malfunction represent risk factors for life-threatening infections with bacteria [250, 251].

PMN switching from N-to S-morphology could represent a fast identification factor for fungal as well as bacterial infections in combination with automated image analysis, since this morphological change was not observed in PMN isolated from mock-infected blood.

Furthermore, using AMIT algorithm improvement allowed the enhancement of recognition of whole cell tracks [192] as well as of dynamically changing cell shapes. Based on these improvements it was possible to combine human whole-blood infection model with live cell imaging of isolated PMN to detect features that are automatically computed to distinguish *C. albicans* from *C. glabrata* infection. On the other hand, our work presented some limitations like the high donor variability, the small censored cohort of blood donors (9 healthy individual aged between 25-40 years) and the limited number of pathogens considered. It would be also interesting to deeply investigate also in mixed pathogen population, which is which is a common condition in patients, and collect information about behavior and morphology of others immune cells involved in

the infection fight (monocytes, macrophages). After having investigated all the above points, the next step could be validation of the distinction between PMN in a spreading- and non-spreading phenotype, and all the characteristics related to this characteristic morphology, as a diagnostic marker based on the label free protocol.

7.2   Response of NK cells to *C. albicans* and *C. glabrata* infection

In this second part of this study, we investigated NK cell effectors mechanisms involved in the immune response against *C. albicans* and *C. glabrata* infections. In particular, we focused on NK cells in a whole-blood infection model, to consider others immune cells and humoral factors in a more complex system, compared to expanded primary NK cells also used in clinical approaches. Human whole-blood infection assay has been used to identify microbial virulence factors, to analyze early immune responses and to test potential therapeutic approaches [252-257]. Further using this model, time-resolved data can be obtained on cell activation, localization and physiological state of the pathogen [258] and there are two important advantages: the minimal pre-analytical handling of the cells and the analysis of host-pathogen interaction in a situation close the one *in vivo* with others humoral factors and immune cells [62]. On the other hand, activated primary NK cells are already used in current clinical approaches. NK cells have been taken into consideration for their importance during fungal infections; even if, on the other hand their role and the activation mechanism has not yet been clarified. More studies on NK cells could bring to the use of these immune cells in the treatment of invasive fungal infection in the clinical setting.

7.2.1 Different levels of NK cell stimulation

In this study, an important first finding was that NK cell stimulation patterns depended on the milieu and *Candida* species. Indeed, a comparison between cytokine-activated human NK cells and blood NK cells regulation was performed in response to *C. albicans* and *C. glabrata* infections and it has been clarified how these cells responded in this two different fungal infection. Our data reveal that primary NK cells have a significantly stronger response against *C. albicans* than *C. glabrata.* This response was characterized by an up-regulation of the degranulation pathway and down-modulation of Fcγ receptor III on the NK cell surface and requires direct contact between NK cells and fungi [184]. It was already shown that primary NK cells are able to establish a contact with C. albicans but they are also involved in similar interactions which lead to phagocytosis [184]. However, human NK cell activation has a low efficiency for *C. albicans* killing and is followed by destruction of the immune cells due to elongation of engulfed *C. albicans* [184, 259]. In contrast, isolated mouse NK cells are able to kill *C. glabrata* upon direct interaction [185]. From this and

previous study, we concluded that primed human NK cells were activated by direct contact of fungal cells of these two different species.

None of these effects could be observed during infection of human whole blood which showed important and several differences compared to primary NK cells. The first difference with primary activated NK cells is that activation of blood NK cells was more pronounced during *C. glabrata* than *C. albicans* infection. Furthermore, the activation phenotype differed from that observed in isolated NK cells. Indeed, activation of blood NK cells was characterized by an up-regulation of both CD69 and death receptor ligand TRAIL. In contrast, the degranulation pathway represented by CD107a and the Fcγ receptor III are not involved in the effector mechanisms of blood NK cells during *Candida* infection. We concluded that compared to primary NK cells, blood NK cells were activated by soluble factors released by other immune cells.

Immune response against *Candida* infections requires the combination of several mechanisms which involved for example the recognition of fungal wall components, the activation of immune cell signaling cascade and release of cytokines and chemokines (innate immune cell response upon candida albicans infection) [260]. In this contest, professional immune cells present different important role, for example, PMN mostly have the role of engulfing. Among all immune cells, monocytes and DC are able to release large amount of cytokines and chemokines once they are activated. Once the use of monocytes has been excluded, we focused on the cross-talk between DC and NK cell. It was already shown can bring to activation of cell types during infection with Aspergillus fumigates and that this reciprocal interaction and activation need the release of soluble and contact factors [138, 189].

The blood activation phenotype could be mimicked by co-incubation with *Candida*-activated DC. This supports the hypothesis that the lower degree of blood NK cell activation during *C. albicans* infection can be explained by different levels of secreted cytokines as detected during DC-NK cell-*Candida* co-incubation experiments.

The different activation profiles expressed by NK cells dependent on the milieu and *Candida* species were also reflected by different IFN-γ secretion. IFN-γ was highly secreted by primary NK cells in response to *C. albicans* infection. For blood NK cells and during NK cell-moDC co-culture levels were higher for *C. glabrata*.

The important role of IFN-γ as pro-inflammatory cytokine to control *Candida* infections was already demonstrated *in vivo* [261]. IFN-γ knockout mice are more sensitive to invasive *C. albicans* infection than wild-type mice, where IFN-γ is able to improve *C. albicans* phagocytosis and killing by PMN and macrophages [262-264]. IFN-γ is also known to enhance the activity of antigen-presenting cells [136], driving among other things the secretion of Th1-inducing cytokines. Among

all functions described, different roles of IFN-γ were suggested during *Candida* infection: increasing of fungal killing upon DC treatment with IFN-γ through the NADPH oxidase modulation [265] and/or indoleamine 2,3-dioxygenase (IDO) activation responsible for the activation of killing systems in PMN and DC response in controlling Th1 or Treg immune response [266, 267]. Release of IFN-γ by NK cells could represent a possible mechanism involved in the immune response during *C. glabrata* infection, as we showed the secretion of this proinflammatory cytokine is higher during *C. glabrata* infection compared to *C. albicans* in the whole blood infection model.

Looking at the possible blood-specific stimulus able to regulate NK cells function and screening between 34 cytokines, we found IL-12 to be differentially secreted in response to *C. albicans* and *C. glabrata* infection with higher levels induced by *C. glabrata* in whole blood. NK cells on their surface expose the high-affinity receptor (IL-12Rβ1/β2) able to bind IL-12. This binding can induce activation of tyrosine kinase 2 (TYR2) and JAK2, leading among other things to production of IFN-γ by NK cells [268].

Further, levels of IL-12 in whole blood and released by DC showed equal differences between *C. albicans* and *C. glabrata*. Difference in of IL-12 release during the infection by these two fungal species could be correlated to the fungal morphology, indeed, it is already well documented that higher secretion of IL-12 occurs in response to yeasts by human blood monocytes as well as mouse and human DC, whereas a reduced IL-12 production is elicited upon exposure to hyphae [252, 269-272].

Using a Transwell system, we could demonstrate that NK cells are indirectly activated by soluble factor(s) released by DC upon infection by *C. albicans* and *C. glabrata*.

The regulatory function of DC-derived IL-12 on NK cell activation was verified using a IL-12 neutralizing antibody. With that, we could show that DC-derived IL-12 is responsible for the IFN-γ secretion by NK cells. Presence of the IL-12 blocking antibody completely inhibited IFN-γ production. The lower *C. albicans* activation degree could reflect the less amount of IL-12 found in the plasma after blood infection and in the supernatant after moDC stimulation in response to *C. albicans*. In line with this, differences in IL-12 secretion in response to both *Candida* species are also partially responsible for different levels of NK cell activation in blood. However, our data revealed the contribution of additional and until unknown cytokines or humoral factors to fully stimulate NK cells.

A key virulence factor of *C. albicans* is the secretion of aspartic proteases (Sap), which are involved in *Candida* adhesion [210, 211] as well as invasion of, and damage to epithelial cells and tissue. furthermore, it was shown that SAPs are able to cleave a broad range of proteins and could be possibly also responsible for modulation of the cytokine milieu [210].

Immune response against fungal pathogens is accompanied by a strong pro-inflammatory reaction by a secretion of a broad range of cytokines by different immune cells (Cytokines and fungal infections paper).

Whole-blood infection revealed different levels of cytokines production between *C. albicans* and *C. glabrata*. Indeed, IL-1β, IL-6, TNF-α and IL-12 were highly produced in response to *C. glabrata* then *C. albicans* infection after 4 hours of confrontation and although this profile disappeared after 8 hours, different in plasma of IL-1β and IL-12 were clearly present.

The impact of *C. albicans* SAPs on the lower detected cytokine levels (IL-1β, IL-6, TNF-α, and IL-12) compared to *C. glabrata* confrontation was checked using inactivated fungi for infection and revealed no differences using either alive or thimerosal inactivated fungal cells. Thus, the impact of SAP protease activity during *C. albicans* infection is not responsible for the species-specific difference in IL-12 levels.

Another key virulence factor of *C. albicans* is its morphological plasticity which has been linked to its pathogenicity as filamentous forms are associated with tissue invasion and infection [59]. *C. albicans* filamentation was observed during whole-blood [62] and for this reason made sense to check *Candida* morphology switching influence on blood NK cell activation. Interesting, no differences in blood NK cell activation during infection with *C. albicans* wild type and the non-filamentous *C. albicans* mutant *cph1Δ/efg1Δ* were detected. Differences in NK cells stimulation induced by *C. albicans* and *C. glabrata* were still evident, especially the higher IL-12 secretion in response to *C. glabrata*. Consequently, blood NK cell stimulation as well as cytokine secretion are not dependent on *Candida* morphology.

Taken together, our data showed that differences in IL-12p70 secretion by moDC in response to both *Candida* spp. are responsible for the IFN-γ secretion by the NK cells. The different secretion of IFN-γ in response to *C. albicans* and *C. glabrata* could represent an important finding especially for the use of this cytokine in the treatment of patients with severe invasive fungal infections. It was already showed that treatment with IFN-γ presents beneficial clinical effect as the general leukocyte immune response improvement [273].

8 Bibliography

1. Viscoli, C., *Bloodstream Infections: The peak of the iceberg.* Virulence, 2016. **7**(3): p. 248-251.

2. Huerta, L.E. and T.W. Rice, *Pathologic Difference between Sepsis and Bloodstream Infections.* 2019. **3**(4): p. 654-663.

3. Prowle, J.R., et al., *Acquired bloodstream infection in the intensive care unit: incidence and attributable mortality.* Critical care (London, England), 2011. **15**(2): p. R100-R100.

4. Pittet, D., D. Tarara, and R.P. Wenzel, *Nosocomial bloodstream infection in critically ill patients. Excess length of stay, extra costs, and attributable mortality.* Jama, 1994. **271**(20): p. 1598-601.

5. Soufir, L., et al., *Attributable morbidity and mortality of catheter-related septicemia in critically ill patients: a matched, risk-adjusted, cohort study.* Infect Control Hosp Epidemiol, 1999. **20**(6): p. 396-401.

6. Garrouste-Orgeas, M., et al., *Excess risk of death from intensive care unit-acquired nosocomial bloodstream infections: a reappraisal.* Clin Infect Dis, 2006. **42**(8): p. 1118-26.

7. Laupland, K.B., et al., *Population-based assessment of intensive care unit-acquired bloodstream infections in adults: Incidence, risk factors, and associated mortality rate.* Crit Care Med, 2002. **30**(11): p. 2462-7.

8. Renaud, B. and C. Brun-Buisson, *Outcomes of primary and catheter-related bacteremia. A cohort and case-control study in critically ill patients.* Am J Respir Crit Care Med, 2001. **163**(7): p. 1584-90.

9. Schwab, F., et al., *ICU mortality following ICU-acquired primary bloodstream infections according to the type of pathogen: A prospective cohort study in 937 Germany ICUs (2006-2015).* PLoS One, 2018. **13**(3): p. e0194210.

10. Horn, D.L., et al., *Presentation of the PATH Alliance registry for prospective data collection and analysis of the epidemiology, therapy, and outcomes of invasive fungal infections.* Diagn Microbiol Infect Dis, 2007. **59**(4): p. 407-14.

11. Wisplinghoff, H., et al., *Nosocomial bloodstream infections in US hospitals: analysis of 24,179 cases from a prospective nationwide surveillance study.* Clin Infect Dis, 2004. **39**(3): p. 309-17.

12. Kett, D.H., et al., *Candida bloodstream infections in intensive care units: analysis of the extended prevalence of infection in intensive care unit study.* Crit Care Med, 2011. **39**(4): p. 665-70.

13. Perlroth, J., B. Choi, and B. Spellberg, *Nosocomial fungal infections: epidemiology, diagnosis, and treatment.* Med Mycol, 2007. **45**(4): p. 321-46.

14.   Brunke, S. and B. Hube, *Two unlike cousins: Candida albicans and C. glabrata infection strategies.* Cell Microbiol, 2013. **15**(5): p. 701-8.

15.   Cole, G.T., A.A. Halawa, and E.J. Anaissie, *The role of the gastrointestinal tract in hematogenous candidiasis: from the laboratory to the bedside.* Clin Infect Dis, 1996. **22 Suppl 2**: p. S73-88.

16.   Fidel, P.L., Jr., J.A. Vazquez, and J.D. Sobel, *Candida glabrata: review of epidemiology, pathogenesis, and clinical disease with comparison to C. albicans.* Clin Microbiol Rev, 1999. **12**(1): p. 80-96.

17.   Jones, T., et al., *The diploid genome sequence of Candida albicans.* Proc Natl Acad Sci U S A, 2004. **101**(19): p. 7329-34.

18.   Hoyer, L.L., *The ALS gene family of Candida albicans.* Trends Microbiol, 2001. **9**(4): p. 176-80.

19.   Ghannoum, M.A., *Potential role of phospholipases in virulence and fungal pathogenesis.* Clin Microbiol Rev, 2000. **13**(1): p. 122-43, table of contents.

20.   Calderone, R.A. and W.A. Fonzi, *Virulence factors of Candida albicans.* Trends Microbiol, 2001. **9**(7): p. 327-35.

21.   de Groot, P.W., et al., *The cell wall of the human pathogen Candida glabrata: differential incorporation of novel adhesin-like wall proteins.* Eukaryot Cell, 2008. **7**(11): p. 1951-64.

22.   Kaur, R., B. Ma, and B.P. Cormack, *A family of glycosylphosphatidylinositol-linked aspartyl proteases is required for virulence of Candida glabrata.* Proceedings of the National Academy of Sciences of the United States of America, 2007. **104**(18): p. 7628-7633.

23.   Sudbery, P.E., *Growth of Candida albicans hyphae.* Nature Reviews Microbiology, 2011. **9**(10): p. 737-748.

24.   Saville, S.P., et al., *Engineered control of cell morphology in vivo reveals distinct roles for yeast and filamentous forms of Candida albicans during infection.* Eukaryot Cell, 2003. **2**(5): p. 1053-60.

25.   Hoyer, L.L., et al., *Discovering the secrets of the Candida albicans agglutinin-like sequence (ALS) gene family--a sticky pursuit.* Med Mycol, 2008. **46**(1): p. 1-15.

26.   Staab, J.F., et al., *Adhesive and mammalian transglutaminase substrate properties of Candida albicans Hwp1.* Science, 1999. **283**(5407): p. 1535-8.

27.   Wachtler, B., et al., *Candida albicans-epithelial interactions: dissecting the roles of active penetration, induced endocytosis and host factors on the infection process.* PLoS One, 2012. **7**(5): p. e36952.

28.   Almeida, R.S., et al., *the hyphal-associated adhesin and invasin Als3 of Candida albicans mediates iron acquisition from host ferritin.* PLoS pathogens, 2008. **4**(11): p. e1000217-e1000217.

29.   Silverman, R.J., et al., *Interaction of Candida albicans cell wall Als3 protein with Streptococcus gordonii SspB adhesin promotes development of mixed-species communities.* Infect Immun, 2010. **78**(11): p. 4644-52.

30.   Phan, Q.T., et al., *Als3 is a Candida albicans invasin that binds to cadherins and induces endocytosis by host cells.* PLoS Biol, 2007. **5**(3): p. e64.

31.   Rodrigues, C.F., et al., *Candida glabrata Biofilms: How Far Have We Come?* Journal of fungi (Basel, Switzerland), 2017. **3**(1): p. 11.

32.   Cormack, B.P., N. Ghori, and S. Falkow, *An adhesin of the yeast pathogen Candida glabrata mediating adherence to human epithelial cells.* Science, 1999. **285**(5427): p. 578-82.

33.   Riera, M., et al., *New regulators of biofilm development in Candida glabrata.* Res Microbiol, 2012. **163**(4): p. 297-307.

34.   De Las Penas, A., et al., *Virulence-related surface glycoproteins in the yeast pathogen Candida glabrata are encoded in subtelomeric clusters and subject to RAP1- and SIR-dependent transcriptional silencing.* Genes Dev, 2003. **17**(18): p. 2245-58.

35.   Wachtler, B., et al., *From attachment to damage: defined genes of Candida albicans mediate adhesion, invasion and damage during interaction with oral epithelial cells.* PLoS One, 2011. **6**(2): p. e17046.

36.   Watts, H.J., et al., *Thigmotropism and stretch-activated channels in the pathogenic fungus Candida albicans.* Microbiology, 1998. **144 (Pt 3)**: p. 689-95.

37.   Li, Z. and K. Nielsen, *Morphology Changes in Human Fungal Pathogens upon Interaction with the Host.* Journal of fungi (Basel, Switzerland), 2017. **3**(4): p. 66.

38.   Jacobsen, I.D., et al., *Candida albicans dimorphism as a therapeutic target.* Expert Rev Anti Infect Ther, 2012. **10**(1): p. 85-93.

39.   Naglik, J.R., et al., *Differential expression of Candida albicans secreted aspartyl proteinase and phospholipase B genes in humans correlates with active oral and vaginal infections.* J Infect Dis, 2003. **188**(3): p. 469-79.

40.   Allert, S., et al., *Candida albicans-Induced Epithelial Damage Mediates Translocation through Intestinal Barriers.* 2018. **9**(3): p. e00915-18.

41.   Moyes, D.L., et al., *Candidalysin is a fungal peptide toxin critical for mucosal infection.* Nature, 2016. **532**(7597): p. 64-8.

42.   Silva, S., et al., *Candida glabrata and Candida albicans co-infection of an in vitro oral epithelium.* J Oral Pathol Med, 2011. **40**(5): p. 421-7.

43.   Coco, B.J., et al., *Mixed Candida albicans and Candida glabrata populations associated with the pathogenesis of denture stomatitis.* Oral Microbiol Immunol, 2008. **23**(5): p. 377-83.

44.   Okada, K., et al., *A Clinical Study of Candida albicans and Candida glabrata Co-infection of Oral Candidiasis.* Ronen Shika Igaku, 2016. **31**(3): p. 346-353.

45.   Tsay, S., et al., *A Tale of Two Healthcare-associated Infections: Clostridium difficile Coinfection Among Patients With Candidemia.* Clin Infect Dis, 2019. **68**(4): p. 676-679.

46.   Tati, S., et al., *Candida glabrata Binding to Candida albicans Hyphae Enables Its Development in Oropharyngeal Candidiasis.* PLoS Pathog, 2016. **12**(3): p. e1005522.

47.   Li, L. and A. Dongari-Bagtzoglou, *Epithelial GM-CSF induction by Candida glabrata.* J Dent Res, 2009. **88**(8): p. 746-51.

48.   Fatahinia, M., M. Halvaeezadeh, and A. Rezaei-Matehkolaei, *Comparison of enzymatic activities in different Candida species isolated from women with vulvovaginitis.* J Mycol Med, 2017. **27**(2): p. 188-194.

49.   Riceto, E.B., et al., *Enzymatic and hemolytic activity in different Candida species.* Rev Iberoam Micol, 2015. **32**(2): p. 79-82.

50.   Atalay, M.A., et al., *Investigation of possible virulence factors in Candida strains isolated from blood cultures.* Niger J Clin Pract, 2015. **18**(1): p. 52-5.

51.   Pandey, N., M.K. Gupta, and R. Tilak, *Extracellular hydrolytic enzyme activities of the different Candida spp. isolated from the blood of the Intensive Care Unit-admitted patients.* Journal of laboratory physicians, 2018. **10**(4): p. 392-396.

52.   Rodrigues, C.F., S. Silva, and M. Henriques, *Candida glabrata: a review of its features and resistance.* Eur J Clin Microbiol Infect Dis, 2014. **33**(5): p. 673-88.

53.   Brown, G.D. and S. Gordon, *Fungal beta-glucans and mammalian immunity.* Immunity, 2003. **19**(3): p. 311-5.

54.   Erwig, L.P. and N.A. Gow, *Interactions of fungal pathogens with phagocytes.* Nat Rev Microbiol, 2016. **14**(3): p. 163-76.

55.   Netea, M.G., et al., *An integrated model of the recognition of Candida albicans by the innate immune system.* Nat Rev Microbiol, 2008. **6**(1): p. 67-78.

56.   Miramon, P., L. Kasper, and B. Hube, *Thriving within the host: Candida spp. interactions with phagocytic cells.* Med Microbiol Immunol, 2013. **202**(3): p. 183-95.

57.   Brunke, S. and B. Hube, *Two unlike cousins: Candida albicans and C. glabrata infection strategies.* Cellular microbiology, 2013. **15**(5): p. 701-708.

58.   Duggan, S., et al., *Neutrophil activation by Candida glabrata but not Candida albicans promotes fungal uptake by monocytes.* Cell Microbiol, 2015. **17**(9): p. 1259-76.

59.   Wozniok, I., et al., *Induction of ERK-kinase signalling triggers morphotype-specific killing of Candida albicans filaments by human neutrophils.* Cell Microbiol, 2008. **10**(3): p. 807-20.

60.   Ramirez-Ortiz, Z.G. and T.K. Means, *The role of dendritic cells in the innate recognition of pathogenic fungi (A. fumigatus, C. neoformans and C. albicans).* Virulence, 2012. **3**(7): p. 635-646.

61.   Wuthrich, M., G.S. Deepe, Jr., and B. Klein, *Adaptive immunity to fungi.* Annu Rev Immunol, 2012. **30**: p. 115-48.

62.   Hunniger, K., et al., *A virtual infection model quantifies innate effector mechanisms and Candida albicans immune escape in human blood.* PLoS Comput Biol, 2014. **10**(2): p. e1003479.

63.   Lehnert, T., et al., *Bottom-up modeling approach for the quantitative estimation of parameters in pathogen-host interactions.* Front Microbiol, 2015. **6**: p. 608.

64.   Seider, K., et al., *The facultative intracellular pathogen Candida glabrata subverts macrophage cytokine production and phagolysosome maturation.* J Immunol, 2011. **187**(6): p. 3072-86.

65.   Borregaard, N., *Neutrophils, from marrow to microbes.* Immunity, 2010. **33**(5): p. 657-70.

66.   Mayadas, T.N. and X. Cullere, *Neutrophil beta2 integrins: moderators of life or death decisions.* Trends Immunol, 2005. **26**(7): p. 388-95.

67.   Dancey, J.T., et al., *Neutrophil kinetics in man.* J Clin Invest, 1976. **58**(3): p. 705-15.

68.   Basu, S., et al., *Evaluation of role of G-CSF in the production, survival, and release of neutrophils from bone marrow into circulation.* Blood, 2002. **100**(3): p. 854-61.

69.   Hunniger, K. and O. Kurzai, *Phagocytes as central players in the defence against invasive fungal infection.* Semin Cell Dev Biol, 2019. **89**: p. 3-15.

70.   Delgado-Rizo, V., et al., *Neutrophil Extracellular Traps and Its Implications in Inflammation: An Overview.* Frontiers in immunology, 2017. **8**: p. 81-81.

71.   Rosales, C. and E. Uribe-Querol, *Phagocytosis: A Fundamental Process in Immunity.* BioMed research international, 2017. **2017**: p. 9042851-9042851.

72.   Nordenfelt, P. and H. Tapper, *Phagosome dynamics during phagocytosis by neutrophils.* J Leukoc Biol, 2011. **90**(2): p. 271-84.

73.   Allen, L.A. and A. Aderem, *Molecular definition of distinct cytoskeletal structures involved in complement- and Fc receptor-mediated phagocytosis in macrophages.* J Exp Med, 1996. **184**(2): p. 627-37.

74.   Faurschou, M. and N. Borregaard, *Neutrophil granules and secretory vesicles in inflammation.* Microbes Infect, 2003. **5**(14): p. 1317-27.

75.   Kuijpers, T. and R. Lutter, *Inflammation and repeated infections in CGD: two sides of a coin.* Cell Mol Life Sci, 2012. **69**(1): p. 7-15.

76.   Williams, R., *Killing controversy.* J Exp Med, 2006. **203**(11): p. 2404.

77.   Estúa-Acosta, G.A., et al., *Neutrophil Extracellular Traps: Current Perspectives in the Eye.* Cells, 2019. **8**(9).

78.   Papayannopoulos, V., et al., *Neutrophil elastase and myeloperoxidase regulate the formation of neutrophil extracellular traps.* The Journal of cell biology, 2010. **191**(3): p. 677-691.

79.   Mantovani, A., et al., *Neutrophils in the activation and regulation of innate and adaptive immunity.* Nat Rev Immunol, 2011. **11**(8): p. 519-31.

80.   Amulic, B., et al., *Neutrophil function: from mechanisms to disease.* Annu Rev Immunol, 2012. **30**: p. 459-89.

81.   Kolaczkowska, E. and P. Kubes, *Neutrophil recruitment and function in health and inflammation.* Nat Rev Immunol, 2013. **13**(3): p. 159-75.

82.   Yang, D., et al., *Alarmins link neutrophils and dendritic cells.* Trends Immunol, 2009. **30**(11): p. 531-7.

83.   Charmoy, M., et al., *Neutrophil-derived CCL3 is essential for the rapid recruitment of dendritic cells to the site of Leishmania major inoculation in resistant mice.* PLoS Pathog, 2010. **6**(2): p. e1000755.

84.   Abi Abdallah, D.S., et al., *Mouse neutrophils are professional antigen-presenting cells programmed to instruct Th1 and Th17 T-cell differentiation.* Int Immunol, 2011. **23**(5): p. 317-26.

85.   Gudlaugsson, O., et al., *Attributable mortality of nosocomial candidemia, revisited.* Clin Infect Dis, 2003. **37**(9): p. 1172-7.

86.   McDonald, B., et al., *Intravascular danger signals guide neutrophils to sites of sterile inflammation.* Science, 2010. **330**(6002): p. 362-6.

87.   Gazendam, R.P., et al., *Human Neutrophils Use Different Mechanisms To Kill Aspergillus fumigatus Conidia and Hyphae: Evidence from Phagocyte Defects.* J Immunol, 2016. **196**(3): p. 1272-83.

88.   Gazendam, R.P., et al., *Two independent killing mechanisms of Candida albicans by human neutrophils: evidence from innate immunity defects.* Blood, 2014. **124**(4): p. 590-7.

89.   Winkelstein, J.A., et al., *Chronic granulomatous disease. Report on a national registry of 368 patients.* Medicine (Baltimore), 2000. **79**(3): p. 155-69.

90.   Lanternier, F., et al., *Primary immunodeficiencies underlying fungal infections.* Current opinion in pediatrics, 2013. **25**(6): p. 736-747.

91.   Lanza, F., *Clinical manifestation of myeloperoxidase deficiency.* J Mol Med (Berl), 1998. **76**(10): p. 676-81.

92.   Zhu, L.L., et al., *C-type lectin receptors Dectin-3 and Dectin-2 form a heterodimeric pattern-recognition receptor for host defense against fungal infection.* Immunity, 2013. **39**(2): p. 324-34.

93.   Kennedy, A.D., et al., *Dectin-1 promotes fungicidal activity of human neutrophils.* Eur J Immunol, 2007. **37**(2): p. 467-78.

94.   Ifrim, D.C., et al., *Role of Dectin-2 for host defense against systemic infection with Candida glabrata.* Infect Immun, 2014. **82**(3): p. 1064-73.

95.   LeibundGut-Landmann, S., et al., *Syk- and CARD9-dependent coupling of innate immunity to the induction of T helper cells that produce interleukin 17.* Nat Immunol, 2007. **8**(6): p. 630-8.

96.   Rubin-Bejerano, I., et al., *Phagocytosis by human neutrophils is stimulated by a unique fungal cell wall component.* Cell Host Microbe, 2007. **2**(1): p. 55-67.

97.   Byrd, A.S., et al., *An extracellular matrix-based mechanism of rapid neutrophil extracellular trap formation in response to Candida albicans.* J Immunol, 2013. **190**(8): p. 4136-48.

98.   van Bruggen, R., et al., *Complement receptor 3, not Dectin-1, is the major receptor on human neutrophils for beta-glucan-bearing particles.* Mol Immunol, 2009. **47**(2-3): p. 575-81.

99.   Fradin, C., et al., *Stage-specific gene expression of Candida albicans in human blood.* Mol Microbiol, 2003. **47**(6): p. 1523-43.

100.   Kaloriti, D., et al., *Combinatorial stresses kill pathogenic Candida species.* Med Mycol, 2012. **50**(7): p. 699-709.

101.   Kaloriti, D., et al., *Mechanisms underlying the exquisite sensitivity of Candida albicans to combinatorial cationic and oxidative stress that enhances the potent fungicidal activity of phagocytes.* mBio, 2014. **5**(4): p. e01334-14.

102.   Miramon, P., et al., *Cellular responses of Candida albicans to phagocytosis and the extracellular activities of neutrophils are critical to counteract carbohydrate starvation, oxidative and nitrosative stress.* PLoS One, 2012. **7**(12): p. e52850.

103.   Chayakulkeeree, M., et al., *SEC14 is a specific requirement for secretion of phospholipase B1 and pathogenicity of Cryptococcus neoformans.* Mol Microbiol, 2011. **80**(4): p. 1088-101.

104.   Essig, F., et al., *Human neutrophils dump Candida glabrata after intracellular killing.* Fungal Genet Biol, 2015. **84**: p. 37-40.

105.   Spits, H., et al., *Innate lymphoid cells--a proposal for uniform nomenclature.* Nat Rev Immunol, 2013. **13**(2): p. 145-9.

106.   Campbell, K.S. and J. Hasegawa, *Natural killer cell biology: an update and future directions.* J Allergy Clin Immunol, 2013. **132**(3): p. 536-544.

107.   Schmidt, S., L. Tramsen, and T. Lehrnbecher, *Natural Killer Cells in Antifungal Immunity.* Front Immunol, 2017. **8**: p. 1623.

108.   Algarra, I., et al., *Suppression of splenic macrophage Candida albicans phagocytosis following in vivo depletion of natural killer cells in immunocompetent BALB/c mice and T-cell-deficient nude mice.* FEMS Immunol Med Microbiol, 2002. **33**(3): p. 159-63.

109.   Pegram, H.J., et al., *Activating and inhibitory receptors of natural killer cells.* Immunol Cell Biol, 2011. **89**(2): p. 216-24.

110.   Vivier, E., et al., *Functions of natural killer cells.* Nat Immunol, 2008. **9**(5): p. 503-10.

111.   Paul, S. and G. Lal, *The Molecular Mechanism of Natural Killer Cells Function and Its Importance in Cancer Immunotherapy.* Front Immunol, 2017. **8**: p. 1124.

112.   Duke, R.C., et al., *Purified perforin induces target cell lysis but not DNA fragmentation.* J Exp Med, 1989. **170**(4): p. 1451-6.

113.   Law, R.H., et al., *The structural basis for membrane binding and pore formation by lymphocyte perforin.* Nature, 2010. **468**(7322): p. 447-51.

114.   Ernst, W.A., et al., *Granulysin, a T cell product, kills bacteria by altering membrane permeability.* J Immunol, 2000. **165**(12): p. 7102-8.

115.   Gamen, S., et al., *Granulysin-induced apoptosis. I. Involvement of at least two distinct pathways.* J Immunol, 1998. **161**(4): p. 1758-64.

116.   Kaspar, A.A., et al., *A distinct pathway of cell-mediated apoptosis initiated by granulysin.* J Immunol, 2001. **167**(1): p. 350-6.

117.   Krensky, A.M. and C. Clayberger, *Biology and clinical relevance of granulysin.* Tissue Antigens, 2009. **73**(3): p. 193-8.

118.   Okada, S., et al., *Intracellular mediators of granulysin-induced cell death.* J Immunol, 2003. **171**(5): p. 2556-62.

119.   Alter, G., J.M. Malenfant, and M. Altfeld, *CD107a as a functional marker for the identification of natural killer cell activity.* J Immunol Methods, 2004. **294**(1-2): p. 15-22.

120.   Krzewski, K., et al., *LAMP1/CD107a is required for efficient perforin delivery to lytic granules and NK-cell cytotoxicity.* Blood, 2013. **121**(23): p. 4672-83.

121.   French, L.E. and J. Tschopp, *Protein-based therapeutic approaches targeting death receptors.* Cell Death Differ, 2003. **10**(1): p. 117-23.

122.   Wajant, H., K. Pfizenmaier, and P. Scheurich, *Tumor necrosis factor signaling.* Cell Death Differ, 2003. **10**(1): p. 45-65.

123.   Thorburn, A., *Death receptor-induced cell killing.* Cell Signal, 2004. **16**(2): p. 139-44.

124.   Chinnaiyan, A.M., et al., *FADD, a novel death domain-containing protein, interacts with the death domain of Fas and initiates apoptosis.* Cell, 1995. **81**(4): p. 505-12.

125.   Salvesen, G.S. and V.M. Dixit, *Caspase activation: the induced-proximity model.* Proc Natl Acad Sci U S A, 1999. **96**(20): p. 10964-7.

126.   Fischer, U., R.U. Jänicke, and K. Schulze-Osthoff, *Many cuts to ruin: a comprehensive update of caspase substrates.* Cell Death Differ, 2003. **10**(1): p. 76-100.

127. Degli-Esposti, M., *To die or not to die--the quest of the TRAIL receptors.* J Leukoc Biol, 1999. **65**(5): p. 535-42.

128. Smyth, M.J., et al., *Activation of NK cell cytotoxicity.* Mol Immunol, 2005. **42**(4): p. 501-10.

129. Gyurkovska, V. and N. Ivanovska, *Distinct roles of TNF-related apoptosis-inducing ligand (TRAIL) in viral and bacterial infections: from pathogenesis to pathogen clearance.* Inflamm Res, 2016. **65**(6): p. 427-37.

130. Leverkus, M., et al., *Regulation of tumor necrosis factor-related apoptosis-inducing ligand sensitivity in primary and transformed human keratinocytes.* Cancer Res, 2000. **60**(3): p. 553-9.

131. Alexander, E.H., et al., *Staphylococcus aureus - induced tumor necrosis factor - related apoptosis - inducing ligand expression mediates apoptosis and caspase-8 activation in infected osteoblasts.* BMC Microbiol, 2003. **3**: p. 5.

132. Ashkenazi, A. and R.S. Herbst, *To kill a tumor cell: the potential of proapoptotic receptor agonists.* J Clin Invest, 2008. **118**(6): p. 1979-90.

133. Unwalla, H., et al., *Potent inhibition of HIV-1 gene expression and TAT-mediated apoptosis in human T cells by novel mono- and multitarget anti-TAT/Rev/Env ribozymes and a general purpose RNA-cleaving DNA-enzyme.* Antiviral Res, 2006. **72**(2): p. 134-44.

134. Wang, W., et al., *NK Cell-Mediated Antibody-Dependent Cellular Cytotoxicity in Cancer Immunotherapy.* Frontiers in immunology, 2015. **6**: p. 368-368.

135. Caligiuri, M.A., *Human natural killer cells.* 2008. **112**(3): p. 461-469.

136. Wallach, D., M. Fellous, and M. Revel, *Preferential effect of gamma interferon on the synthesis of HLA antigens and their mRNAs in human cells.* Nature, 1982. **299**(5886): p. 833-6.

137. Filipe-Santos, O., et al., *Inborn errors of IL-12/23- and IFN-gamma-mediated immunity: molecular, cellular, and clinical features.* Semin Immunol, 2006. **18**(6): p. 347-61.

138. Cooper, M.A., et al., *NK cell and DC interactions.* Trends Immunol, 2004. **25**(1): p. 47-52.

139. Ljunggren, H.G. and K. Karre, *In search of the 'missing self': MHC molecules and NK cell recognition.* Immunol Today, 1990. **11**(7): p. 237-44.

140. Liu, L.L., et al., *Ex Vivo Expanded Adaptive NK Cells Effectively Kill Primary Acute Lymphoblastic Leukemia Cells.* Cancer Immunol Res, 2017. **5**(8): p. 654-665.

141. Schlegel, P., et al., *NKG2D Signaling Leads to NK Cell Mediated Lysis of Childhood AML.* J Immunol Res, 2015. **2015**: p. 473175.

142. Castriconi, R., et al., *Natural killer cell-mediated killing of freshly isolated neuroblastoma cells: critical role of DNAX accessory molecule-1-poliovirus receptor interaction.* Cancer Res, 2004. **64**(24): p. 9180-4.

143.   Kloess, S., et al., *IL-2-activated haploidentical NK cells restore NKG2D-mediated NK-cell cytotoxicity in neuroblastoma patients by scavenging of plasma MICA.* Eur J Immunol, 2010. **40**(11): p. 3255-67.

144.   Smyth, M.J., N.Y. Crowe, and D.I. Godfrey, *NK cells and NKT cells collaborate in host protection from methylcholanthrene-induced fibrosarcoma.* Int Immunol, 2001. **13**(4): p. 459-63.

145.   O'Sullivan, T., et al., *Cancer immunoediting by the innate immune system in the absence of adaptive immunity.* J Exp Med, 2012. **209**(10): p. 1869-82.

146.   Kaplan, D.H., et al., *Demonstration of an interferon gamma-dependent tumor surveillance system in immunocompetent mice.* Proc Natl Acad Sci U S A, 1998. **95**(13): p. 7556-61.

147.   Smyth, M.J., et al., *NKG2D function protects the host from tumor initiation.* J Exp Med, 2005. **202**(5): p. 583-8.

148.   Smyth, M.J., et al., *Perforin-mediated cytotoxicity is critical for surveillance of spontaneous lymphoma.* J Exp Med, 2000. **192**(5): p. 755-60.

149.   Iannello, A., et al., *p53-dependent chemokine production by senescent tumor cells supports NKG2D-dependent tumor elimination by natural killer cells.* J Exp Med, 2013. **210**(10): p. 2057-69.

150.   Miller, J.S., et al., *Successful adoptive transfer and in vivo expansion of human haploidentical NK cells in patients with cancer.* Blood, 2005. **105**(8): p. 3051-7.

151.   Curti, A., et al., *Successful transfer of alloreactive haploidentical KIR ligand-mismatched natural killer cells after infusion in elderly high risk acute myeloid leukemia patients.* Blood, 2011. **118**(12): p. 3273-9.

152.   Shah, N., et al., *Antigen presenting cell-mediated expansion of human umbilical cord blood yields log-scale expansion of natural killer cells with anti-myeloma activity.* PLoS One, 2013. **8**(10): p. e76781.

153.   Veluchamy, J.P., et al., *High-efficiency lysis of cervical cancer by allogeneic NK cells derived from umbilical cord progenitors is independent of HLA status.* Cancer Immunol Immunother, 2017. **66**(1): p. 51-61.

154.   Marçais, A., et al., *The metabolic checkpoint kinase mTOR is essential for IL-15 signaling during the development and activation of NK cells.* Nat Immunol, 2014. **15**(8): p. 749-757.

155.   Chu, J., et al., *CS1-specific chimeric antigen receptor (CAR)-engineered natural killer cells enhance in vitro and in vivo antitumor activity against human multiple myeloma.* Leukemia, 2014. **28**(4): p. 917-27.

156.   Jiang, H., et al., *Transfection of chimeric anti-CD138 gene enhances natural killer cell activation and killing of multiple myeloma cells.* Mol Oncol, 2014. **8**(2): p. 297-310.

157.   Esser, R., et al., *NK cells engineered to express a GD2 -specific antigen receptor display built-in ADCC-like activity against tumour cells of neuroectodermal origin.* J Cell Mol Med, 2012. **16**(3): p. 569-81.

158.   Altvater, B., et al., *2B4 (CD244) signaling by recombinant antigen-specific chimeric receptors costimulates natural killer cell activation to leukemia and neuroblastoma cells.* Clin Cancer Res, 2009. **15**(15): p. 4857-66.

159.   Chang, Y.H., et al., *A chimeric receptor with NKG2D specificity enhances natural killer cell activation and killing of tumor cells.* Cancer Res, 2013. **73**(6): p. 1777-86.

160.   Vey, N., et al., *A phase 1 trial of the anti-inhibitory KIR mAb IPH2101 for AML in complete remission.* Blood, 2012. **120**(22): p. 4317-23.

161.   Korde, N., et al., *A phase II trial of pan-KIR2D blockade with IPH2101 in smoldering multiple myeloma.* Haematologica, 2014. **99**(6): p. e81-3.

162.   Lam, V.C. and L.L. Lanier, *NK cells in host responses to viral infections.* Curr Opin Immunol, 2017. **44**: p. 43-51.

163.   Beziat, V., et al., *CMV drives clonal expansion of NKG2C+ NK cells expressing self-specific KIRs in chronic hepatitis patients.* Eur J Immunol, 2012. **42**(2): p. 447-57.

164.   Garcia-Penarrubia, P., et al., *Antibacterial activity of human natural killer cells.* J Exp Med, 1989. **169**(1): p. 99-113.

165.   Wherry, J.C., R.D. Schreiber, and E.R. Unanue, *Regulation of gamma interferon production by natural killer cells in scid mice: roles of tumor necrosis factor and bacterial stimuli.* Infect Immun, 1991. **59**(5): p. 1709-15.

166.   Schmidt, S., et al., *NK Cells and Their Role in Invasive Mold Infection.* Journal of fungi (Basel, Switzerland), 2017. **3**(2): p. 25.

167.   Schmidt, S., et al., *Human natural killer cells exhibit direct activity against Aspergillus fumigatus hyphae, but not against resting conidia.* J Infect Dis, 2011. **203**(3): p. 430-5.

168.   Hidore, M.R., et al., *Cytoplasmic components of natural killer cells limit the growth of Cryptococcus neoformans.* J Leukoc Biol, 1990. **48**(1): p. 15-26.

169.   Benedetto, N., et al., *Interleukin-2 and increased natural killer activity in mice experimentally infected with Aspergillus niger.* Microbiologica, 1988. **11**(4): p. 339-45.

170.   Li, S.S., et al., *The NK receptor NKp30 mediates direct fungal recognition and killing and is diminished in NK cells from HIV-infected patients.* Cell Host Microbe, 2013. **14**(4): p. 387-97.

171.   Quintin, J., et al., *Differential role of NK cells against Candida albicans infection in immunocompetent or immunocompromised mice.* Eur J Immunol, 2014. **44**(8): p. 2405-14.

172.   Park, Y.W., et al., *Impaired differentiation and cytotoxicity of natural killer cells in systemic lupus erythematosus.* Arthritis Rheum, 2009. **60**(6): p. 1753-63.

173.   Stuehler, C., et al., *Immune Reconstitution After Allogeneic Hematopoietic Stem Cell Transplantation and Association With Occurrence and Outcome of Invasive Aspergillosis.* J Infect Dis, 2015. **212**(6): p. 959-67.

174.   Fernandez-Ruiz, M., et al., *Low Natural Killer Cell Counts and Onset of Invasive Fungal Disease After Solid Organ Transplantation.* J Infect Dis, 2016. **213**(5): p. 873-4.

175.   Palma-Carlos, A.G. and M.L. Palma-Carlos, *Chronic mucocutaneous candidiasis revisited.* Allerg Immunol (Paris), 2001. **33**(6): p. 229-32.

176.   Chiu, S.J., et al., *Chronic mucocutaneous candidiasis in a 6-year-old boy.* J Microbiol Immunol Infect, 2004. **37**(3): p. 196-9.

177.   de Moraes-Vasconcelos, D., et al., *Characterization of the cellular immune function of patients with chronic mucocutaneous candidiasis.* Clin Exp Immunol, 2001. **123**(2): p. 247-53.

178.   Schmidt, S., et al., *Rhizopus oryzae hyphae are damaged by human natural killer (NK) cells, but suppress NK cell mediated immunity.* Immunobiology, 2013. **218**(7): p. 939-44.

179.   Bouzani, M., et al., *Human NK cells display important antifungal activity against Aspergillus fumigatus, which is directly mediated by IFN-gamma release.* J Immunol, 2011. **187**(3): p. 1369-76.

180.   Aimanianda, V., et al., *Surface hydrophobin prevents immune recognition of airborne fungal spores.* Nature, 2009. **460**(7259): p. 1117-21.

181.   Chai, L.Y., et al., *Aspergillus fumigatus conidial melanin modulates host cytokine response.* Immunobiology, 2010. **215**(11): p. 915-20.

182.   Kozel, T.R. and E.C. Gotschlich, *The capsule of cryptococcus neoformans passively inhibits phagocytosis of the yeast by macrophages.* J Immunol, 1982. **129**(4): p. 1675-80.

183.   Rappleye, C.A. and W.E. Goldman, *Fungal stealth technology.* Trends Immunol, 2008. **29**(1): p. 18-24.

184.   Voigt, J., et al., *Human natural killer cells acting as phagocytes against Candida albicans and mounting an inflammatory response that modulates neutrophil antifungal activity.* J Infect Dis, 2014. **209**(4): p. 616-26.

185.   Vitenshtein, A., et al., *NK Cell Recognition of Candida glabrata through Binding of NKp46 and NCR1 to Fungal Ligands Epa1, Epa6, and Epa7.* Cell Host Microbe, 2016. **20**(4): p. 527-534.

186.   Ziegler, S., et al., *CD56 Is a Pathogen Recognition Receptor on Human Natural Killer Cells.* Sci Rep, 2017. **7**(1): p. 6138.

187.   Ogbomo, H. and C.H. Mody, *Granule-Dependent Natural Killer Cell Cytotoxicity to Fungal Pathogens.* Front Immunol, 2016. **7**: p. 692.

188.   Robinet, P., et al., *A polysaccharide virulence factor of a human fungal pathogen induces neutrophil apoptosis via NK cells.* J Immunol, 2014. **192**(11): p. 5332-42.

189. Weiss, E., et al., *First Insights in NK—DC Cross-Talk and the Importance of Soluble Factors During Infection With Aspergillus fumigatus.* 2018. **8**(288).

190. Gillum, A.M., E.Y. Tsay, and D.R. Kirsch, *Isolation of the Candida albicans gene for orotidine-5'-phosphate decarboxylase by complementation of S. cerevisiae ura3 and E. coli pyrF mutations.* Mol Gen Genet, 1984. **198**(2): p. 179-82.

191. Dujon, B., et al., *Genome evolution in yeasts.* Nature, 2004. **430**(6995): p. 35-44.

192. Al-Zaben, N., et al., *Automated tracking of label-free cells with enhanced recognition of whole tracks.* Sci Rep, 2019. **9**(1): p. 3317.

193. Brandes, S., et al., *Automated segmentation and tracking of non-rigid objects in time-lapse microscopy videos of polymorphonuclear neutrophils.* Med Image Anal, 2015. **20**(1): p. 34-51.

194. Brandes, S., et al., *Migration and interaction tracking for quantitative analysis of phagocyte-pathogen confrontation assays.* Med Image Anal, 2017. **36**: p. 172-183.

195. Belyaev I, P.J., Medyukhina A, Figge MT, *Enhanced segmentation of label-free cells for automated migration and interaction tracking.* Submitted, 2020.

196. Schuster, M., et al., *Surveillance of Myelodysplastic Syndrome via Migration Analyses of Blood Neutrophils: A Potential Prognostic Tool.* J Immunol, 2018. **201**(12): p. 3546-3557.

197. Köhler, A., et al., *G-CSF-mediated thrombopoietin release triggers neutrophil motility and mobilization from bone marrow via induction of Cxcr2 ligands.* Blood, 2011. **117**(16): p. 4349-4357.

198. Alves-Filho, J.C., et al., *The role of neutrophils in severe sepsis.* Shock, 2008. **30 Suppl 1**: p. 3-9.

199. Adamzik, M., et al., *Aquaporin 5 gene promoter--1364A/C polymorphism associated with 30-day survival in severe sepsis.* Anesthesiology, 2011. **114**(4): p. 912-7.

200. Wilcox, R.R., *Comparing Two Independent Groups Via Multiple Quantiles.* Journal of the Royal Statistical Society. Series D (The Statistician), 1995. **44**(1): p. 91-99.

201. Kozel, T.R., *Activation of the complement system by pathogenic fungi.* Clinical Microbiology Reviews, 1996. **9**(1): p. 34-46.

202. Shin, H.S., et al., *Chemotactic and Anaphylatoxic Fragment Cleaved from the Fifth Component of Guinea Pig Complement.* Science, 1968. **162**(3851): p. 361-363.

203. Goldstein, I.M. and G. Weissmann, *Generation of C5-Derived Lysosomal Enzyme-Releasing Activity (C5a) by Lysates of Leukocyte Lysosomes.* The Journal of Immunology, 1974. **113**(5): p. 1583-1588.

204. Sacks, T., et al., *Oxygen radicals mediate endothelial cell damage by complement-stimulated granulocytes. An in vitro model of immune vascular damage.* J Clin Invest, 1978. **61**(5): p. 1161-7.

205.   Hunniger, K., et al., *A second stimulus required for enhanced antifungal activity of human neutrophils in blood is provided by anaphylatoxin C5a.* J Immunol, 2015. **194**(3): p. 1199-210.

206.   Denk, S., et al., *Complement C5a-Induced Changes in Neutrophil Morphology During Inflammation.* Scandinavian journal of immunology, 2017. **86**(3): p. 143-155.

207.   Manne, B.K., S.C. Xiang, and M.T. Rondina, *Platelet secretion in inflammatory and infectious diseases.* Platelets, 2017. **28**(2): p. 155-164.

208.   Deuel, T.F., et al., *Chemotaxis of monocytes and neutrophils to platelet-derived growth factor.* The Journal of clinical investigation, 1982. **69**(4): p. 1046-1049.

209.   Alli, R.S. and A. Khar, *Interleukin-12 secreted by mature dendritic cells mediates activation of NK cell function.* FEBS Lett, 2004. **559**(1-3): p. 71-6.

210.   Naglik, J.R., S.J. Challacombe, and B. Hube, *Candida albicans secreted aspartyl proteinases in virulence and pathogenesis.* Microbiol Mol Biol Rev, 2003. **67**(3): p. 400-28, table of contents.

211.   Schaller, M., et al., *Candida albicans-Secreted Aspartic Proteinases Modify the Epithelial Cytokine Response in an In Vitro Model of Vaginal Candidiasis.* 2005. **73**(5): p. 2758-2765.

212.   Gabaldón, T., *Recent trends in molecular diagnostics of yeast infections: from PCR to NGS.* FEMS Microbiol Rev, 2019. **43**(5): p. 517-547.

213.   Clancy, C.J., et al., *Detecting Infections Rapidly and Easily for Candidemia Trial, Part 2 (DIRECT2): A Prospective, Multicenter Study of the T2Candida Panel.* Clin Infect Dis, 2018. **66**(11): p. 1678-1686.

214.   Tang, D.-L., et al., *Pooled analysis of T2 Candida for rapid diagnosis of candidiasis.* BMC Infectious Diseases, 2019. **19**(1): p. 798.

215.   Dix, A., et al., *Biomarker-based classification of bacterial and fungal whole-blood infections in a genome-wide expression study.* Front Microbiol, 2015. **6**: p. 171.

216.   Westh, H., et al., *Multiplex real-time PCR and blood culture for identification of bloodstream pathogens in patients with suspected sepsis.* Clin Microbiol Infect, 2009. **15**(6): p. 544-51.

217.   Riedel, S. and K.C. Carroll, *Early Identification and Treatment of Pathogens in Sepsis: Molecular Diagnostics and Antibiotic Choice.* Clin Chest Med, 2016. **37**(2): p. 191-207.

218.   Ansari-Lari, M.A., T.S. Kickler, and M.J. Borowitz, *Immature granulocyte measurement using the Sysmex XE-2100. Relationship to infection and sepsis.* Am J Clin Pathol, 2003. **120**(5): p. 795-9.

219.   Wenz, B., et al., *The clinical utility of the leukocyte differential in emergency medicine.* Am J Clin Pathol, 1986. **86**(3): p. 298-303.

220.   Cornbleet, P.J., *Clinical utility of the band count.* Clin Lab Med, 2002. **22**(1): p. 101-36.

221.   Berger, C., et al., *Comparison of C-reactive protein and white blood cell count with differential in neonates at risk for septicaemia.* Eur J Pediatr, 1995. **154**(2): p. 138-44.

222.   Groeneveld, A.B., et al., *Circulating inflammatory mediators in patients with fever: predicting bloodstream infection.* Clin Diagn Lab Immunol, 2001. **8**(6): p. 1189-95.

223.   Hausfater, P., et al., *Usefulness of procalcitonin as a marker of systemic infection in emergency department patients: a prospective study.* Clin Infect Dis, 2002. **34**(7): p. 895-901.

224.   Zonneveld, R., G. Molema, and F.B. Plötz, *Analyzing Neutrophil Morphology, Mechanics, and Motility in Sepsis: Options and Challenges for Novel Bedside Technologies.* Crit Care Med, 2016. **44**(1): p. 218-28.

225.   Baharlou, H., et al., *Mass Cytometry Imaging for the Study of Human Diseases-Applications and Data Analysis Strategies.* Front Immunol, 2019. **10**: p. 2657.

226.   Antinori, S., M. Corbellino, and C. Parravicini, *Challenges in the Diagnosis of Invasive Fungal Infections in Immunocompromised Hosts.* Curr Fungal Infect Rep, 2018. **12**(1): p. 12-22.

227.   Arvanitis, M., et al., *Molecular and nonmolecular diagnostic methods for invasive fungal infections.* Clin Microbiol Rev, 2014. **27**(3): p. 490-526.

228.   Kozel, T.R. and B. Wickes, *Fungal diagnostics.* Cold Spring Harb Perspect Med, 2014. **4**(4): p. a019299.

229.   Barnes, R.A., *Early diagnosis of fungal infection in immunocompromised patients.* J Antimicrob Chemother, 2008. **61 Suppl 1**: p. i3-6.

230.   Shoham, S. and S.M. Levitz, *The immune response to fungal infections.* Br J Haematol, 2005. **129**(5): p. 569-82.

231.   Horn, D.L., et al., *Epidemiology and outcomes of candidemia in 2019 patients: data from the prospective antifungal therapy alliance registry.* Clin Infect Dis, 2009. **48**(12): p. 1695-703.

232.   Medyukhina, A., et al., *Image-based systems biology of infection.* Cytometry A, 2015. **87**(6): p. 462-70.

233.   Chenouard, N., et al., *Objective comparison of particle tracking methods.* Nat Methods, 2014. **11**(3): p. 281-9.

234.   Masuzzo, P., et al., *Taking Aim at Moving Targets in Computational Cell Migration.* Trends Cell Biol, 2016. **26**(2): p. 88-110.

235.   Meijering, E., et al., *Tracking in cell and developmental biology.* Semin Cell Dev Biol, 2009. **20**(8): p. 894-902.

236.   Al-Zaben, N., et al., *Automated tracking of label-free cells with enhanced recognition of whole tracks.* Scientific reports, 2019. **9**(1): p. 3317-3317.

237.	Hoffstein, S.T., R.S. Friedman, and G. Weissmann, *Degranulation, membrane addition, and shape change during chemotactic factor-induced aggregation of human neutrophils.* J Cell Biol, 1982. **95**(1): p. 234-41.

238.	Wang, L., C.E. Castro, and M.C. Boyce, *Growth strain-induced wrinkled membrane morphology of white blood cells.* Soft Matter, 2011. **7**(24): p. 11319-11324.

239.	Jumaa, M.A.A., S. Dewitt, and M.B. Hallett, *Topographical interrogation of the living cell surface reveals its role in rapid cell shape changes during phagocytosis and spreading.* Sci Rep, 2017. **7**(1): p. 9790.

240.	Roberts, R.E. and M.B. Hallett, *Neutrophil Cell Shape Change: Mechanism and Signalling during Cell Spreading and Phagocytosis.* International journal of molecular sciences, 2019. **20**(6): p. 1383.

241.	Dewitt, S., R.J. Francis, and M.B. Hallett, *Ca²⁺ and calpain control membrane expansion during the rapid cell spreading of neutrophils.* J Cell Sci, 2013. **126**(Pt 20): p. 4627-35.

242.	Hallett, M.B. and S. Dewitt, *Ironing out the wrinkles of neutrophil phagocytosis.* Trends Cell Biol, 2007. **17**(5): p. 209-14.

243.	Dewitt, S. and M. Hallett, *Leukocyte membrane "expansion": a central mechanism for leukocyte extravasation.* J Leukoc Biol, 2007. **81**(5): p. 1160-4.

244.	Pettit, E.J., E.V. Davies, and M.B. Hallett, *The microanatomy of calcium stores in human neutrophils: relationship of structure to function.* Histol Histopathol, 1997. **12**(2): p. 479-90.

245.	Renkawitz, J. and M. Sixt, *Mechanisms of force generation and force transmission during interstitial leukocyte migration.* EMBO Rep, 2010. **11**(10): p. 744-50.

246.	Lepidi, H., et al., *Morphological polarization of human polymorphonuclear leucocytes in response to three different chemoattractants: an effector response independent of calcium rise and tyrosine kinases.* J Cell Sci, 1995. **108 (Pt 4)**: p. 1771-8.

247.	Reis, E.S., et al., *C5a receptor-dependent cell activation by physiological concentrations of desarginated C5a: insights from a novel label-free cellular assay.* J Immunol, 2012. **189**(10): p. 4797-805.

248.	Cheng, S.C., et al., *Complement plays a central role in Candida albicans-induced cytokine production by human PBMCs.* Eur J Immunol, 2012. **42**(4): p. 993-1004.

249.	Marolda, A., et al., *Candida species-dependent release of IL-12 by dendritic cells induces different levels of NK cell stimulation.* J Infect Dis, 2020.

250.	Teng, T.-S., et al., *Neutrophils and Immunity: From Bactericidal Action to Being Conquered.* Journal of immunology research, 2017. **2017**: p. 9671604-9671604.

251.	Leliefeld, P.H., et al., *The role of neutrophils in immune dysfunction during severe inflammation.* Crit Care, 2016. **20**: p. 73.

252.   Echenique-Rivera, H., et al., *Transcriptome analysis of Neisseria meningitidis in human whole blood and mutagenesis studies identify virulence factors involved in blood survival.* PLoS Pathog, 2011. **7**(5): p. e1002027.

253.   Tena, G.N., et al., *Failure to control growth of mycobacteria in blood from children infected with human immunodeficiency virus and its relationship to T cell function.* J Infect Dis, 2003. **187**(10): p. 1544-51.

254.   Plested, J.S., J.A. Welsch, and D.M. Granoff, *Ex vivo model of meningococcal bacteremia using human blood for measuring vaccine-induced serum passive protective activity.* Clin Vaccine Immunol, 2009. **16**(6): p. 785-91.

255.   Jemmett, K., et al., *A cyanobacterial lipopolysaccharide antagonist inhibits cytokine production induced by Neisseria meningitidis in a human whole-blood model of septicemia.* Infect Immun, 2008. **76**(7): p. 3156-63.

256.   Deslouches, B., et al., *Activity of the de novo engineered antimicrobial peptide WLBU2 against Pseudomonas aeruginosa in human serum and whole blood: implications for systemic applications.* Antimicrob Agents Chemother, 2005. **49**(8): p. 3208-16.

257.   Sprong, T., et al., *Inhibition of C5a-induced inflammation with preserved C5b-9-mediated bactericidal activity in a human whole blood model of meningococcal sepsis.* Blood, 2003. **102**(10): p. 3702-10.

258.   Duggan, S., et al., *Host response to Candida albicans bloodstream infection and sepsis.* Virulence, 2015. **6**(4): p. 316-26.

259.   Kurzai, O., et al., *Polymorphism of Candida albicans is a major factor in the interaction with human dendritic cells.* Int J Med Microbiol, 2005. **295**(2): p. 121-7.

260.   Morrell, M., V.J. Fraser, and M.H. Kollef, *Delaying the empiric treatment of candida bloodstream infection until positive blood culture results are obtained: a potential risk factor for hospital mortality.* Antimicrob Agents Chemother, 2005. **49**(9): p. 3640-5.

261.   Brieland, J., et al., *Comparison of pathogenesis and host immune responses to Candida glabrata and Candida albicans in systemically infected immunocompetent mice.* Infection and immunity, 2001. **69**(8): p. 5046-5055.

262.   Balish, E., et al., *Candidiasis in interferon-gamma knockout (IFN-gamma-/-) mice.* J Infect Dis, 1998. **178**(2): p. 478-87.

263.   Cenci, E., et al., *IFN-gamma is required for IL-12 responsiveness in mice with Candida albicans infection.* J Immunol, 1998. **161**(7): p. 3543-50.

264.   Káposzta, R., et al., *Characteristics of invasive candidiasis in gamma interferon- and interleukin-4-deficient mice: role of macrophages in host defense against Candida albicans.* Infection and immunity, 1998. **66**(4): p. 1708-1717.

265.   Donini, M., et al., *NADPH oxidase of human dendritic cells: role in Candida albicans killing and regulation by interferons, dectin-1 and CD206.* Eur J Immunol, 2007. **37**(5): p. 1194-203.

266.   Bozza, S., et al., *A crucial role for tryptophan catabolism at the host/Candida albicans interface.* J Immunol, 2005. **174**(5): p. 2910-8.

267.   Romani, L. and P. Puccetti, *Protective tolerance to fungi: the role of IL-10 and tryptophan catabolism.* Trends Microbiol, 2006. **14**(4): p. 183-9.

268.   Wu, Y., Z. Tian, and H. Wei, *Developmental and Functional Control of Natural Killer Cells by Cytokines.* Front Immunol, 2017. **8**: p. 930.

269.   Giri, S. and A.J. Kindo, *A review of Candida species causing blood stream infection.* Indian J Med Microbiol, 2012. **30**(3): p. 270-8.

270.   Reuss, O., et al., *The SAT1 flipper, an optimized tool for gene disruption in Candida albicans.* Gene, 2004. **341**: p. 119-27.

271.   Walther, A. and J. Wendland, *An improved transformation protocol for the human fungal pathogen Candida albicans.* Curr Genet, 2003. **42**(6): p. 339-43.

272.   Mollnes, T.E., et al., *Essential role of the C5a receptor in E coli-induced oxidative burst and phagocytosis revealed by a novel lepirudin-based human whole blood model of inflammation.* Blood, 2002. **100**(5): p. 1869-77.

273.   Delsing, C.E., et al., *Interferon-gamma as adjunctive immunotherapy for invasive fungal infections: a case series.* BMC Infect Dis, 2014. **14**: p. 166.

9 List of Abbreviation

Abbreviation	Meaning
NK	Natural killer
C.	Candida
TRAIL	Tumor necrosis factor-related apoptosis-inducing ligand
IFN	Interferon
moDC	Monocyte-derived dendritic cells
IL	Interleukin
PMN	Polymorphonuclear
BSI	Bloodstream infections
ICU	Intensive care unit
E. coli	Escherichia coli
Spp	species
EPIC	Extended prevalence of infection in intensive care
Als	Agglutinin-like sequence
GPI	Glycosylphosphatidylinositol
Hwp1	Hyphal wall protein 1
Epa	Epithelial adhesin
SAP	Secreted Aspartyl Proteinases
ECE	Endothelin Converting Enzyme
PAMP	Pathogen associated molecular pattern
PRR	Pattern recognition receptor
CLR	C-type lectin receptor
NOD	Nucleotide-binding oligomerization domain
NLR	NOD-like receptor
TLR	Toll-like receptor
IgG	Immunogobulin G
C3b	Complement component 3
CR3	Complement receptor 3
G-CSF	Granulocyte colony-stimulating factor
NET	Neutrophil extracellular traps
NAPDH	Nicotinamide adenine dinucleotide phosphate oxidase
MPO	Myeloperoxidase
CG	Cathepsin G
NGAL	Neutrophil gelatinase-associated lipocalin
MMP	Metalloproteinases
DNA	Deoxyribonucleic acid
NE	Neutrophils elastase
LTF	Lactoferrin
PR3	Leukocyte proteinase 3
ROS	Reactive oxygen species
CXCL8	Chemokine (C-X-C motif) ligand 8
GRO-α	Growth-regulated alpha protein
MIP-1α	Macrophage inflammatory proteins
CCL3	Chemokine (C-C motif) ligand 3
DC	Dendritic cells
Th	T helper
CGD	Chronic granulomatous disease

LAD	Leukocyte adhesion deficiency
PRR	Pattern recognition receptor
PXT3	Pentraxin 3
Syk	Tyrosine-protein kinase
Sik	Serine/threonine-protein kinase
CARD9	Caspase recruitment domain-containing protein 9
PI3K	Phosphoinositide 3-kinases
ILC1	Innate lymphoid cells
ITAM	Immunoreceptor tyrosine-based activation motif
ITIM	Immunoreceptor tyrosine-based inhibition motif
TNF	Tumor necrosis factor
MTOC	Microtubule organizing center
LAMP	Lysosomal-associated membrane protein
TNFR	TNF receptor
NGFR	Nerve growth factor receptor
DD	Death domain
FADD	Fas associated death domain
DED	Death effector domain
DISC	Death inducing signalling complex
ADCC	Antibody-dependent cell-mediated cytotoxicity
NF-kB	Nuclear factor kappa-light-chain-enhancer of activated B cells
MAPK	mitogen-activated protein kinase
Akt	Protein kinase B
ERK	Extracellular signal-regulated kinases
JNK	c-Jun N-terminal kinase
MHC	Major histocompatibility complex
MCA	Mucin-like carcinoma-associated antigen
CAR	Chimeric antigen receptor
Ab	antibody
AML	Acute myeloid leukemia
CMV	Cytomegalovirus
HSCT	Hematopoietic stem cell transplantation
GFP	Green fluorescent protein
HBSS	Hanks balanced solution
PBMCs	Peripheral blood mononuclear cells
MOI	Multiplicity of infection
hS	Human serum
hiFBS	Heat inactivated human serum
PI	Propidium iodine
DIC	Differential interference contrast
S-morphology	Spreading morphology
N-morphology	Non-spreading morphology
PDGF	Platelet-derived growth factor
fMLP	N-formylmethionine-leucyl-phenylalanine

Ehrenwörtliche Erklärung

Hiermit teile ich ehrenwörtlich mit, dass mir die geltende Promotionsordnung der Friedrich-Schiller-Universität Jena bekannt ist.

Ich habe die vorliegende Dissertation selbstständig verfasst. Alle verwendeten Hilfsmittel, Quellen und persönliche Mitteilungen habe ich angegeben.

Personen, welche mir bei der Auswahl und Auswertung der Materialien geholfen haben, habe ich benannt und in der Danksagung erwähnt.

Alle Personen, die bei der Erstellung des Manuskripts geholfen haben, sind in der Publikationsliste aufgeführt.

Die Hilfe eines Promotionsberaters wurde nicht in Anspruch genommen.
Für meine Arbeiten, die im Zusammenhang mit dem Inhalt der vorgelegten Dissertation stehen, habe ich weder unmittelbar noch mittelbar geldwerte Leistungen erhalten.

Die vorliegende Arbeit wurde bisher weder an der Friedrich-Schiller-Universität Jena noch an einer anderen Hochschule als Dissertation oder in Form einer Prüfungsarbeit für eine staatliche oder andere wissenschaftliche Prüfung eingereicht.

Jena, September 2020

_____

Alessandra Marolda